ISSN 0169-6548

Communications on Hydraulic and Geotechnical Engineering

Stationary and oscillatory flow through coarse porous media

June 1993

M.R.A. van Gent

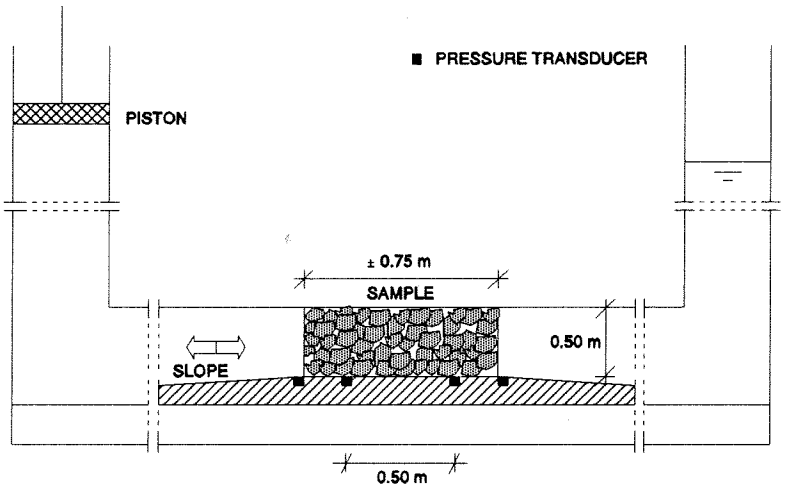

TU Delft
Delft University of Technology

Faculty of Civil Engineering

STATIONARY AND OSCILLATORY FLOW THROUGH COARSE POROUS MEDIA

by

M.R.A. van Gent

June 1993

Communications on Hydraulic and Geotechnical Engineering

Report No. 93-9

Faculty of Civil Engineering
Delft University of Technology

ABSTRACT

Measurements in a U-tube tunnel were carried out to study flow through coarse granular material. Tests with stationary flow and tests with oscillatory flow were done to study the differences between both. The coefficients from the extended Forchheimer equation, which is supposed to describe non-stationary porous flow, were determined. It appeared that for oscillatory flow the turbulent resistance is larger than under stationary flow conditions. This additional resistance is depending on the flow-field, expressed by the Keulegan-Carpenter number. The contribution of the inertial resistance is depending on the flow field as well. Its contribution to the total resistance was rather limited. The influence of the non-stationary flow conditions have been implemented in the expressions for the turbulent resistance and the inertial resistance. Comparisons of the results from the stationary flow tests with other measurements show that the results correspond reasonably well. This is not the case for existing expressions for stationary flow. The existing formulae under-predict the a-values while they over-predict the b-values. Further research must be concentrated on the influence of parameters such as grading, the aspect ratio and shape. These dependencies can be determined under stationary flow conditions.

CONTENTS

Chapter 1

1. Introduction.

Physical modelling of rubble mound structures has been studied often using small-scale models. Scale effects occur using such small scale models. For instance the flow through the permeable part of a permeable or partially permeable structure causes scale effects. In a small scale model the flow may be laminar in a certain area of the permeable part while under prototype circumstances the flow can be turbulent in that area. To study such scale effects, knowledge concerning the flow through the porous part is necessary.

In recent years much effort is put into the modelling of wave motion on and in coastal structures. For the modelling of the flow in the porous part, reliable expressions for the flow resistance are needed.

Due to the relatively large velocities and relatively large accelerations, porous flow through coarse material differs from Darcy-flow. Many researchers have investigated this stationary porous flow (see Hannoura and Barends, 1981). However, it resulted also in many different expressions for the porous friction terms. Most expressions consist of a term linear with the flow velocity (laminar contribution containing the coefficient "a") and a term quadratic with the flow velocity (turbulent contribution containing the coefficient "b"). Two major drawbacks appear if we consider the existing knowledge:

- The expressions for the porous friction terms show large deviations from the data-set from which they were derived. This is partially due to scatter, inherent to the complexity of the studied phenomena, but also due to the over-simplified expressions.
- Almost all measurements were performed with stationary flow. Therefore, all expressions were derived for stationary flow. Non-stationary flow gives an extra term in the equation describing the flow through porous media (term containing a coefficient "c"). Theoretical considerations of some researchers (see for instance Burcharth and Christensen, 1991 or Van Gent, 1991) predict deviations of the porous friction terms due to the influence of inertia as well (different coefficients "a" and "b").

To contribute to the solution of the first problem, accurate measurements must be performed with variation of many parameters such as porosity, diameter, grading, aspect ratio, shape (gross shape, roughness and surface texture) and orientation of the stones with regard to the direction of the mean flow. Measures must be taken to limit wall effects; in many experimental set-ups, wall effects cause relatively large deviations in the flow resistance.

Only very limited measurements have been performed with oscillatory flow. Smith (1991) created a data-set for non-stationary flow through porous media. Those measurements were concentrated on flow through spheres with different packing arrangements. The size of the spheres and the type of packing were varied. This valuable data-set is however not sufficient for the description of flow through coarse granular material since little measurements were performed with rock.

The measurements described in this report were concentrated on the flow through coarse granular material, in particular on the aspects of non-stationary flow and its differences with stationary flow. Unlike previous tests, the estimated inertia contribution had to be relatively large compared to the estimated contribution of the turbulent flow to study non-stationary aspects of porous flow.

The measurements described in this report were performed in the oscillating water tunnel at Delft Hydraulics. They were carried out within the European MAST-G6 "Coastal Structures" program, project 1, "Wave Action on and in Rubble Mound Structures". The proposal for the test was made within this project. The actual tests were performed by G. Smith (Delft Hydraulics), O.H. Andersen (D.H.I.) and M.R.A. van Gent (Delft University of Technology) with assistance of the laboratory staff of Delft Hydraulics. The initial analysis described in the paper "Non-steady oscillatory flow in coarse granular materials" by Andersen, Van Gent, Van der Meer, Burcharth and Den Adel (1993). The coefficients in the present report differ from the coefficients in the mentioned paper. The a and b-coefficients are in the same order of magnitude but differ as a result of slightly different assumptions and a slightly different analysis. The procedure to derive the c-coefficients used in the mentioned paper, was found to be incorrect. Also measurements with cylinders in a "squared" packing arrangement have been performed, see Andersen et al.(1993). The present study is concentrated on rock material. Therefore, no further analysis on those measurements with cylinders will be performed here.

Chapter 2

2. Theoretical background.

2.1 Stationary flow.

Most of the existing knowledge concerning porous flow through coarse granular material concerns stationary flow. In this section some of the research and measurements with stationary flow will be discussed briefly.

A coarse porous medium causes flow resistance that can reasonably well be expressed with a term linear with the flow velocity and a term quadratic with the flow velocity. The first term can be seen as the laminar contribution and the second term can be seen as the turbulent contribution. This can we written as:

$$I = au + bu^2 \qquad (1)$$

where

I	:	hydraulic gradient.
u	:	bulk/filter velocity.
a	:	dimensional coefficient (s/m).
b	:	dimensional coefficient (s^2/m^2).

This formula is referred to as the Forchheimer equation because Forchheimer was one of the first (1901) to suggest this formula. The coefficients "a" and "b" are dimensional and contain several parameters. Many empirical and semi-empirical formulae have been derived from measurements. See for a literature survey Hannoura and Barends (1981). Below, some of those formulae are shown. The following notation has been used:

n	:	porosity.
D	:	particle size.
D_{EQ}	:	equivalent sphere diameter defined as the $D_{EQ}=(6M_{50}/\pi\rho_a)^{1/3}$
M_{50}	:	average mass of a rock grading, determined by the 50% value on the mass distribution curve.
ρ_a	:	density of the material.

a	b	Source
$\alpha_{ERG}\ \frac{(1-n)^2}{n^3}\ \frac{\nu}{g\,D^2}$	$\beta_{ERG}\ \frac{1-n}{n^3}\ \frac{1}{g\,D}$	Ergun (1952)
$\alpha_{ENG}\ \frac{(1-n)^3}{n^2}\ \frac{\nu}{g\,D_{EQ}^2}$	$\beta_{ENG}\ \frac{1-n}{n^3}\ \frac{1}{g\,D_{EQ}}$	Engelund (1953)
$\alpha_{K}\ \frac{(1-n)^2}{n^3}\ \frac{\nu}{g\,D_{15}^2}$	$\beta_{K}\ \frac{1}{n^5}\ \frac{1}{g\,D_{15}}$	Koenders (1985)
$\alpha_{DA}\ \frac{(1-n)^2}{n^3}\ \frac{\nu}{g\,D_{15}^2}$	$\beta_{DA}\ \frac{1}{n^2}\ \frac{1}{g\,D_{15}}$	Den Adel (1987)
$\alpha_{S}\ \frac{(1-n)^2}{n^3}\ \frac{\nu}{g\,D_{15}^2}$	$\beta_{S}\ \frac{1-n}{n^3}\ \frac{1}{g\,D_{15}}$	Shih (1990)

Table 1 Some existing formulae for stationary porous flow.

For the coefficients α and β in those equations, the following values were found (between brackets the 95% confidence levels are given):

- Ergun: $\alpha_{ERG}=150$ $\beta_{ERG}=1.75$
- Engelund: $\alpha_{ENG}=780$ $\beta_{ENG}=1.8\text{-}3.6$
- Koenders: $\alpha_{K}=290$ (250-330) $\beta_{K}=1.4$
- Den Adel: $\alpha_{DA}=160$ (75-350) $\beta_{DA}=2.2$ (0.9-5.3)

Shih (1990) proposed the following formulae for α_S and β_S:

$$\alpha_S = 1684 + 3.12\cdot 10^{-3}\left(\frac{g}{\nu^2}\right)^{\frac{2}{3}} D_{15}^2$$
$$\beta_S = 1.72 + 1.57\ \exp\left[-5.10\cdot 10^{-3}\left(\frac{g}{\nu^2}\right)^{\frac{1}{3}} D_{15}\right] \qquad (12)$$

For wide graded material Shih proposed to replace D_{15} by:

$$D_* = D_{15}\left(\frac{D_{15}}{D_{50}}\right)^{-1.11}\left(\frac{D_{50}}{D_{85}}\right)^{0.52} \qquad (13)$$

The above mentioned expressions result in "a" and "b" values in rather wide ranges. This indicates that measuring porous flow through coarse granular material is a very complex matter, even for stationary flow. It also indicates that the existing formulae are over-simplified. The expressions are rather sensitive for small errors in the measured porosities since these porosities are incorporated in the expressions with the porosity to a certain power.

The expressions for "a" and "b" first proposed by Ergun (1952), can also be derived theoretically (see for instance Van Gent, 1991). The non-dimensional coefficients α and β are not the same for all types of stones. It may well be possible that parameters such as grading, aspect ratio or shape must be implemented in the expressions.

The following set of expressions for the a and b-coefficients will be used in this report:

$$a = \alpha \frac{(1-n)^2}{n^3} \frac{\nu}{g D^2}$$
$$b = \beta \frac{1-n}{n^3} \frac{1}{g D} \qquad (14)$$

It can be argued whether the D_{n15}, the D_{n50} or the D_{EQ} is the most appropriate characteristic length-scale for the porous medium. The D_{n15} ,can be seen as a representative scale for the size of the pores. On the other hand, the D_{EQ} can be used as a characteristic length-scale while the influence of grading (affecting the size of the pores) can be included separately in the expressions for α and β. The D_{n50} has also been used as a characteristic length-scale. In this report the values α and β, calculated with the D_{n15}, D_{n50} and the D_{EQ} will all be presented.

2.2 Non-stationary flow.

General.

In many circumstances porous flow is not stationary. In most coastal structures that contain a permeable part, wave action causes non-stationary flow. For many practical purposes knowledge concerning non-stationary flow is necessary. First the basic formula for non-stationary flow will be discussed, subsequently the influence of inertia will be regarded and finally the relevance of previous experiments and the described experiments will be clarified.

Formula for non-stationary flow.

The Forchheimer equation (equation 1) is valid for stationary flow. Polubarinova Kochina (1962) added a time-dependent term. This formula is referred to as the extended Forchheimer equation:

$$I = au + bu|u| + c\frac{du}{dt} \tag{15}$$

where "c" is a dimensional coefficient (s^2/m). This formula can also be derived from the Navier-Stokes/Reynolds equation, see for instance Van Gent (1991).

For the coefficient "c" some expressions exist. Gu and Wang (1991) and Van Gent (1991) derived the same type of expression for "c" after a theoretical derivation:

$$c = \frac{1 + \gamma \frac{(1-n)}{n}}{n\,g} \tag{16}$$

where γ is a non-dimensional coefficient that takes the phenomenon added mass into account. To accelerate a certain volume of water, a certain amount of momentum is needed. The amount of momentum that is needed to accelerate the same volume of water in a porous medium is larger. This is called "added mass" because the extra amount of momentum suggests that a larger volume of water has to be accelerated.

Theoretical considerations of some researchers predict deviations of the porous friction terms with coefficients "a" and "b" due to the influence of inertia (see for instance Van Gent, 1991 or Burcharth and Christensen, 1991).

Estimation of the relative importance of inertia.

Gu and Wang (1991) discussed the influence of inertia for a wide range of practical applications. A discussion using a very similar approach is given below.

The relative importance of resistance forces can be estimated using two non-dimensional parameters. The contributions of inertial, laminar and turbulent resistance are regarded. The magnitude of the turbulent resistance relative to the laminar resistance is linear with the Reynolds-number, Re, defined as UD/ν where

ν is the kinematic viscosity and U is a characteristic velocity. The magnitude of the turbulent resistance relative to the inertial resistance is linear with the Keulegan-Carpenter number, KC, defined as UT/D where T is the wave/oscillation period. The magnitude of the inertial resistance relative to the laminar resistance is linear with $Re/KC = D^2/T\nu$.

With the estimations $\alpha \sim O(1000)$, $\beta \sim O(1)$ and $\gamma \sim O(1)$, where α, β and γ are the coefficients in equations 14 and 16, the relative magnitude of the resistance forces can be estimated:

$$\left|\frac{f_I}{f_L}\right| = \frac{\text{inertial resistance}}{\text{laminar resistance}} \sim 10^{-2}\,\frac{RE}{KC}$$

$$\left|\frac{f_T}{f_L}\right| = \frac{\text{turbulent resistance}}{\text{laminar resistance}} \sim 10^{-2}\,RE \qquad (17)$$

$$\left|\frac{f_T}{f_I}\right| = \frac{\text{turbulent resistance}}{\text{inertial resistance}} \sim KC$$

MATERIAL DESCRIPTION	SIZE (m)	U (m/s)	Re (UD/ν)	Re/KC ($D^2/T\nu$)	DOMINANT RESISTANCE
Sand	< 0.002	< $O(10^{-3})$	< $O(10^0)$	< $O(10^0)$	Laminar
Pebble Small gravel	0.01	$O(10^{-2})$	$O(10^2)$	$O(10^2)$	Laminar Turbulent Inertial
Large gravel Crusted stone	0.10	$O(10^{-1})$	$O(10^4)$	$O(10^4)$	Turbulent Inertial
Boulder Crusted stone	0.3-1.0	$O(10^0)$	$O(10^6)$	$O(10^6)$	Turbulent Inertial
Artificial blocks Large rock	> 1.0	> $O(10^0)$	> $O(10^6)$	> $O(10^6)$	Turbulent Inertial

Table 2 Dominant resistance under coastal wave conditions, according Gu and Wang (1991).

In Figure 1, the regions with different dominant resistance components are shown. In Table 2 an illustration of the dominant resistance components under coastal wave

conditions is given. Figure 1 and Table 2 have both been derived from Gu and Wang (1991).

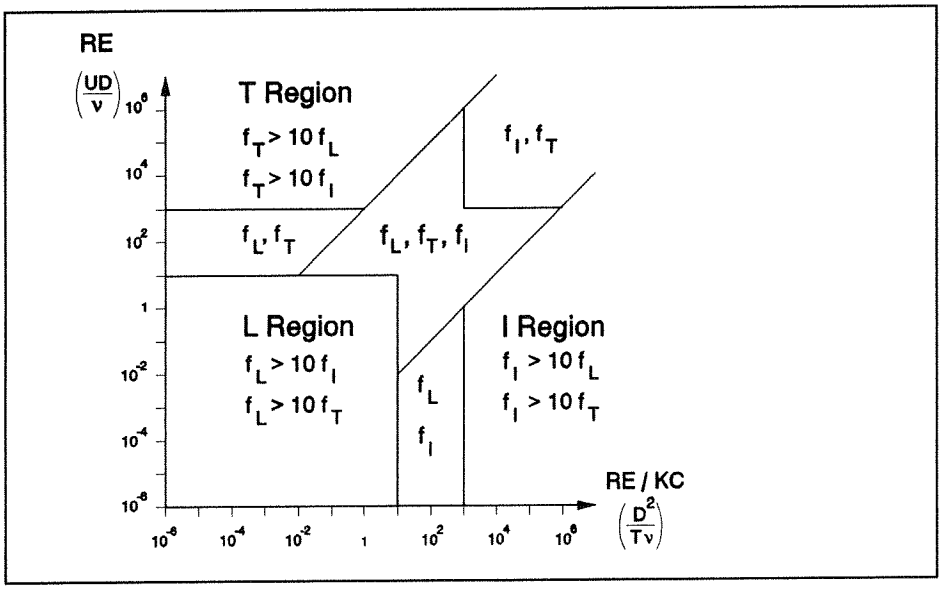

Fig.1 Regions with different dominant resistance components.

Relevance of previous and present oscillatory flow tests.

The empirical and semi-empirical formulae described in the previous section are all based on experiments with stationary flow. Only very limited measurements have been performed with oscillatory flow. Smith (1991) did experiments in an oscillating water tunnel through different arrangements of packing of spheres. Two sizes of spheres and two arrangements of the packing were tested with different amplitudes of the velocity and different oscillation periods. Also stationary tests were performed. Non of the existing formulae could be applied for the measured friction coefficients, not for the stationary flow results and not for the non-stationary flow results. This will be discussed in section 4.2. The data-set of Smith (1991) is not sufficient to improve or extend the existing formulae for rock material since only one sample with rock material was tested.

New measurements have been carried out, not in the first place to improve or extend the formulae for stationary flow, but to study the differences between stationary flow and non-stationary flow. If differences appear, they are supposed to be relatively large in a flow regime where inertia is relatively important

compared to the turbulent contribution. The experiments that have been carried out now, have been done in the regime were the ratio of the inertia contribution compared to the turbulent contribution is larger than in the measurements of Smith (1991). The tests were done over a larger range of Re-numbers and with smaller KC-numbers. The magnitude of the dominant resistance components in the tests by Smith (1991) and in the new tests, described in this report, have been illustrated in Figure 2. The figure shows that non of the three components can be neglected in the tested region. The figure shows the relevant areas for sand, small gravel, large gravel and large rock under coastal wave conditions. It can be concluded that the tested region is of importance for applications with coastal wave conditions.

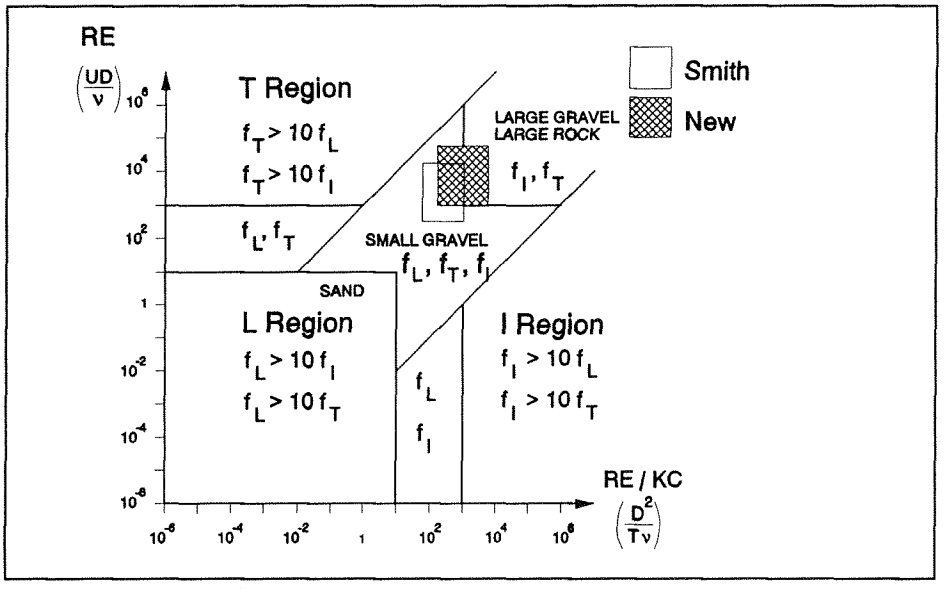

Fig.2 Dominant resistance in previous and present tests.

Chapter 3

3. Description of the measurements.

3.1 Description of the experimental set up.

The experiments were carried out in the oscillating water tunnel at Delft Hydraulics. This tunnel is a U-tube tunnel with a horizontal section of 15 m long and 0.30 m wide. The piston can produce oscillating water movement. Various combinations of amplitudes and oscillation periods can be generated. A stationary flow can be produced with a discharge up to 0.10 m^3/s. Measures have been taken to remove air from the horizontal section.

In the middle of the horizontal section a box with material was placed. The box was about 0.75 m in length, 0.50 m in height and 0.30 m in width. To obtain a sufficient large discharge through the samples, the cross section of the horizontal section of the U-tube was reduced. An additional bottom was placed 0.30 m above the bottom of the tunnel. A slope was created on both sides of the test section. The height of the cross section near the sample was 0.50 m. A sketch of the experimental set up is given in Figure 3.

At the bottom side of the box, pressure transducers and pressure difference transducers were positioned, both inside the box and just outside the box. The distance between the internal transducers was 0.50 m. The distance between the external transducers was about 0.8 m. The movement of the piston was recorded (the steered signal and the actual signal). The velocity through the sample could be derived from the actual movement of the piston. This velocity was checked with LDV-equipment which was placed above the slope and outside the range of the water particles moving through the sample. For the stationary flow tests the discharge generated by the pump was measured (steered discharge and actual discharge) and checked with the LDV-equipment. All signals where recorded during one minute with a sampling frequency of 100 Hz.

Half spheres were glued to the vertical sides of the boxes containing rock material, in order to reduce the wall effects. See Figure 4.

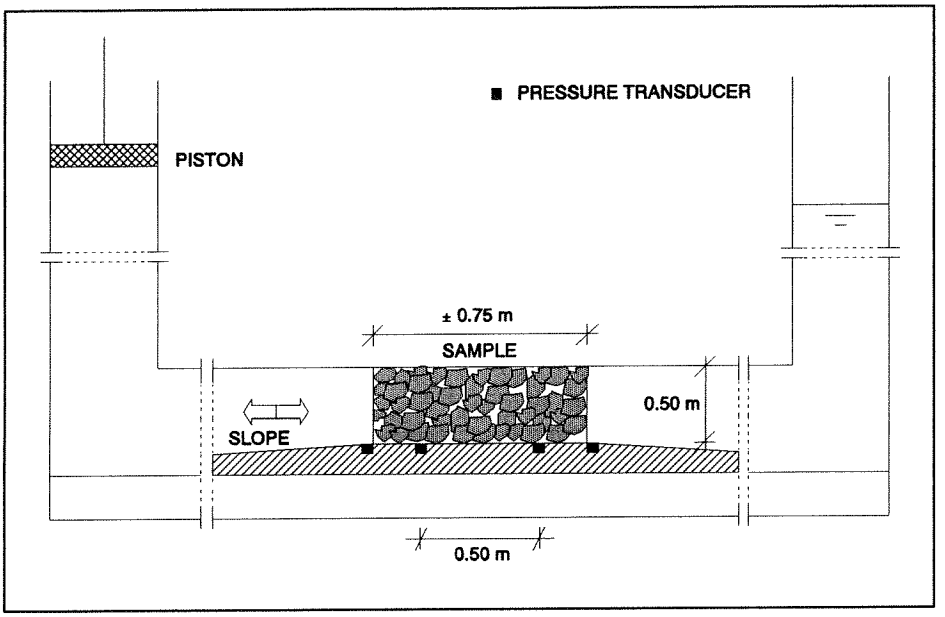

Fig.3 Experimental set up.

3.2 Description of the tested material.

Five samples with different types of stones have been tested. Pictures of the stones can be found in Appendix 0. Some relevant properties are given in Table 3. Test materials R1, R3 and R4 were sent by Hydraulic Research, Wallingford. Test material R3 was rounded by abrasion of material R1 to achieve a 5 to 10% weight loss. R4 was rounded by abrasion of material R1 to achieve a 20 to 25% weight loss. A full description is given by Bradbury et al. (1988) and Williams (1992). Material R8 was used as core material in tests at Hannover, see Ouméraci (1991). The porosity n was measured by weighing the stone sample in a box with a volume equal to the box placed in the oscillating water tunnel. The volume of the stones was found by division by the stone density. The porosity of the sample with spheres was theoretically derived. Because the wooden spheres expand in water, the actual porosity might have been slightly smaller. The aspect ratio l/t is defined as the average length of the longest axis of the stones (l) divided by the minimum length perpendicular to this axis (t).

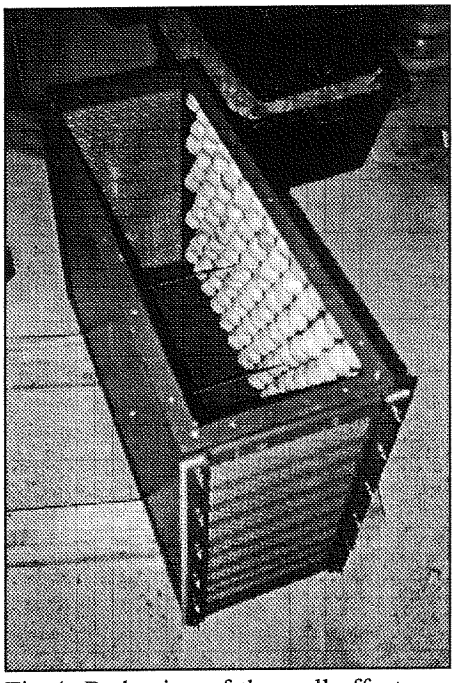

Fig.4 Reduction of the wall effects.

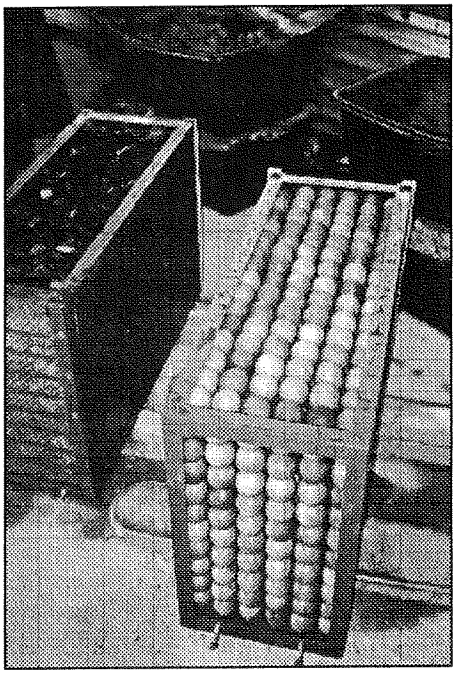

Fig.5 Sample with spheres.

DESCRIPTION OF TESTED MATERIAL							
CODE	MATERIAL	D_{EQ}	D_{n50}	D_{n15}	D_{n85}/D_{n15}	l/t	n
R1	Irregular rock	0.0760	0.061	0.052	1.27	1.9	0.442
R3	Semi round rock	0.0607	0.048	0.041	1.27	2.0	0.454
R4	Very round rock	0.0606	0.048	0.042	1.26	2.2	0.393
R5	Irregular rock	0.0251	0.020	0.017	1.03	2.3	0.449
R8	Irregular rock	0.0385	0.031	0.023	1.74	2.0	0.388
S1	Spheres-cubic packing	0.0460	0.046	0.046	1.0	1.0	0.476

Table 3 Description of the tested material.

Besides the five samples with stones, a sample with wooden spheres in a cubic packing arrangement has been tested. See Figure 5. Also three samples with cylinders in a "squared packing" arrangements have been tested. An analysis of the results with cylinders can be found in Andersen et al.(1993).

The number of samples is not sufficient for a full parameter study. Parameters as porosity, diameter, grading, aspect ratio and shape (gross shape, roughness and surface texture) have been varied. Since more parameters have been varied than the number of tested samples, existing formulae can not be extended with more parameters. However, results can be compared with existing formulae.

3.3 Procedure of testing and analysis.

Procedure of testing.

The rock samples were constructed in such a way that the underlayer of the sample was parallel to the mean flow direction; the direction of the gravitational acceleration during construction of the sample was perpendicular to the mean flow direction. The longest axis of the stones is supposed to be perpendicular to the gravitational acceleration during construction of the sample. Stones with an aspect ratio (maximum length divided by the length perpendicular to the direction of the maximum length) larger than one are supposed to have a horizontal orientation. The samples were compacted before testing so that they could not be compacted during testing. After positioning of the sample in the tunnel, the maximum constant discharge was imposed through the sample to remove air bubbles. The actual test-runs started with a constant flow with a discharge of 0.01 m^3/s. The discharge was increased with steps of 0.01 m^3/s up to 0.10 m^3/s. The imposed displacement was sinusoidal for the oscillatory flow tests. The tests were done with three oscillation periods. For each oscillation period the stroke of the piston was increased with steps of about 1% ($\approx$ 0.015 m) of the maximum stroke of the piston ($\approx$ 1.50 m). This stroke was increased till the maximum capacity of the tunnel was reached. This maximum capacity was achieved if the pressure reached its maximum allowable. The average maximum stroke of the piston was about 10% of its maximum. This corresponds to a maximum velocity of about 0.50 m/s near the sample. This indicates that the tests were done in the lower range of the capacity of the piston displacement.

Signal analysis.

The imposed displacement of the piston was sinusoidal for the oscillatory flow tests. However, it appeared that for the tests with relatively small piston displacements, the signals were not sinusoidal. The displacement signals were relatively flat at the point were the piston changed its direction. This had a rather large influence on the signals of the pressure gradient. Local maxima occurred as shown in Figure 6 (at t=14.5s, t=16.5s, etc.). This figure shows an extreme case (rock sample R3,

T=4s and an amplitude of 2% of the maximum amplitude). This has a large influence on the derivation of the friction coefficients since this local maximum could not always be found in the velocity signal. Techniques to derive the coefficients, for instance regression analysis, are hard to perform because for some tests a part of the signal must be excluded from the analysis (near zero-crossings). The extremely large local maxima near the zero-crossings, as for instance shown in Figure 6, are supposed not to be caused by phenomena that can be described with the extended Forchheimer equation. However, the contribution of the c-term from the extended Forchheimer equation is supposed to be relatively important in this part of the signal. Therefore, it is hard or impossible to derive c-coefficients for these tests with such small amplitudes of the piston displacement with techniques as regression analysis.

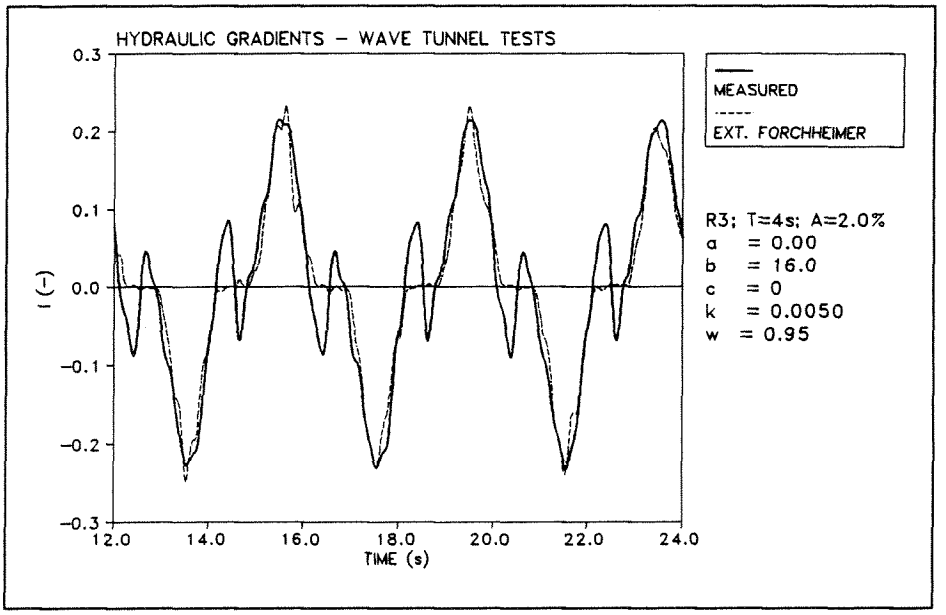

Fig.6 Example of a extremely disturbed signal; probably caused by deviations of the piston displacement at very low percentages of its maximum capacity (2%).

Pressures were measured with pressure transducers and pressure difference transducers, both inside the sample and just outside the sample. Due to possible disturbance of the flow just outside the sample, analysis with the internal transducers was preferred. Comparisons between the maximum pressure differences outside the sample and inside the sample, showed differences of about 5%-10%. The peak values of the external pressure differences were larger. Differences in the same order of magnitude occurred between the calculated signals from the two

internal pressure transducers compared and the signals from the internal pressure difference transducers. The signals from the internal pressure difference transducer have been used after band-pass filtering. Cut-off frequencies of 0.05 Hz and 4 Hz were chosen after spectral analysis of the signals; frequencies outside this range, including the zero-component, were removed by this filtering procedure.

A phase-shift occurred between the displacement signals from the piston and the pressure gradient at the sample. This phase-shift was not constant. No further analysis concerning this phase-shift has been performed.

Treatment of the underflow.

As shown in the experimental set up, an additional bottom was placed 0.30 m above the actual bottom of the tunnel. Underneath the sample, the space between the extra bottom and the real bottom of the tunnel was filled with foam. It appeared that a certain flow beneath the extra bottom, through the section with foam, took place. Because the estimated water velocities through the sample were derived from the piston displacement, a correction must be made for this loss underneath the extra bottom. The magnitude of this underflow has been measured with the LDV-equipment. This has been done for rock sample R1. The estimated underflow velocity was about 15% of the velocity through the sample. This corresponds to about 10% of the flux through the sample. By assuming a quadratic resistance of the area filled with foam, the friction coefficient of the foam-section could be estimated. In this way the velocities derived from the piston displacement, u_p, could be corrected for the underflow: $u := u_p - k \cdot I \sqrt{|I|}$ where k is the estimated friction coefficient for the foam section (0.005) and I the measured hydraulic gradient.

Treatment of wall effects.

The wall effects for the rock samples have been reduced because half spheres were glued to two sides of the box, see Figure 4. Wall effects are supposed to be important in case the stones are large compared to the size of the box. From measurements with spheres of the same size, it appeared that the friction coefficients of those spheres were in the same order of magnitude as the friction coefficients from the largest tested rock material. Therefore, it has been assumed that no wall effects occurred near those two sides of the box. However, the two sides at the top and the bottom of the box were smooth. Therefore, a correction for wall effects has been applied. The equivalent diameter of the box is 0.45 m. With an average stone size of about 0.04 m, the ratio $D_{box}/D_{50\text{-stone}}$ was about 11. Because the wall effect has been reduced at 63% of the four sides of the box, this ratio is multiplied with 1/0.63. The adapted ratio $D_{box}/D_{50\text{-stone}}$ becomes about 18. Burcharth

and Christensen (1991) show curves for wall effect correction factors derived from some existing data and a curve suggested by Rose (1950). The curves show wall effect correction factors corresponding to the β-values (which is the coefficient in the Forchheimer friction term with the squared velocity). Using the ratio 18, one can find a correction factor of about 0.88 for the β-values. In this study the correction factor was not applied on the β-values but on the velocities. A correction factor of 0.88 for the β-values corresponds to a correction factor $\sqrt{0.88}$ for the velocities. The value 0.95 has been applied. Obviously no correction for the sample with spheres has been applied.

Chapter 4

4. Stationary flow tests.

4.1 Results of the stationary flow tests.

The coefficients "a" and "b" from the Forchheimer equation (equation 1) could be derived using linear regression analysis. If we assume that those coefficients are constant for the tested range, a plot I/u versus u would give a straight line. I is the measured hydraulic gradient and u is the calculated velocity, derived from the piston displacement. The correction for wall effects (0.95) and the correction for the underflow have been implemented. Extrapolations of the lines in Figure 7 give the a-values at the vertical axis. The b-values can be derived from the slopes of the lines. In Appendix 1, figures are shown of each sample separately. It appears that the assumption that the a and b-values are constant for the tested range, is valid since the measured data correspond remarkably well with the fitted line except for the two lowest measuring points with sample R8 (excluded from further analysis). One data-point from sample R4 has been excluded as well, see the figure on page A1-2; this point is supposed to be caused by an error in the data-acquisition or by failure of the equipment. All other data points, resulting in rather straight lines, do not indicate that the validity of the Forchheimer equation (prescribing straight lines in Figure 7) should be questioned. Therefore, these three divergent points have not been included in the further analysis.

Table 4 shows the results from the stationary flow tests. The coefficients "a" and "b" from the Forchheimer equation (equation 1) are given as well as their standard deviation (std). The values of α and β from equation 14 are calculated using three characteristic length-scales: D_{n15}, D_{n50} and D_{EQ}. The kinematic viscosity of water at 10°C is 1.3E-6 m^2/s. Due to the relative large standard deviations of the a-values (std a), the absolute errors in the α-values are large.

The coefficients α and β are not constant. This indicates that the expressions for "a" and "b" (equation 14) are over-simplified. Probably parameters such as grading, aspect ratio and shape (gross shape, roughness and surface texture) may still have to be implemented in the expressions. The present tests are not sufficient to extend the existing formulae.

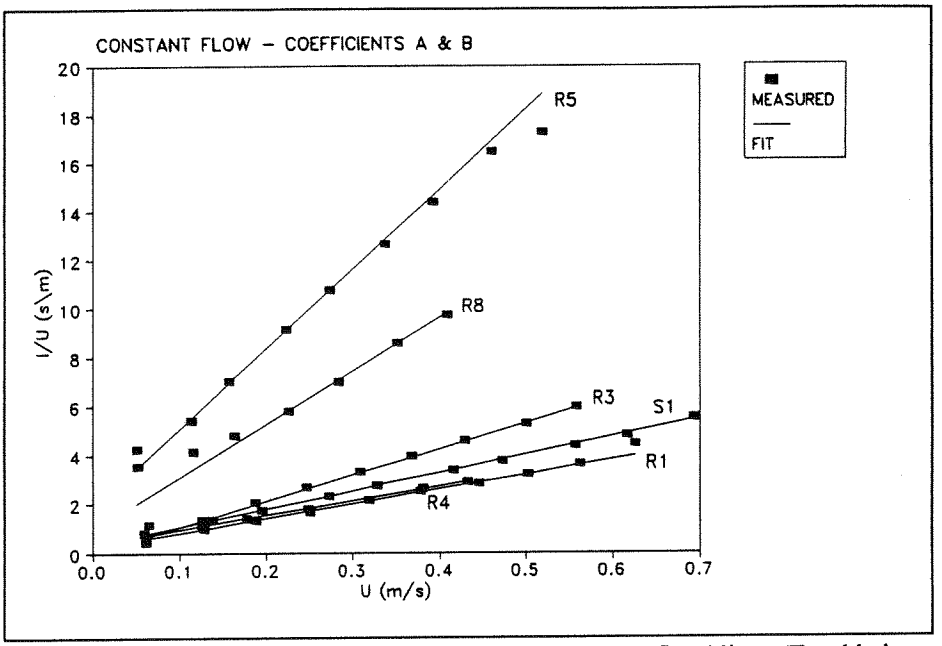

Fig.7 Measurement points from stationary flow tests and fitted lines (Forchheimer equation).

RESULTS STATIONARY FLOW TESTS										
MATERIAL	a	std a	α-D_{n15}	α-D_{n50}	α-D_{EQ}	b	std b	β-D_{n15}	β-D_{n50}	β-D_{EQ}
R1	0.23	0.037	1327	1791	2780	6.0	0.076	0.48	0.55	0.69
R3	0	0.016	0	0	0	10.7	0.05	0.75	0.88	1.09
R4	0.34	0.015	808	1066	1644	6.0	0.06	0.25	0.29	0.36
R5	1.81	0.093	1204	1662	2566	32.8	0.75	0.91	1.07	1.33
R8	0.89	0.055	554	1007	1552	21.7	0.4	0.47	0.63	0.78
S1	0.33	0.023	2070	2070	2070	7.4	0.16	0.69	0.69	0.69

Table 4 Results from the stationary flow tests. The values of α and β are related to eq.14.

4.2 Comparison with other data.

Influence of the orientation of the stones.

Before the comparison between the coefficients derived from the present tests and other tests is made, a discussion concerning the influence of the orientation of the stones with regard to the mean flow direction is given. A brief discussion about this subject has been presented by Den Adel (1991).

It is proposed to include the influence of the orientation of the stones, with regard to the mean flow direction in the expression for "b" (equation 14). This influence of the orientation of the stones is assumed to be dependent on the projected area of stones, perpendicular to the flow direction. This projected area differs from the average projected area in case the aspect ratios of the stones are not equal to one. In case the smallest projected area of the stones is perpendicular to the flow direction, the resistance is smaller than in case the largest projected area of the stones is perpendicular to the flow direction.

In the present tests the orientation of the stones was not varied. However, it is proposed to implement the influence of this orientation in the expression for b. In the following discussion, an expression containing this influence, is proposed. However, this expression must be verified with measurements. The relatively large deviations in test results, obtained with tests with different orientations of the stones, may be explained this way.

In the expression for b (equation 14) the influence of the orientation of the stones with respect to the mean flow direction can be implemented by including the term $(l/t)^{0.5 \cdot \tan(\psi - 45°)}$ where l/t is the aspect ratio and ψ the (absolute) angle between the mean flow direction and the longest axis of the stones. The longest axis of the stones is supposed to be perpendicular to the gravitational acceleration during construction of the sample. Some existing data were derived with a set-up where this was parallel to the mean flow direction (0°). In other measurement set-ups this was perpendicular to this mean flow direction (90°). The b-values vary linearly with the characteristic length-scale D. The influence of the orientation of the stones is assumed to be linear with $(l/t)^{0.5 \cdot \tan(\psi - 45°)}$. This expression results in a difference of a factor l/t between samples tested with an angle (ψ) of 0° and samples tested with an angle of 90°. This is still a rather rough simplification of the phenomenon. The sizes and the shape of the box containing the sample, might also influence the orientation of the stones; the stones may be slightly forced to be orientated in such a way that the direction of the longest axis of the stones is in the direction of the longest axis of the box. It might also be possible that the sample is not isotope and

that the directional porosity is different (probably slightly smaller) in the direction of the gravitational acceleration. These last two phenomena have been neglected.

Measurements where the orientation of the stones with regard to the mean flow direction is being varied, must show whether the following expression is sufficient to take the orientation of the stones into account.

$$b = \beta \frac{1-n}{n^3} \left(\frac{l}{t}\right)^{0.5\tan(\psi - 45°)} \frac{1}{g\ D} \tag{18}$$

where

ψ	:	the (absolute) angle between the mean flow direction and the direction of the underlayer during construction of the sample (the direction of the longest axis of the stones).
l/t	:	aspect ratio.
l	:	length of the longest axis of a particle.
t	:	length of the smallest axis perpendicular to the longest axis of a particle.

Comparison with existing formulae.

In section 2.1 some existing formulae for stationary flow were described. These formulae were based on experiments. Comparisons of the α-values, see Table 1 and Table 4, show that the α-values from the present tests are higher. A comparison was made between the measured b-values and the various expressions for "b".

Because the samples tested by various authors were constructed differently, a comparison is rather difficult. In the present tests the angle ψ was 0° while some other tests were done with an angle of 90°. This has been denoted as b(0°) and b(90°). To compare the present tests (ψ=0°) with tests where ψ was 90°, the "measured b(90°)" is calculated as discussed earlier in this chapter. This gives b(90°)=l/t b(0°). The coefficient β=0.75 for equation 14 has been derived from the present tests using the D_{EQ} as the characteristic stone diameter. This corresponds to a value β=0.6 in case for D the D_{n50} is taken.

For the coefficient in Engelund's formula 2.8 was used. Den Adel gave a 95% confidence interval 0.9-5.3 for the coefficient of his formula: $b=2.2/gD_{15}n^2$. The measured b-values are lower than the predicted b-values, see Table 5 and Figures 8 and 9. However, the wide confidence levels of the coefficients from the existing formulae indicate that the measured coefficients are not unrealistic.

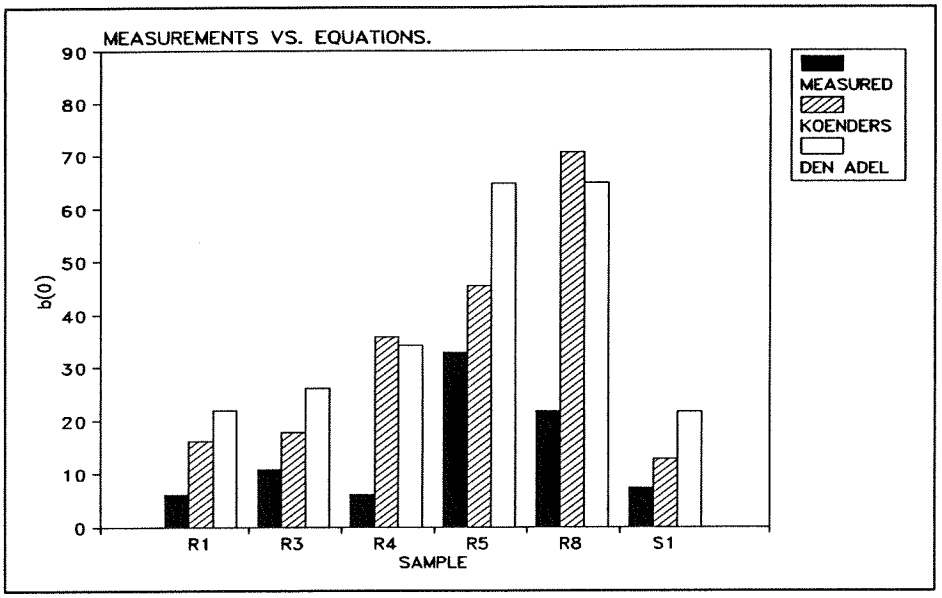

Fig.8 Comparison of measured b(0°)-values and two expressions for b.

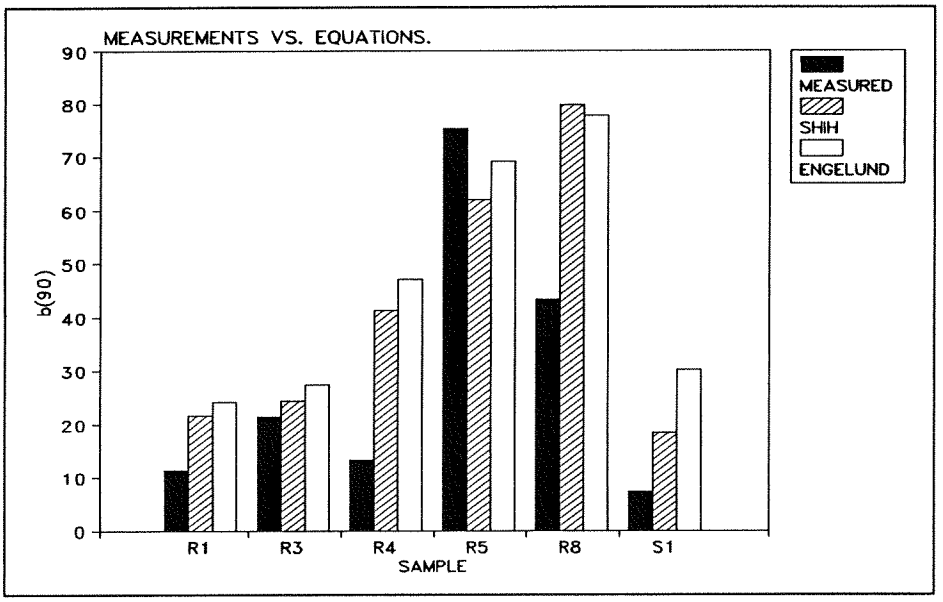

Fig.9 Comparison of measured b(90°)-values and two expressions for b.

COMPARISON b-VALUES WITH EQUATIONS							
MATERIAL	MEASURED		Eq.14	Shih	Koenders	Den Adel	Engelund
	b(0°)	b(90°)	b(0°)	b(90°)	b(0°)	b(0°)	b(90°)
R1	6.0	11.3	9.4	21.6	16.1	21.9	24.3
R3	10.7	21.4	10.7	24.4	17.7	26.0	27.4
R4	6.0	13.2	18.0	41.3	35.8	34.2	47.1
R5	32.8	75.4	27.0	62.1	45.5	64.7	69.2
R8	21.7	43.4	34.8	79.9	70.6	64.8	77.7
S1	7.4	7.4	8.1	18.5	12.7	21.5	30.1

Table 5 Comparison of measured b-values with some existing formulae for "b". For eq.14, the D_{EQ} and $\beta=0.75$ have been used.

Smith (1991) did stationary flow tests with five samples (four with spheres and one with rock). He found similar results comparing his data with the formulae from Koenders and Engelund. Comparison with his tests showed that the equation by Koenders over-predicts the b-values with an average of about 150% while the equation from Engelund over-predicts the b-values with an average of roughly 300%. For both data-sets, the corresponding expressions for the a-coefficient predicted relatively low a-values. Therefore, it is not unrealistic that the b-values are relatively high.

It can be concluded that the existing formulae over-predict the friction coefficient b. Smith (1991) came to the same conclusion based on his tests. The β coefficient from equation 14, is not constant for all types of stones. However, the coefficient β seems to be near 0.6 in case for D, the D_{n50} is taken and 0.75 in case for D, the D_{EQ} is taken. In case the orientation of the stones is implemented as written in equation 18, the most appropriate β coefficient is near 1.1 with $D=D_{n50}$ or 1.4 with $D=D_{EQ}$. Not enough types of material were tested to improve or extend equation 14 or equation 18 (for stationary flow conditions).

Comparison with other experiments.

At Hydraulic Research, Wallingford material R1, R3 and R4 were also tested with a constant flow, see Williams (1992). However, a real comparison can not be made since the construction of the samples was done differently. In those tests the mean flow was perpendicular to the longest axis of the stones (denoted with b(90°)) while the mean flow was parallel to this axis (denoted with b(0°)) in the present tests. Therefore, it could be expected that the total resistance would be smaller in the

present tests than in the tests at Hydraulic Research, Wallingford. This way the smaller b-values found in the present tests can be explained. In the present tests the relative importance of the laminar term with coefficient "a" is small but larger than in the tests at Hydraulic Research, Wallingford. The relative importance of the term with coefficient "a" may have been so small at the tests at Hydraulic Research, Wallingford that it could be neglected. This indicates that the a-values for which zero was found at the tests at Hydraulic Research, Wallingford are correct and that the a-values, not equal to zero in the present tests, are correct as well. The b-values for R1, R3 and R4 were respectively 27.9, 26.1 and 32.1. So, as expected, these b-values are larger. However, the differences are larger as one would expect.

Burcharth and Christensen (1991) did stationary flow tests as well. Some relevant data are given in Table 6. The stones had aspect ratios between 2.1 and 2.6. Six samples with irregular rock were tested. The α-values show relatively large variations. Comparisons of the α-values for irregular rock with those from samples R1, R5 and R8 show that Burcharth and Christensen (1991) found, in average, higher values. Taking into account the large variations of the α-values, it can be concluded that they are in the same order of magnitude. Unlike the present tests, the underlayer (of the sample) during construction of the sample was not perpendicular to the mean flow direction. Since the aspect ratio was about 2.3 in average, differences were to be expected comparing the b-values with those from the present tests. The values of $\beta(90°)$ found by Burcharth and Christensen (1991) are about three times higher than the values of $\beta(0°)$, found in the present tests. Differences of a factor of about 2.3 were to be expected as a result of a different orientation of the stones. Therefore, it can be concluded that the β-values correspond reasonably well.

STATIONARY FLOW DATA FROM BURCHARTH AND CHRISTENSEN (1991)						
MATERIAL	D_{15}	D_{50}	α-D_{15}	α-D_{50}	β-D_{15}	β-D_{50}
Irregular	0.0066-0.031	0.0094-0.0368	700-9200	1400-13000	1.8-2.5	2.4-3.5
Semi round	0.013	0.0181	1550	3000	1.8	2.45
Very round	0.0323	0.0375	7400	10000	1.9	2.15

Table 6 Data from Burcharth and Christensen. The values of α and β are related to eq.14.

Smith (1991) did stationary flow tests with five samples. Four of them were with spheres. The results are summarized in Table 7. Because the construction of the sample was done in the same way as for the present tests, a clear comparison can be made. The comparison of the values for α shows that they are in the same range except for samples R3 and C75, see Figure 10. The β-values vary in the same range, see Figure 11. It can be concluded that the β-values correspond well.

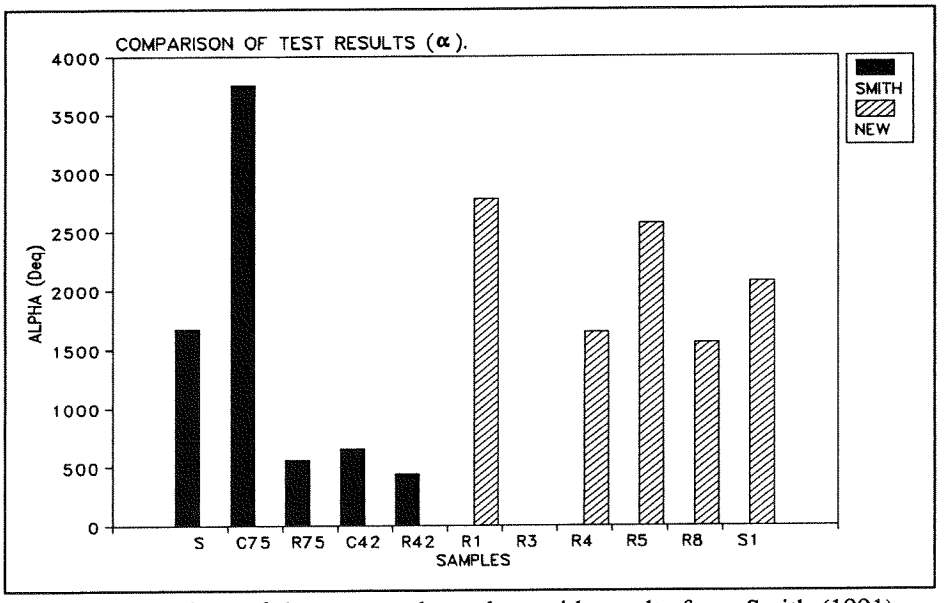

Fig.10 Comparison of the measured α-values with results from Smith (1991).

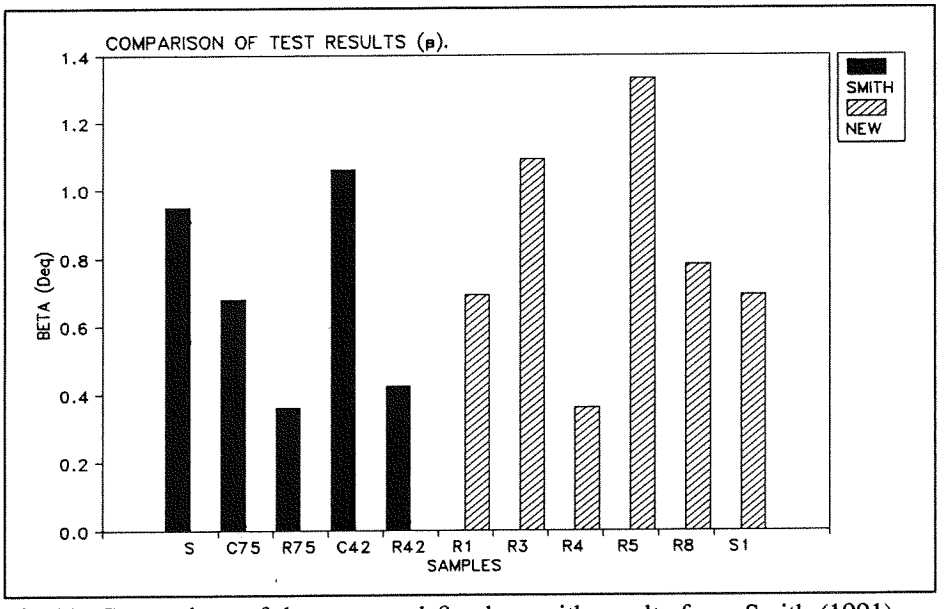

Fig.11 Comparison of the measured β-values with results from Smith (1991).

STATIONARY FLOW DATA FROM SMITH (1991)						
MATERIAL	D_{EQ}	n	a	b	α-D_{EQ}	β-D_{EQ}
Rock (S)	0.100	0.47	0.06	4.94	1673	0.95
Spheres-cubic packing (C75)	0.075	0.51	0.16	3.43	3752	0.68
Spheres-rhombohedral packing (R75)	0.075	0.26	0.41	19.2	559	0.36
Spheres-cubic packing (C42)	0.042	0.52	0.08	8.77	650	1.06
Spheres-rhombohedral packing (R42)	0.042	0.33	0.43	39.6	437	0.424

Table 7 Stationary flow data from Smith (1991). The values of α and β are related to eq.14.

4.3 Conclusions stationary flow tests.

From the stationary flow tests the following can be concluded:

- The coefficients α and β from equation 14 are not the same for all types of stone.
- Comparisons of the results from the stationary flow tests show that the results correspond reasonably well with existing stationary flow tests from Smith (1991) and Burcharth and Christensen (1991). This is not the case for existing formulae. The existing formulae under-predict the a-values while they over-predict the b-values.
- It is proposed to include the influence of the orientation of the stones in the expression for "b" as written in equation 18. As long as no full parameter study has been done, for β (equation 18), the value 1.1 is proposed in case the D_{n50} is taken as a representative stone diameter or 1.4 in case for D the D_{EQ} is taken. For the value of α, the rough estimation of $\alpha=1000$ with $D=D_{n50}$ or $\alpha=1500$ with $D=D_{EQ}$, can be used.
- A full parameter study must be performed to examine the influence of gradation, aspect ratio and shape (gross shape, roughness and surface texture). Those parameters probably contribute to the variation of α and β-values.

Chapter 5

5. Oscillatory flow tests.

5.1 Description of the results.

Determination of the coefficients.

As discussed in section 3.3, the signals derived with relatively low displacements of the piston, gave disturbed signals. Therefore, the coefficients "a", "b" and "c" from the extended Forchheimer equation (equation 15) could not be determined using regression analysis or other advanced techniques. The coefficients were determined with a graphical approach; comparisons were made between the signal from the measured pressure gradient I and the calculated signal using the extended Forchheimer equation. The term $c \cdot \partial u/\partial t$ is supposed to be zero at the peak of the velocity signal ($u = \hat{U}$). Therefore, the term $a \cdot u + b \cdot u \cdot |u|$ could be determined from these maximum velocities. The c-term causes deviations from the sinusoidal signal, especially around the zero-crossings of the velocity signals ($u \ll \hat{U}$).

A problem arose distinguishing the contribution of the term $a \cdot u$ from the contribution of the term $b \cdot u \cdot |u|$. This problem could not be solved without the assumption that the a-coefficient is the same as in the stationary flow tests. The results of the oscillatory tests show that the term $a \cdot u + b \cdot u \cdot |u|$ is larger for oscillatory flow than for stationary flow. The difference is assumed to be caused by a different b-value (turbulence contribution) rather that a different a-value (laminar contribution). From a practical point of view, this assumption is not that important since it does not really matter whether the extra resistance is caused by a larger a-value or a larger b-value (or a combination) as long as this extra resistance can be included in an expression for "a" or "b" accurately. From a theoretical point of view one can expect that an oscillatory movement of the fluid causes extra turbulence rather than extra laminar flow compared with a stationary flow. This indicates that it is more likely that the b-values are larger for oscillatory flow than that the a-values are larger. Therefore, the a-values found from the stationary flow tests were assumed to be the same for the oscillatory flow tests.

The b-values could be determined by comparing the maximum of the measured pressure gradient I with the calculated maximum of the Forchheimer equation

$a \cdot u + b \cdot u \cdot |u|$ where "b" is the unknown value. The c-value could then be determined by choosing a certain c-value and comparing the measured signal (I) with the calculated signal using the extended Forchheimer equation. The c-value was determined by iteration. This will be clarified later in this section. Despite the complicated way to determine the c-values, the accuracy is estimated to be about 10%.

The determination of the c-values for the measurements where the signals were disturbed due to relatively small displacements of the piston (non-sinusoidal signals, see Figure 6), was more complicated. The signals from the measured pressure gradients "I" showed local maxima while the velocity signals, calculated from the piston displacement did not show these disturbed signals. Often it was found that including a c-value for those measurements did not result in a better correspondence between the measured pressure gradient and the extended Forchheimer equation. Therefore, those c-values were set at zero.

Tested conditions.

In section 2.2 the relevance of the present tests has been discussed. The tests were done for relative large Reynolds numbers and for small Keulegan-Carpenter numbers. The ranges of some relevant parameters for the oscillatory flow tests have been listed in Table 8. Note that in the Re-number and the KC-number, the pore velocity is taken as a representative velocity. The Ac-number is introduced. It is a measure for the accelerations in the porous medium.

TESTED RANGES FOR OSCILLATORY TESTS					
MATERIAL	$\hat{U}$	T	Re/1000	KC	Ac*1000
R1	0.13-0.50	2-4	15-66	8-60	7-49
R3	0.12-0.45	2-4	12-46	8-65	7-33
R4	0.12-0.49	2-4	16-58	11-82	7-58
R5	0.05-0.25	2-4	2-10	9-88	3-22
R8	0.09-0.34	2-4	6-25	13-91	7-36
S1	0.07-0.51	2-4	5-38	6-93	7-52

Table 8 Ranges from the oscillatory flow tests. $Re = \hat{U}D_{EQ}/n\nu$; $KC = \hat{U}T/nD_{EQ}$; $Ac = \hat{U}/nTg$.

Results from the oscillatory flow tests.

In Appendix 2, figures with the measured pressured gradient I and the corresponding fit to the extended Forchheimer equation are shown for all measurements. In Appendix 3, tables with the results are given. Figure 12 shows an example for rock sample R5, an oscillation period of 2 seconds and an amplitude of the piston of 4% which corresponds to a maximum velocity $\hat{U}=0.20$ m/s. The value k denotes the resistance factor related to the underflow correction (see section 3.3). The value w=0.95 denotes that the velocities are multiplied with 0.95 to take the wall effects into account (see section 3.3).

The a-coefficient is the same as for the stationary flow tests, the b-coefficient is derived from the peaks of the signal and the c-coefficient is derived by choosing a c-value which gives the best resemblance of the signal near the zero-crossings.

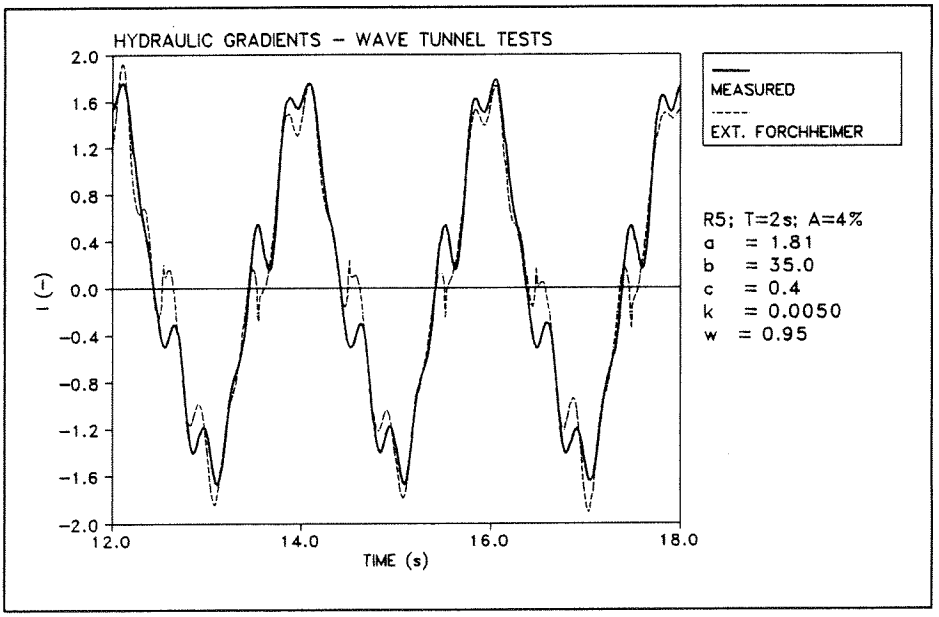

Fig.12 Example of a measured hydraulic gradient (I) and a fit to the extended Forchheimer equation.

Figure 13 shows a single oscillation from a test with rock sample R3. Several time-series, derived with the extended Forchheimer equation, with varying c-values are shown. For c=0.4, the fluctuations near the zero-crossings give the best resemblance with the measured signal. Figure 13 shows that for c=0.6 the

fluctuations are to large while for c=0 and c=0.2 smaller fluctuations appear than those appearing in the measured signal. The c-values have been determined by iteration; for instance series with c=0.2; c=0.5; c=0.35; c=0.40; c=0.42; c=0.38 have been compared (⇒ c=0.40).

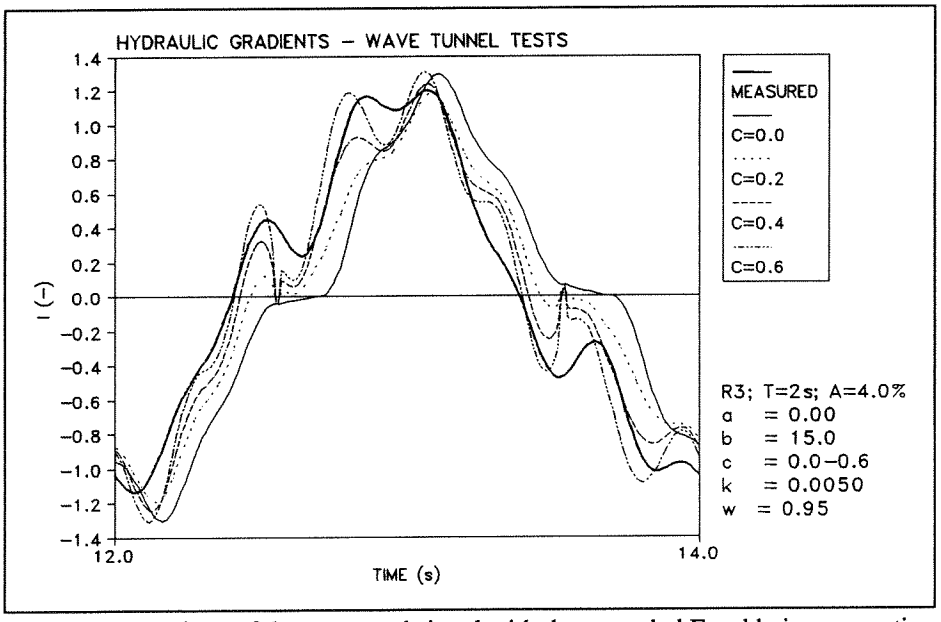

Fig.13 Comparison of the measured signal with the extended Forchheimer equation with various c-values.

RESULTS OSCILLATORY FLOW TESTS							
MATERIAL	b(stat)	b(av)	b(std)	b(range)	c(av)	c(std)	c(range)
R1	6.0	8.5	1.23	7.2-11.5	0.21	0.14	0-0.40
R3	10.7	13.6	2.02	12-17	0.27	0.14	0-0.45
R4	6.0	9.2	0.84	8.1-12	0.30	0.14	0-0.45
R5	32.8	35	5.23	31-50	0.12	0.16	0-0.40
R8	21.7	23	1.80	21-28	0.31	0.14	0-0.45
S1	7.4	9.3	3.34	6-21	0.15	0.13	0-0.3

Table 9 Results from the oscillatory flow tests; b(stat) is the b-coefficient from the stationary flow tests; b(av) is the average b-coefficient from the oscillatory flow tests.

In Table 9, the results from the oscillatory flow tests have been summarized. For a comparison, the b-values from the stationary flow tests have been listed as well. The b-values from the oscillatory flow tests are larger. The b and c-values show large standard deviations (and wide ranges). However, as can be seen in Figure 14, these deviations are not random but rather systematic.

Figure 14 shows that the b-values are larger for the tests with small values of the maximum velocity $\hat{U}$. This trend seems to be stronger for the small oscillation periods (T). The difference between the b-values from the oscillatory flow tests and the stationary flow tests seems to be inversely proportional to $\hat{U}T/D$ which is the Keulegan-Carpenter number. This will be discussed further in Chapter 6. The c-values show a trend as well although this trend is much weaker than for the b-values, see Figure 15. From a theoretical point of view it is remarkable that often the value $c=0$ was found. This will be discussed in Chapter 6 as well.

Relative contributions of the Forchheimer terms.

In Figure 16, the contributions of the a, b and c-terms to the complete signal (extended Forchheimer) are shown. This is the same time-series as shown Figure 12. The figure shows that the contribution of the c-term is rather limited. Even for a test with a relatively large c-value ($c=0.4$), the contribution of the c-term is only of relative importance in a small part of the oscillation period (near the zero-crossings).

For each sample the contributions of the three terms from the extended Forchheimer equation are calculated with respect to the maximum hydraulic gradient (I_{MAX}). See Table 10 and Figure 17. The ratio $a\cdot\hat{U}/I_{MAX}$ varied between 0 and 0.41. The term with coefficient "b" is the largest for all samples; $b\cdot\hat{U}\cdot|\hat{U}|/I_{MAX}$ varied between 0.59 and 1.00. The contribution of the term with coefficient "c" reached its maximum just after the zero-crossings. At that point, the ratio $(c\cdot\partial u/\partial t)_{MAX}/I_{MAX}$ reached its maximum contribution of 40% of I_{MAX} for some tests with sample R1. It may look as if the contribution of the a-term is in the same order of magnitude as the contribution of the c-term. However, the contribution of the c-term lasts relatively short.

As one can see in Table 9 or Figure 14, the values of "b" are larger than the b-values from the stationary flow tests. Figures 14 and 17 show that the magnitude of this extra contribution to the b-term can not be neglected. The magnitude of this extra contribution is often larger than the contributions of the a-term or the c-term.

Fig.14 B-VALUES OSCILLATORY FLOW TEST - THE LABELS DENOTE Û IN CM/S.

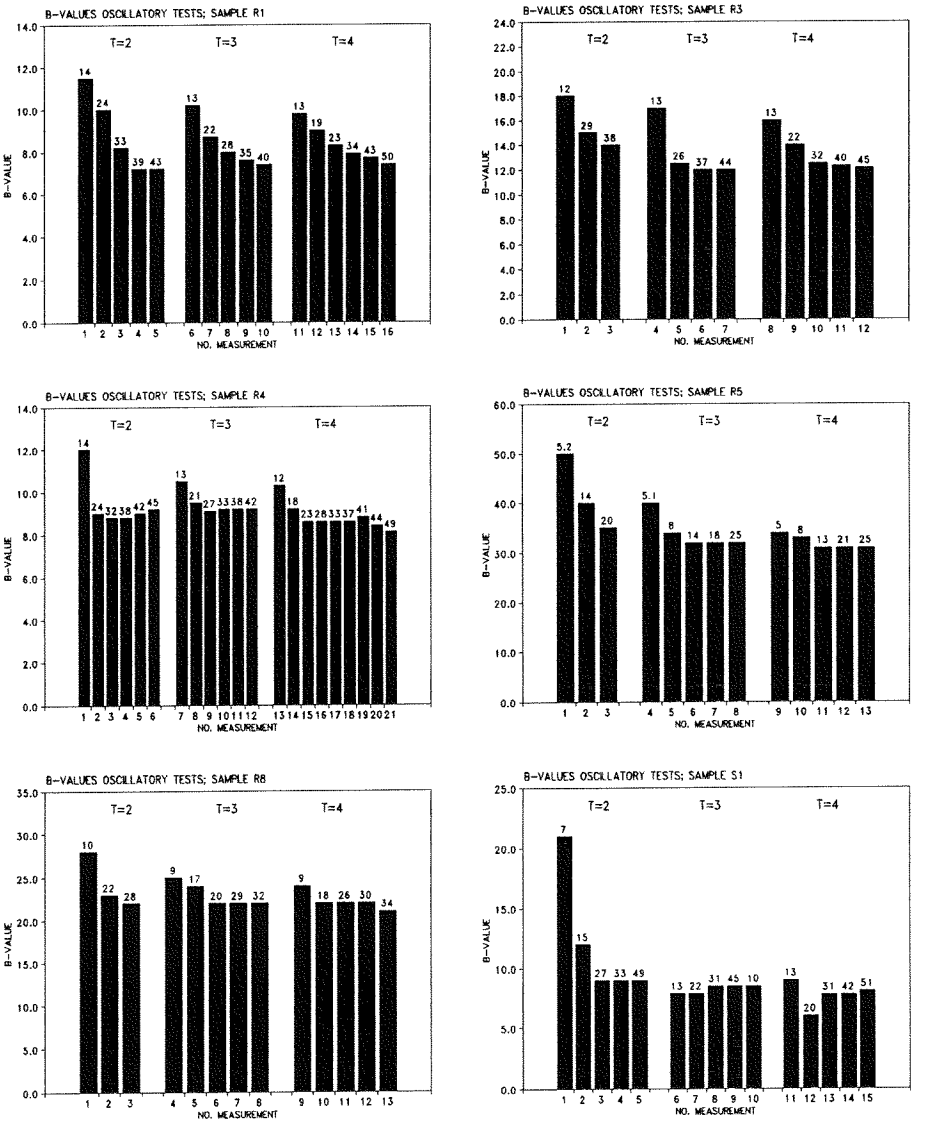

Fig.15 C-VALUES OSCILLATORY FLOW TEST - THE LABELS DENOTE Û IN CM/S.

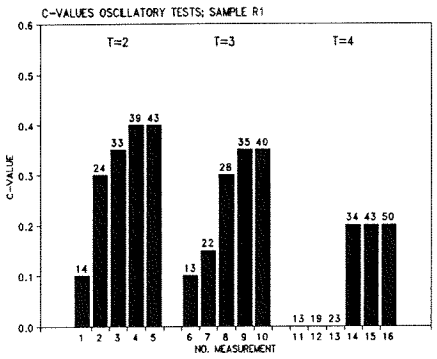

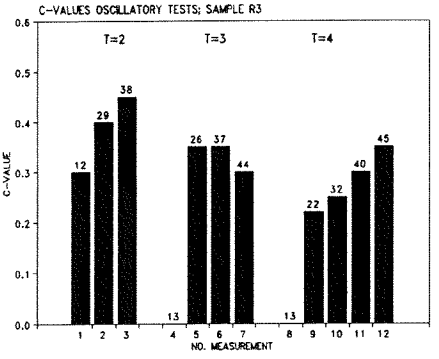

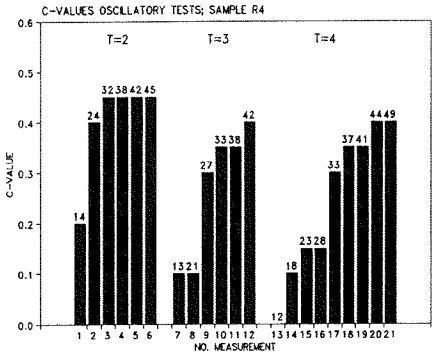

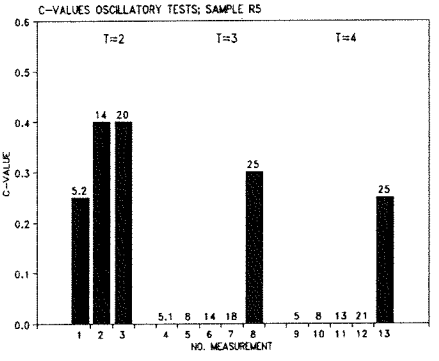

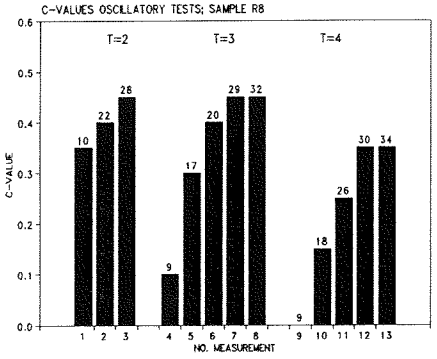

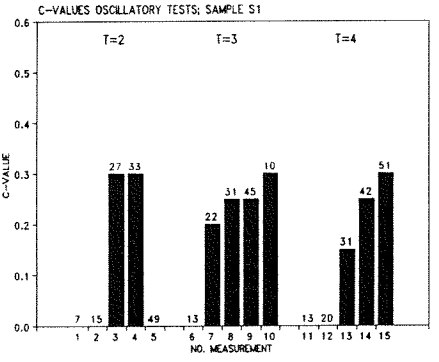

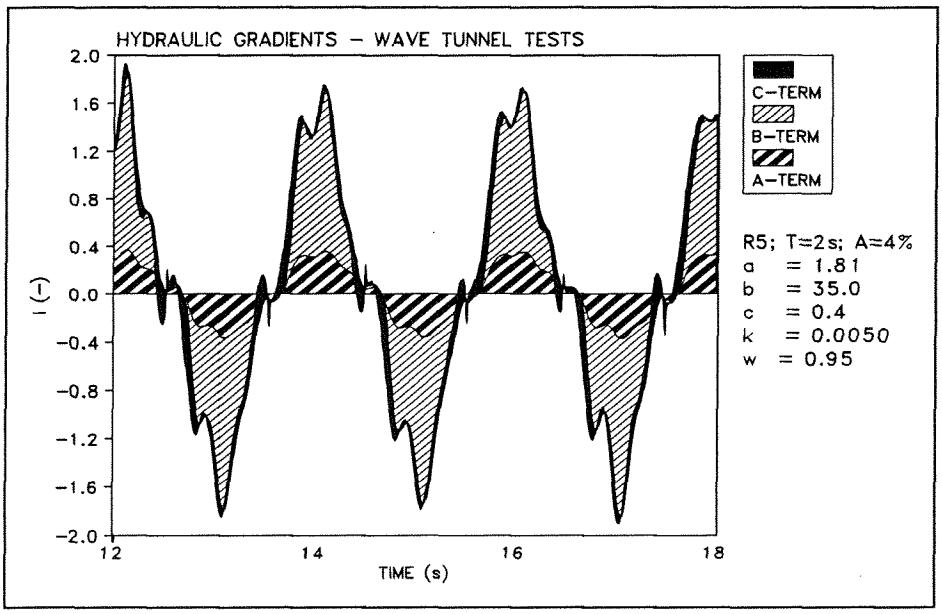

Fig.16 Contributions of the a, b and c-terms to the complete signal.

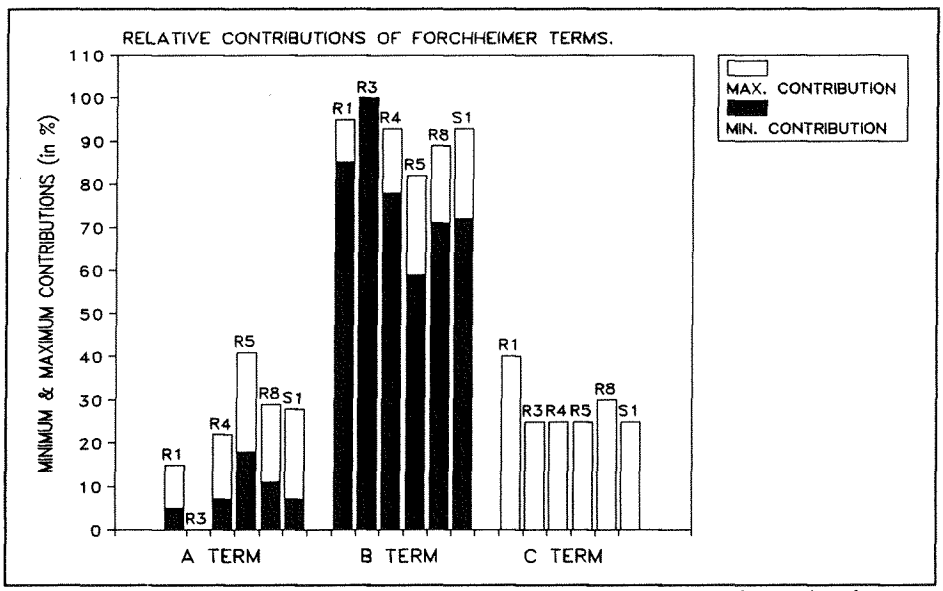

Fig.17 Relative contributions of the Forchheimer terms $a\cdot\hat{U}$, $b\cdot\hat{U}\cdot|\hat{U}|$ and $(c\cdot\partial u/\partial t)_{MAX}$, with respect to the maximum hydraulic gradient (I_{MAX}).

RELATIVE CONTRIBUTIONS OF THE a, b AND c TERMS FROM THE EXTENDED FORCHHEIMER EQUATION IN % OF I_{MAX}.			
MATERIAL	$a \cdot \hat{U}$	$b \cdot \hat{U} \cdot \lvert\hat{U}\rvert$	$(c \cdot \partial u/\partial t)_{MAX}$
R1	5-15	85-95	0-40
R3	0	100	0-25
R4	7-22	78-93	0-25
R5	18-41	59-82	0-25
R8	11-29	71-89	0-30
S1	7-28	72-93	0-25

Table 10 Contributions of the a, b and c term in % of the maximum hydraulic gradient I_{MAX}.

5.2 Comparison with other tests.

The present results have been compared with data from Smith (1991). Smith did experiments in an oscillating water tunnel through different arrangements of packing of spheres. Two sizes of spheres and two arrangements of the packing were tested with different amplitudes of the velocity and different oscillation periods. The tests were done with slightly smaller Re-numbers and larger KC-numbers. No tests were done in the range were in the present tests disturbed signals occurred due to relatively small displacements of the piston.

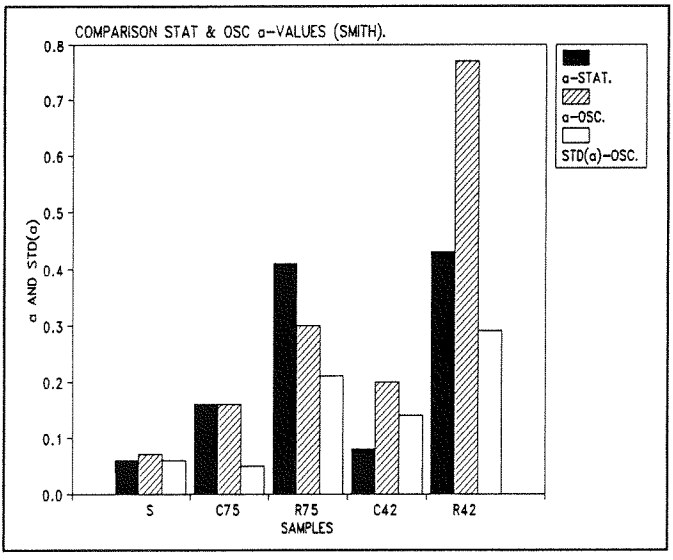

Fig.18 Comparison of a-values from stationary and oscillatory flow tests by Smith (1991).

Unlike the present tests, a-values could be determined from the oscillatory flow tests, see Figure 18. However, taking the relatively large standard deviations into account, it is not unlikely that the a-values are the same for the stationary flow tests as for the oscillatory flow tests (compare Table 7 and Table 11).

No systematic differences between the stationary b-values and the oscillatory flow b-values were found. The differences in the present tests were relatively large for the smallest KC-numbers. Since the tests from Smith (1991) were done with larger KC-numbers it is not strange that no dependency on the KC-number was found. In the present tests this dependency is relatively weak for the very round stones and the spheres. Since four of the five samples from Smith contained spheres, this may indicate that the dependency is weaker for spheres.

The c-values found by Smith (1991) are in the same order of magnitude as the values derived from the present tests. No systematic trend was found.

OSCILLATORY FLOW DATA FROM SMITH (1991)						
MATERIAL	a	std a	b	std b	c	std c
Rock (S)	0.07	0.06	4.7	0.40	0.32	0.04
Spheres-cubic packing (C75)	0.16	0.05	4.2	0.51	0.23	0.05
Spheres-rhombohedral packing (R75)	0.30	0.21	20	7.4	0.37	0.12
Spheres-cubic packing (C42)	0.20	0.14	9.3	2.8	0.24	0.07
Spheres-rhombohedral packing (R42)	0.77	0.29	42	4.2	0.65	0.28

Table 11 Oscillatory flow data from Smith (1991).

5.3 Conclusions oscillatory flow tests.

From the oscillatory flow tests the following can be concluded:

- With the assumption that the a-values for the oscillatory flow tests are the same as for the stationary flow tests, the b-values could be determined rather accurately. To determine the c-values was more difficult.
- The coefficients "b" (see equation 15) derived from the oscillatory flow tests are significantly larger than those derived from the stationary flow tests.
- The differences between the b-values found from the oscillatory flow tests and the stationary flow tests seem to be inversely proportional to the Keulegan-Carpenter number.

- The coefficients "c" seem to increase with increasing peak velocities ($\hat{U}$) and decreasing with increasing oscillation periods (T).
- In the present tests the b-term from the extended Forchheimer equation was dominating. The contribution of the c-term was rather limited.

Chapter 6

6. Formulae for non-stationary porous flow.

6.1 Implementation of unsteadiness in the b-term.

A large number of equations for stationary porous flow exist. They predict the Forchheimer friction coefficients "a" and "b" for stationary flow. For non-stationary porous flow such equations are not available. The present measurements showed that the friction increased for non-stationary porous flow. This can be implemented in the expression for the b-coefficient. This will be described in this chapter. Non-stationary flow causes also a time-depending flow resistance. This is implemented with a coefficient "c". This will be discussed in this chapter as well. The discussion in this chapter is concentrated on rock material.

An expression for the coefficient "b" is written in equation 14. This expression has been theoretically derived. The coefficient β in this expression for "b", must be determined using measurements. The influence of the oscillatory flow can be implemented in the expression for β. How this has been done will be explained now.

The coefficient β can be split into a stationary part and an extra contribution caused by non-stationary flow. This can be expressed by $\beta=\beta_c+\beta'$ where β_c is the stationary part and β' takes the extra resistance into account. This extra term can be explained as follows. The boundary layers and possibly small eddies, will be destroyed in case the flow direction changes. This destruction of the boundary layers requires and extra amount of momentum. The destruction of these boundary layers will be larger in case the inertia term, relative to the turbulence term, is larger. This is inversely proportional to the KC-number since the KC-number can be seen as the ratio of the influence of the turbulent term and the influence of inertia. See also the discussion in section 2.2. Boundary layers are not developed instantaneously. This causes a kind of history effect in the friction term; the friction at a certain point of time is not directly dependent on the (average) velocity at that point of time. A characteristic velocity of the flow field can therefore be more useful than the momentary velocity. This can be implemented by taking $\hat{U}$ for the velocity scale in the KC-number.

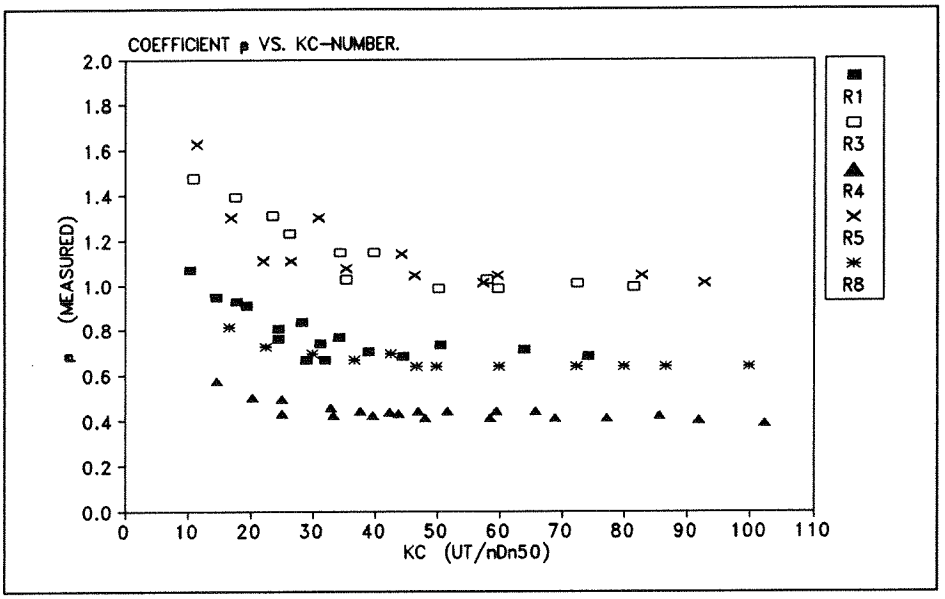

Fig.19 Coefficient β as a function of the KC-number (with D_{n50}).

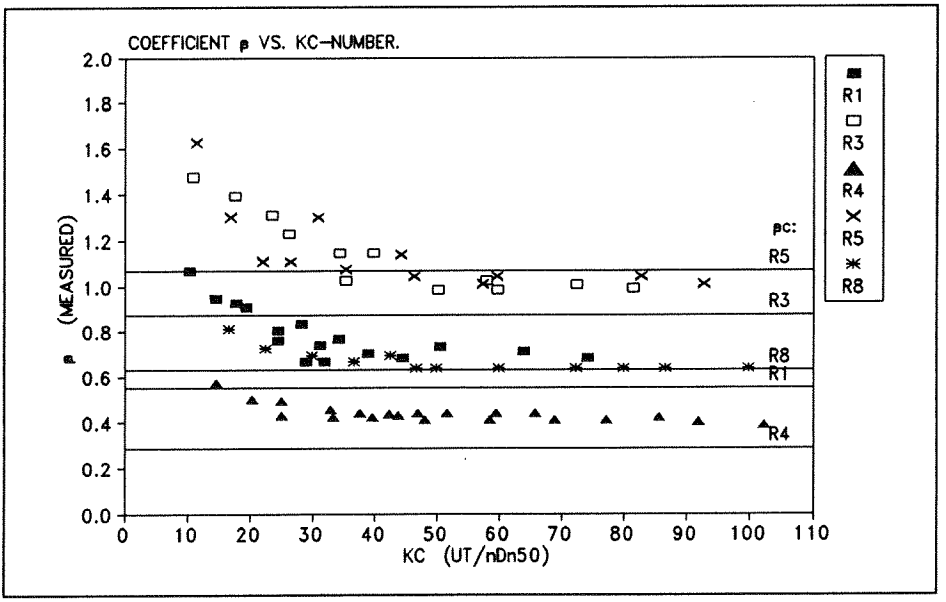

Fig.20 Coefficient β (and β_c) as a function of the KC-number (with D_{n50}).

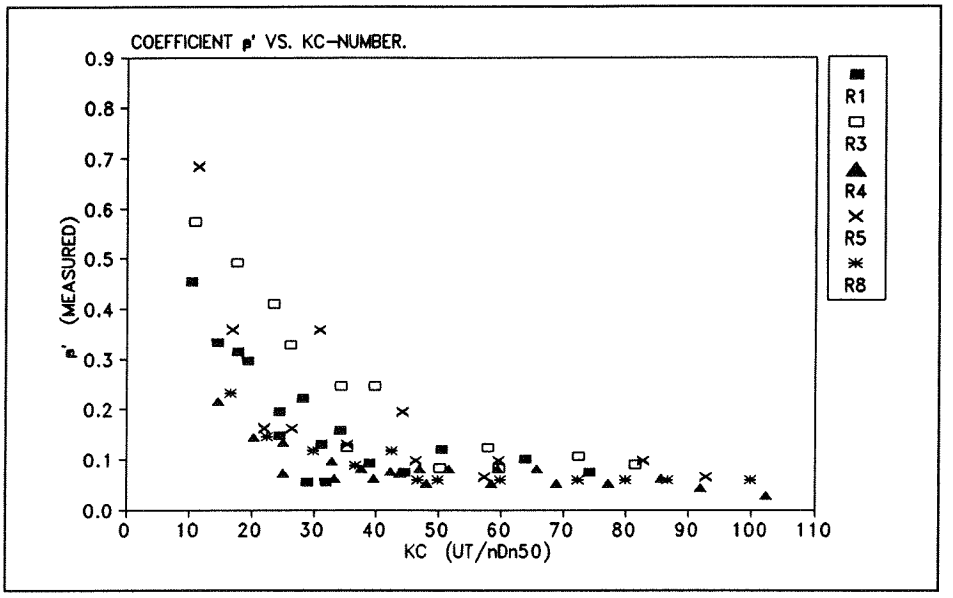

Fig.21 The coefficient β' (extra resistance) as a function of the KC-number.

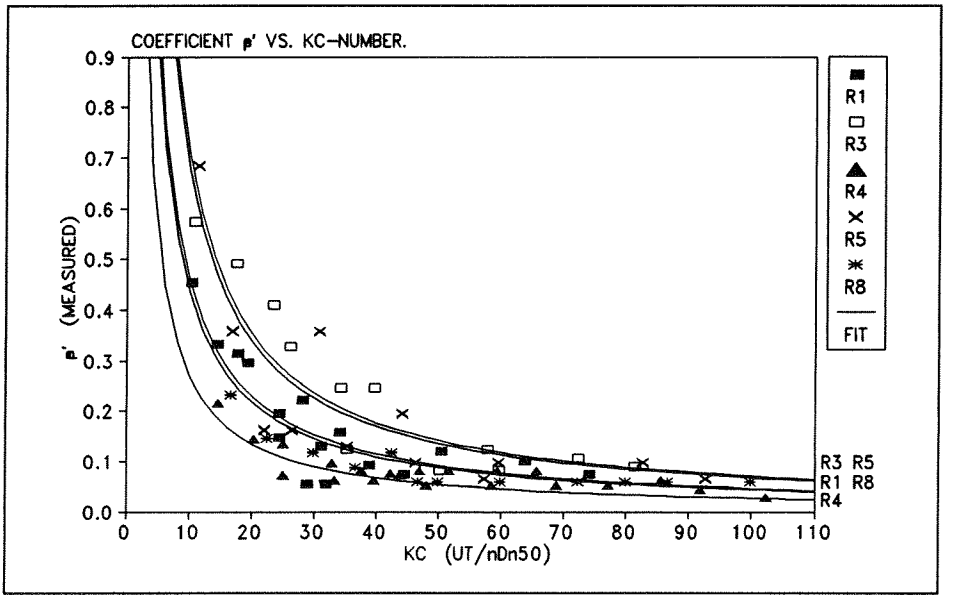

Fig.22 The coefficient β' (extra resistance) as a function of the KC-number (with fit).

Figure 19 shows the β-values ($\beta=\beta_c+\beta'$) from the oscillatory flow tests as a function of the KC-number. For the tests with the relatively low KC-values, the β-values are larger. For the relatively high KC-values, the β-values seem to become less dependent on the KC-number. Stationary flow corresponds to an infinite value of the KC-number ($T=\infty$). Therefore, it would be most likely, from a theoretical point of view, that the β-values approach the β-values from stationary flow (β_c). Figure 20 shows the values of β_c as well. However, these values, derived from the stationary flow tests, as well as the measured β-values from theoscillatory flow tests, both contain inaccuracies. Figure 20 shows that not all β_c-values correspond to the limiting-values that seems to be present for the oscillatory flow measurements. However, the above mentioned theoretical explanation justifies the assumption that these limiting-values and the measured β_c-values are the same. In Figure 21, those limiting-values have been extracted from the measured β-values, resulting in the a plot of β' versus the KC-number.

Since the extra resistance that is present under oscillatory flow conditions is relatively large, especially for the relatively low KC-values, it can not be neglected. Therefore, it is proposed to implement this extra resistance in the expression for β.

As the previous figures show, the values are depending on the value of the KC-number. The value of β decreases with higher KC-values. An expression, inversely proportional with the KC-number is proposed. The preceding theoretical consideration clarified this. The KC-number can also be included to a certain power. The measurements are not accurate enough to determine this power. However, as will be shown, the power one gives satisfactory results. The Figures 19 and 20 show that the increase in β-values at low KC-numbers is larger for the samples where the β_c is relatively large. This indicates that the extra resistance is proportional to the resistance that is already present in the porous medium under stationary flow conditions. This shows that it is reasonable that the β' can be dependent on the value β_c. Again, this dependency could be present in the expression with a certain power. However, the power one gives satisfactory results. The expression becomes $\beta'=c_\beta\ \beta_c\ /\ KC$. The value of c_β is determined with regression analysis. This value is 7.5 in case for the characteristic stone diameter D_{n50} is taken and 5.9 in case the D_{EQ} is used. In Figure 22, the β' and the expression for this coefficient ($\beta'=7.5\beta_c/KC$) are shown. Since each sample has different values for β_c, n and D_{n50}, for each sample a different curve is valid.

The total expression for β becomes: $\beta=\beta_c(1+7.5/KC)$ in case for D, the D_{n50} is used. This results in the following expression for b:

$$b = \beta_c \left(1 + \frac{7.5}{KC}\right) \frac{1-n}{n^3} \frac{1}{g\, D_{n50}} \qquad \text{with} \quad KC = \frac{\hat{U}T}{nD_{n50}} \tag{19}$$

where β_c is a coefficient to be found from stationary flow tests. This coefficient may be dependent on the grading, the aspect ratio and the shape of the tested material.

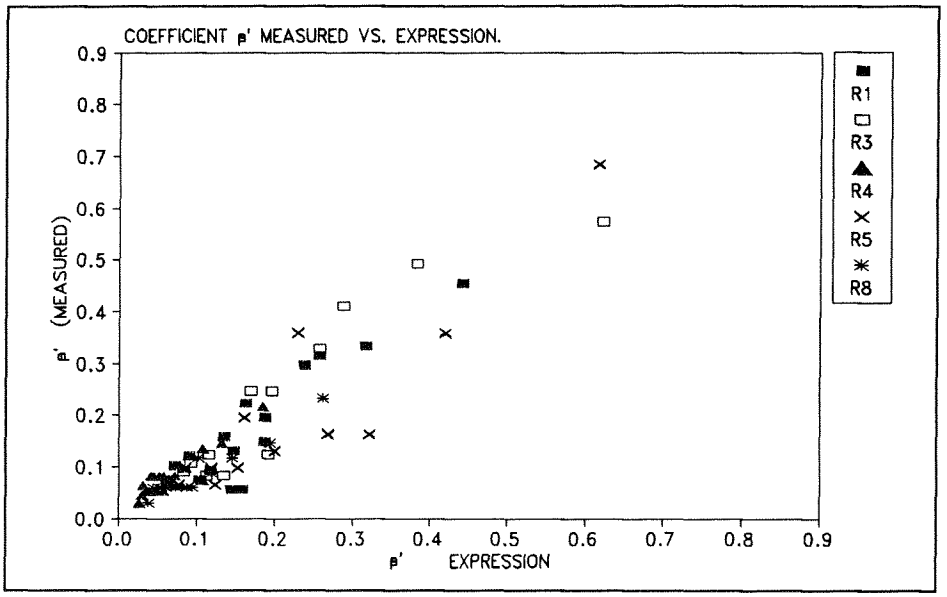

Fig.23 Measured β' versus the expression for β'. The coefficient β' is a measure for the extra resistance due to unsteadiness.

Equation 19 shows that the flow resistance is depending on the flow field; the KC-number contains $\hat{U}$ and T. Figure 23 shows that the coefficient 7.5 is rather accurate; the standard deviation of the differences between measured β' and the value given by the expression is 0.05. However, uncertainties enter the equation since β_c is depending on parameters as grading, aspect ratio and shape. This dependency is not clearly described yet since no full parameter study has been performed. This parameter study can better be done under stationary flow conditions.

6.2 Expression for the c-term.

The c-coefficient is increasing with a larger amplitude of the velocity, $\hat{U}$, and decreasing with a larger oscillation period, T. This can be seen as a dependency on the acceleration field. It is proposed to implement this with the acceleration number, Ac ($\hat{U}$/nTg). The theoretical derived expression, equation 16, contains a parameter, γ, that can be dependent on several parameters, for instance on the Ac-number. The c-coefficients have been plotted versus the Ac-number in Figure 24. The measurements with samples R5 and S1 have been excluded from the analysis because only for a relative small number of tests with those samples, c-values could be determined (see Figure 15). Figure 24 shows that the c-coefficient is dependent on the Ac-number. Since the porosity is present in the equation for "c", the curves are different for each sample (the porosity has been varied).

The measured points in Figure 24 suggest that there is a limiting-value for the c-coefficient, which is being approached for the higher acceleration numbers. The limiting-value of γ (equation 16), denoted as c_L, is being approached for the higher Ac-values (largest accelerations). This can be expressed as $\gamma = c_L - c_\gamma/Ac$. The influence of Ac can also be present in an expression with a power different from one. However, the measurements were not accurate enough to determine this power exactly. Since the power one gives satisfactory results, this value has been used. For the values for c_L and c_γ, respectively 0.85 and 0.015 were found using regression analysis. The influence of the c-term became smaller for the lowest values of the Ac-number. From a theoretical point of view this seems reasonable since this term is zero under stationary flow conditions.

The following expression for "c" results in a satisfactory correspondence with the measured c-values:

$$c = \frac{1 + \frac{1-n}{n}\left(0.85 - \frac{0.015}{Ac}\right)}{ng} \qquad \text{for} \quad Ac > \frac{0.015}{\frac{n}{1-n} + 0.85} \tag{20}$$

In Figure 24, the curves for two samples, R1 and R8, have been plotted as well. The curves for samples R3 and R4 are between those two. The curves seem to be rather close to the corresponding measured points for the higher c-values. The correspondence between the lower c-values is weaker. The relatively low accuracy of the tests with low c-values and the steep inclination of the curves, may be causes for the weaker correspondence in this area. The coefficients in the expression seem to be independent on parameters of the tested material. Since no negative values for

"c" were found, the expression is only valid for positive c-values (no extrapolation of the curves to lower c-values).

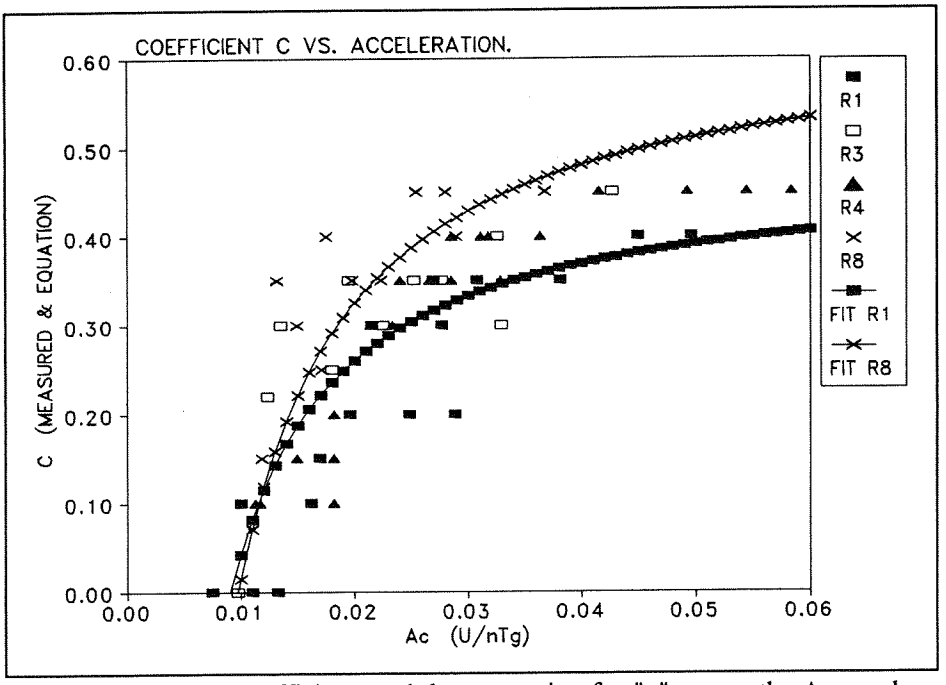

Fig.24 Measured c-coefficients and the expression for "c" versus the Ac-number.

The expression for "c" contains a part representing the momentum needed to accelerate the total amount of fluid present in the porous medium, 1/ng in equation 16, and an extra amount of momentum needed which is known as the added mass term $((1-n)/n\cdot\gamma)/ng$. The c-values became zero for some tests. This may indicate that the added mass term can become negative. A negative value of the added mass term means that a smaller amount of momentum is needed to accelerate the fluid than the amount necessary to accelerate the fluid without porous medium. This may be caused by parts of the water volume in the porous medium that do not flow ("dead parts"). This seems to be the case for $Ac < 0.018$ (very small accelerations).

Chapter 7

7. Summary and conclusions.

Measurements in a U-tube tunnel were carried out to study flow through coarse granular material. Tests with stationary flow and tests with oscillatory flow were done to study the differences between both. Five samples with rocks and one with spheres have been tested. Parameters such as porosity, size, grading and shape, have been varied. Measures to reduce wall effects have been taken. The oscillatory flow tests were done with sinusoidal signals. Problems occurred for very small piston displacements.

The equation which is supposed to describe porous flow is the extended Forchheimer equation (equation 15). The coefficients (a, b and c) from this equation were determined. With the assumption that the a-values for oscillatory flow are the same as for stationary flow, the b-values could be determined rather accurately. To determine the c-values was more difficult. The coefficients (a, b and c) contain many parameters. Theory provides expressions for "a", "b" and "c" (equations 14 and 16). However, these equations contain coefficients (α, β and γ) which are still depending on several parameters.

The differences between the b-values found for stationary flow and for oscillatory flow have been studied. The tested samples gave more resistance (larger b-values) in case of oscillatory flow than in case of stationary flow. This extra resistance can be included in the expression for "b" as written in equation 19. This extra resistance is inversely proportional to the Keulegan-Carpenter number ($KC = \hat{U}T/nD$). This means that resistance is depending on the flow field since the KC-number represents a certain flow field. This has consequences for numerical modelling of porous flow. The resistance is depending on the flow field ($b = f(\hat{U}T/nD)$) and the flow field is depending on the resistance. Therefore, a certain adjustment time (for regular waves) will be necessary to reach a periodical signal (resistance and flow field in harmony).

The coefficient β_c is the coefficient in the expression for the (quadratic) stationary flow resistance (also present in non-stationary flow). This coefficient is supposed to be depending on parameters such as grading, the aspect ratio and shape (gross shape, roughness and surface texture). This dependency must be determined from measurements. Such a parameter-study can be done under stationary flow

conditions. It is proposed to take the influence of the orientation of the stones into account as written in equation 18. This expression must be verified with tests where samples with rock material are constructed differently. As long as no full parameter-study has been done, for β_c the value 1.4 is proposed while the orientation of the stones can be included as written in equation 18.

The coefficient "c" from the extended Forchheimer equation has been determined. This coefficient seems to be depending on the acceleration parameter $Ac=\hat{U}/nTg$. This means that this coefficient is depending on the local flow field as well. The theoretically derived expression for the coefficient "c" (equation 16) has been improved by implementing an empirical expression for γ (see equation 20).

The expressions for the coefficients from the Forchheimer equation, as a result of the present analysis of non-stationary tests, are summarized in equation 21.

$$I = a\,u + b\,u\,|u| + c\frac{\partial u}{\partial t} \quad \text{with}$$

$$a = \alpha\,\frac{(1-n)^2}{n^3}\,\frac{\nu}{g D_{n50}^2}$$

$$b = \beta_c\,(1+\frac{7.5}{KC})\,\frac{1-n}{n^3}\,\frac{1}{g\,D_{n50}} \quad \text{where } KC = \frac{\hat{U}T}{nD_{n50}} \tag{21}$$

$$c = \frac{1 + \frac{1-n}{n}\left(0.85 - \frac{0.015}{Ac}\right)}{ng} \quad \text{with } Ac = \frac{\hat{U}}{ngT} > \frac{0.015}{\frac{n}{1-n} + 0.85}$$

where α, β_c = f(grading, aspect ratio, shape, orientation). From the theoretical consideration as described in section 4.2 it can be concluded that the orientation of the stones can be included in the expression for β_c by $\beta_c=\beta_o(l/t)^{0.5\cdot\tan(\psi-45°)}$ where l/t is the aspect ratio and ψ the (absolute) angle between the mean flow direction and the longest axis of the stones (supposed to be perpendicular to the gravitational acceleration during construction of the sample). However, this expression must be verified with measurements (stationary flow) because the angle ψ has not been varied in the present tests. As long as no full parameter study has been performed, the α and β_o can be approximated with respectively 1000 and 1.1 in case the D_{n50} is used as the characteristic stone diameter. In case the D_{EQ} is taken as the characteristic stone diameter, these coefficients become 1500 and 1.4 while the coefficient 7.5 in the expression for "b" must be replaced by 5.9.

Comparisons of the results from the stationary flow tests with existing stationary flow tests from Burcharth and Christensen (1991) and Smith (1991) show that the results correspond reasonably well. This is not the case for existing formulae (for stationary flow). Comparison with oscillatory flow tests with spheres by Smith (1991) showed that the values found for "c" are in the same order of magnitude. Since those tests were done under slightly different flow conditions (and with spheres in stead of rock material), no clear dependencies of the coefficients on the Keulegan-Carpenter number and the Acceleration-number could be found.

In the present tests, the b-term from the extended Forchheimer equation was dominating. The contribution of the c-term was rather limited.

Further research must provide the dependency of the b-coefficient on grading, aspect ratio, shape (gross shape, roughness and surface texture) and the orientation of the stones with regard to the mean flow direction. These tests can be done under stationary flow conditions. This means that, for the practical purposes for which the accuracy of the present tests is satisfactory, further oscillatory flow tests are not required.

Acknowledgements

The financial support by the Commission of the European Communities by way of the MAST G6-Coastal Structures project (contract 0032-C) and by Rijkswaterstaat, the Dutch Governmental Water Control and Public Works Department, is gratefully acknowledged. I would like to express my appreciation to the participants in the MAST-G6S project, in particular to Dr. J.W. van der Meer and G.M. Smith from Delft Hydraulics and Dr. H. den Adel from Delft Geotechnics for their valuable comments and critical reading.

References

Adel, H. den (1987), *Re-analysis of permeability measurements using Forchheimer's equation*, Report C0-272550/56, Delft Geotechnics (in Dutch).

Adel, H. den (1991), *Inventory of existing knowledge on permeability formulae*, Delft Geotechnics, MAST-G6S report, Project 1.

Andersen, O.H., M.R.A. van Gent, J.W. van der Meer, H.F. Burcharth and H. den Adel (1993), *Non-steady oscillatory flow in coarse granular materials*, Proc. MAST-G6S workshop-Lisbon, Project 1.

Bradbury, A.P., N.W.H. Allshop, J-P. Latham, M. Mannion and A.B. Poole (1988), *Rock armour for rubble mound breakwaters, sea walls and revetments: Recent progress*, H.R.-Wallingford, Report SR 150.

Burcharth, H.F. and C. Christensen (1991), *On stationary and non-stationary porous flow in coarse granular materials*, Aalborg University, Department of Civil Engineering, MAST- G6S report, Project 1.

Engelund, F. (1953), *On the laminar and turbulent flow of ground water through homogeneous sand*, Trans. Danish academy of Technical sciences, Vol. 3.

Ergun, S. (1952), *Fluid flow through packed columns*, Chem. Engrg. Progress, Vol. 48, No. 2, pp.89-94.

Gent, M.R.A. van (1991), *Formulae to describe porous flow*, Communications on Hydraulic and Geotechnical Engineering, ISSN 0169-6548 No.92-2, Delft University of Technology and MAST-G6S report, project 1.

Gu, Z. and H. Wang (1991), *Gravity waves over porous bottoms*, Coastal Engrg. 15 (1991) pp.695-524, Elsevier Science Publ. B.V., Amsterdam.

Hannoura, A.A. and F.B.J. Barends (1981), *Non-Darcy flow: A state of the art*, Proc. EuroMech 143, pp.37-51, Delft.

Koenders, M.A. (1985), *Hydraulic criteria for filters*, Estuary physics, Kew, Unnumbered report.

Ouméraci, H. (1991), *Wave-induced pore pressure in rubble mound breakwaters*, Franzius Institute, MAST-G6S report, Project 1.

Polubarinova Kochina, P.Ya. (1962), *Theory of groundwater movement*, Princeton University Press, Princeton.

Ribberink, J.S. (1989), *The large oscillating water tunnel*, Delft Hydraulics, Report H840.

Shih, R.W.K. (1990), *Permeability characteristics of rubble material, new formulae*, Proc. ICCE 1990 Delft, Vol.2, pp.1499-1512.

Smith, G. (1991), *Comparison of stationary and oscillatory flow through porous media*, M.Sc.-thesis, Queen's University, Canada.

Williams, A.F. (1992), *Permeability of rubble mound material*, MAST-G6S report (draft), Project 1.

List of symbols

a	:	dimensional coefficient in Forchheimer equation, eq.1 (s/m).
A	:	amplitude of the displacement of the piston from the wave tunnel.
Ac	:	non-dimensional number for acceleration, for a porous medium: $Ac=\hat{U}/(nTg)$.
b	:	dimensional coefficient in Forchheimer equation, eq.1 (s^2/m^2).
c	:	dimensional coefficient in ext. Forchheimer equation, eq.15 (s/m).
D	:	particle size.
D_{EQ}	:	equivalent sphere diameter defined as the $D_{EQ}=(6M_{50}/\pi\rho_a)^{1/3}$
D_{n15}	:	diameter (based on weight) of a stone sample, exceeded by 85% of the material.
D_{n50}	:	diameter (based on weight) of a stone sample, exceeded by 50% of the material.
D_{n85}	:	diameter (based on weight) of a stone sample, exceeded by 15% of the material.
f_I	:	resistance force caused by inertia.
f_L	:	resistance force caused by the laminar contribution.
f_T	:	resistance force caused by the turbulent contribution.
g	:	gravitational acceleration.
I	:	hydraulic gradient.
k	:	resistance factor for discharge that does not flow through the tested sample.
KC	:	Keulegan-Carpenter number, for a porous medium: $KC=\hat{U}T/(nD)$.
l	:	length of the longest axis of a particle.
l/t	:	aspect ratio.
M_{50}	:	average mass of a rock grading, determined by the 50% value on the mass distribution curve.
n	:	porosity.
Re	:	Reynolds number, for a porous medium: $\hat{U}D/(n\nu)$.
t	:	length of the smallest axis perpendicular to the longest axis of a particle.
T	:	oscillation period.
u	:	bulk/filter velocity.
$\hat{U}$	:	amplitude of the velocity.
w	:	coefficient to take wall effects into account (w=1 corresponds to no wall effects).

α : coefficient in the expression for "a", eq.14.

α-D_{EQ}: value of α from eq.14 with D_{EQ} as a representative stone diameter.

α-D_{n15}: value of α from eq.14 with D_{n15} as a representative stone diameter.

α-D_{n50}: value of α from eq.14 with D_{n50} as a representative stone diameter.

β : coefficient in the expression for "b", eq.14.

β_c : coefficient in the expression for "b", eq.19 (found from stationary flow tests).

β' : coefficient taking the extra resistance, caused by non-stationary motion, into account.

β-D_{EQ} : value of β from eq.14 with D_{EQ} as a representative stone diameter.

β-D_{n15}: value of β from eq.14 with D_{n15} as a representative stone diameter.

β-D_{n50}: value of β from eq.14 with D_{n50} as a representative stone diameter.

γ : coefficient in the expression for "c", eq.16.

ρ_a : density of the tested material.

ψ : the (absolute) angle between the mean flow direction and the longest axis of the stones. The longest axis of the stones is supposed to be perpendicular to the gravitational acceleration during construction of the sample.

ν : kinematic viscosity.

APPENDIX 0

DESCRIPTION OF TESTED MATERIAL

DESCRIPTION OF TESTED MATERIAL

Test material R1, R3 and R4 was sent by Hydraulic Research, Wallingford. Test material R3 was rounded by abrasion of material R1 to achieve a 5 to 10% weight loss. R4 was rounded by abrasion of material R1 to achieve a 20 to 25% weight loss. A full description is given by Bradbury et al. (1988) and Williams (1992). Material R8 was used as core-material in tests performed at Hannover, see Ouméraci (1991).

DESCRIPTION OF TEST MATERIAL							
CODE	MATERIAL	D_{EQ}	D_{n50}	D_{n15}	D_{n85}/D_{n15}	l/t	n
R1	Irregular rock	0.0760	0.0610	0.0525	1.27	1.9	0.442
R3	Semi round rock	0.0607	0.0487	0.0419	1.27	2.0	0.454
R4	Very round rock	0.0606	0.0488	0.0425	1.26	2.2	0.393
R5	Irregular rock	0.0251	0.0202	0.0170	1.03	2.3	0.449
R8	Irregular rock	0.0385	0.0310	0.0230	1.74	2.0	0.388
S1	Spheres-cubic packing	0.0460	0.0460	0.0460	1.0	1.0	0.476

Table A0-1 Properties of test material.

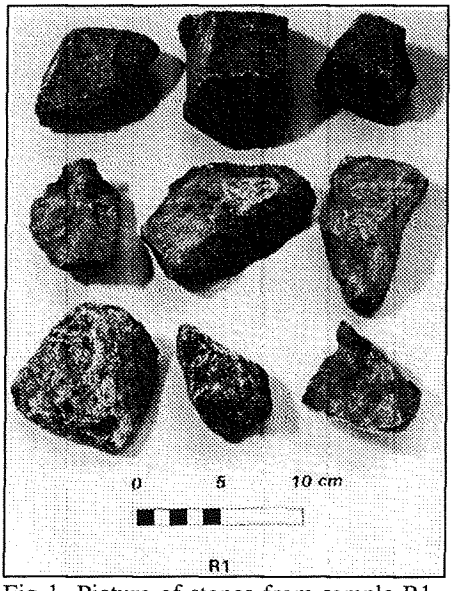

Fig.1 Picture of stones from sample R1.

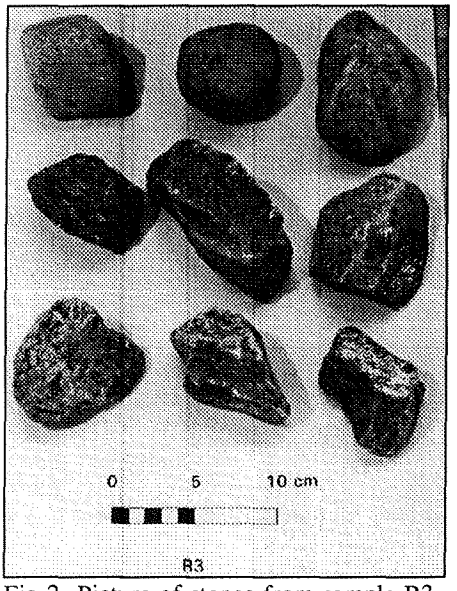

Fig.2 Picture of stones from sample R3.

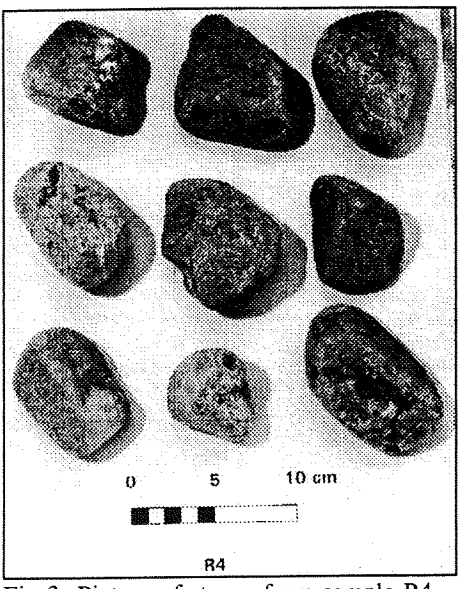

Fig.3 Picture of stones from sample R4.

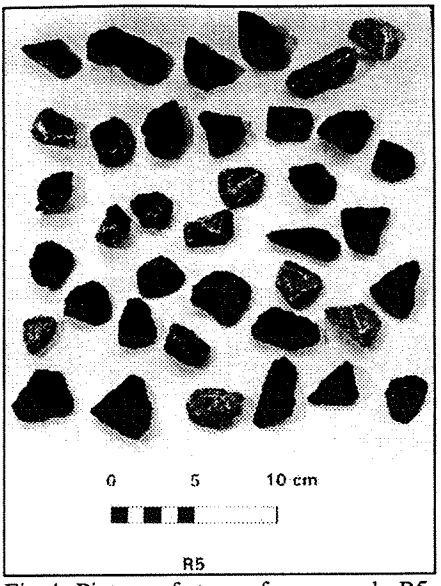

Fig.4 Picture of stones from sample R5.

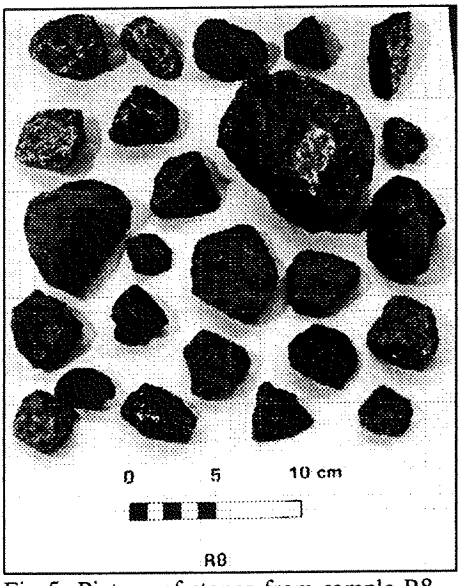

Fig.5 Picture of stones from sample R8.

APPENDIX 1

FIGURES CONSTANT FLOW

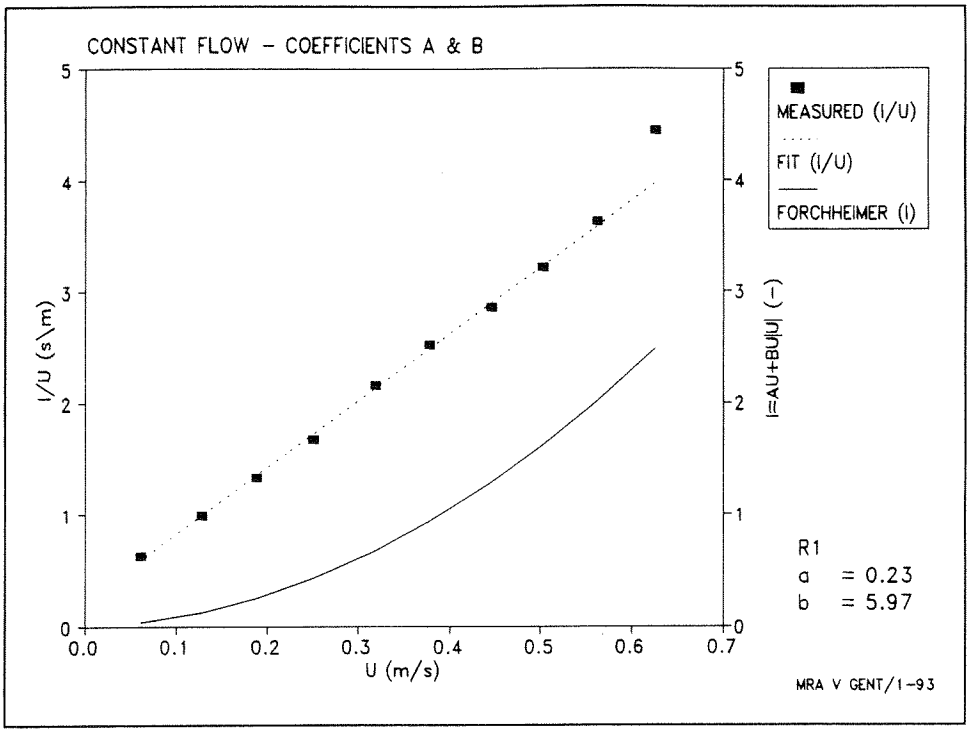
CONSTANT FLOW – COEFFICIENTS A & B
I/U (s\m)
I=AU+BU|U| (–)
U (m/s)
MEASURED (I/U)
FIT (I/U)
FORCHHEIMER (I)
R1
a = 0.23
b = 5.97
MRA V GENT/1-93

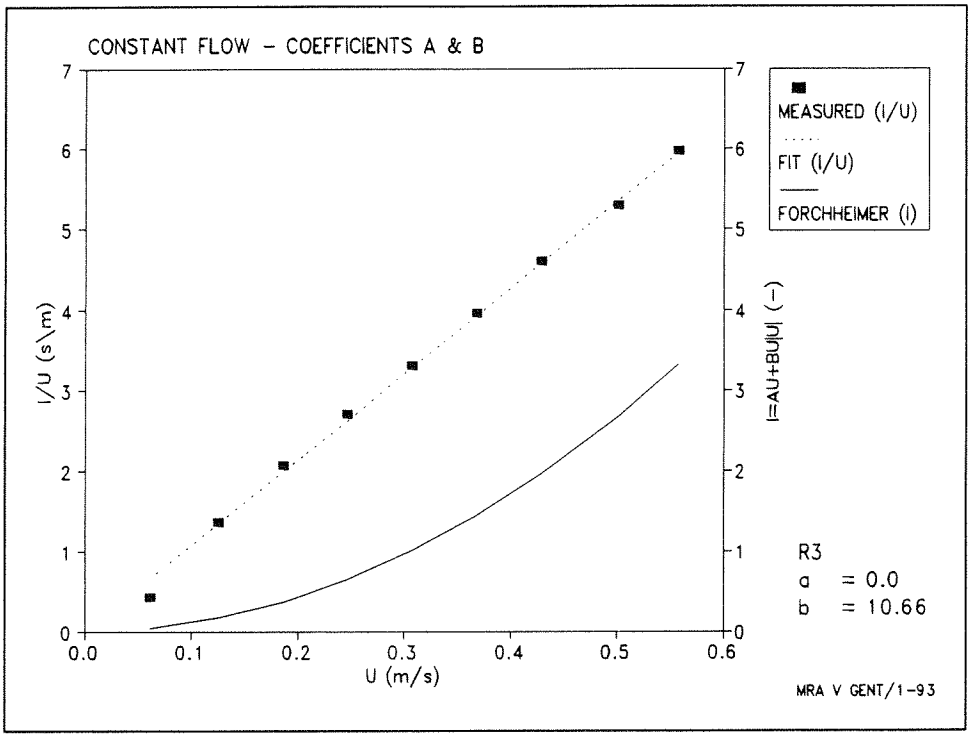
CONSTANT FLOW – COEFFICIENTS A & B
I/U (s\m)
I=AU+BU|U| (–)
U (m/s)
MEASURED (I/U)
FIT (I/U)
FORCHHEIMER (I)
R3
a = 0.0
b = 10.66
MRA V GENT/1-93

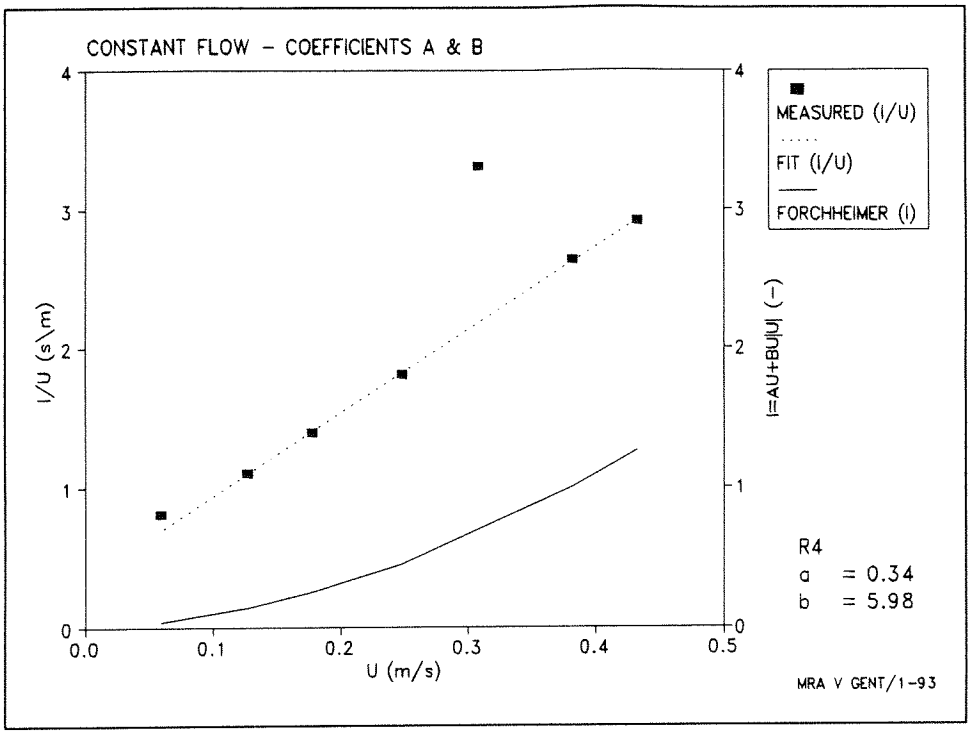
CONSTANT FLOW – COEFFICIENTS A & B
I/U (s\m)
I=AU+BU|U| (–)
U (m/s)
MEASURED (I/U)
FIT (I/U)
FORCHHEIMER (I)
R4
a = 0.34
b = 5.98
MRA V GENT/1-93

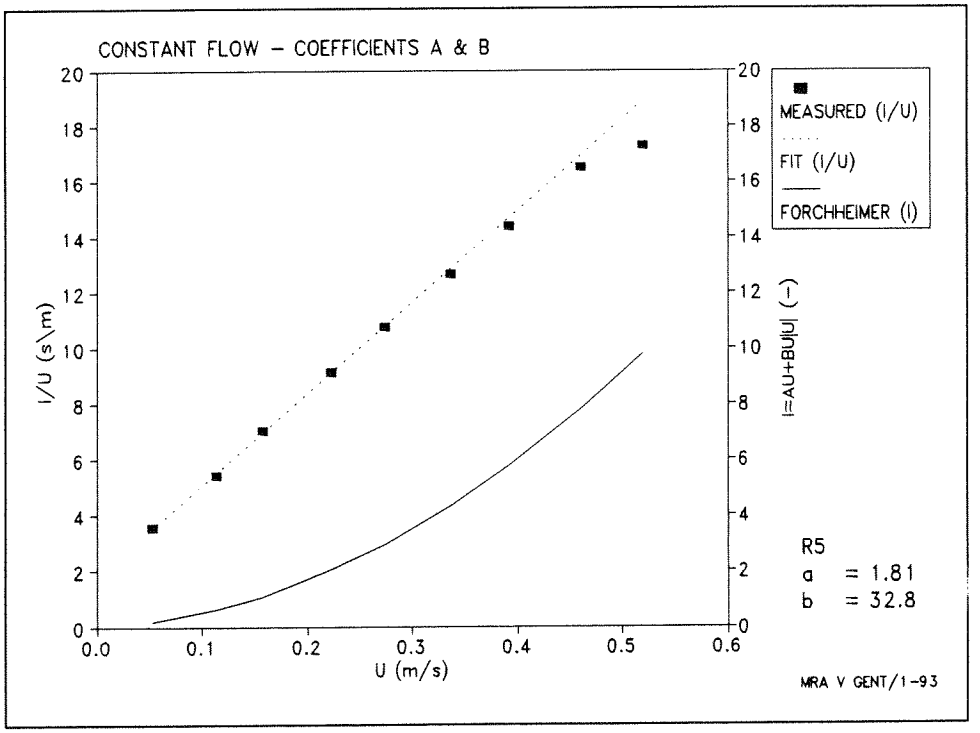
CONSTANT FLOW – COEFFICIENTS A & B
I/U (s\m)
I=AU+BU|U| (–)
U (m/s)
MEASURED (I/U)
FIT (I/U)
FORCHHEIMER (I)
R5
a = 1.81
b = 32.8
MRA V GENT/1-93

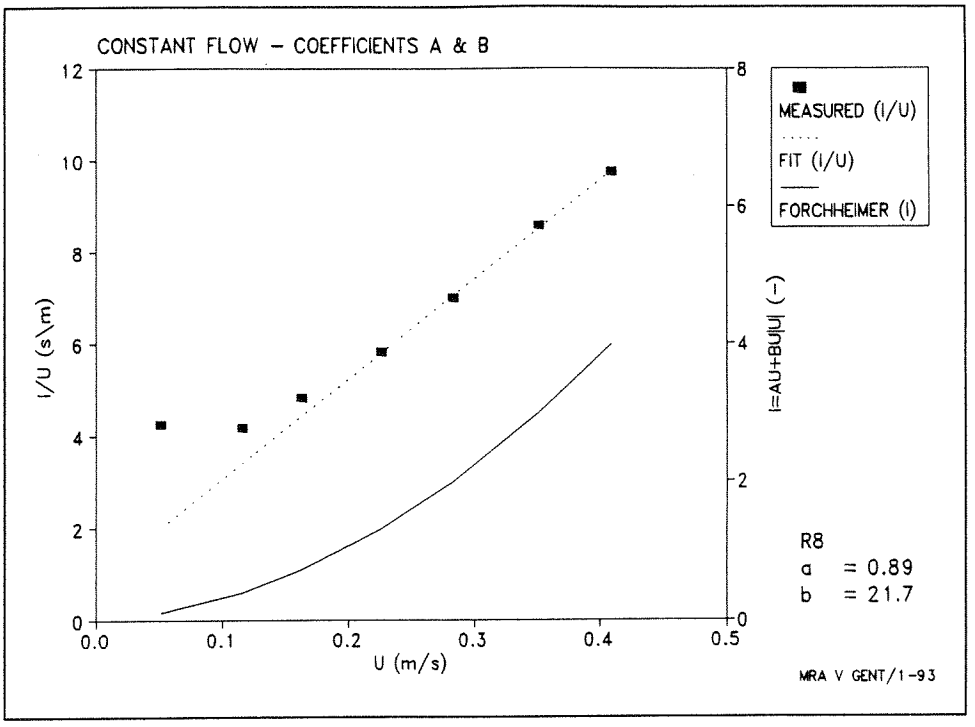
CONSTANT FLOW – COEFFICIENTS A & B
I/U (s\m)
I=AU+BU|U| (–)
U (m/s)
MEASURED (I/U)
FIT (I/U)
FORCHHEIMER (I)
R8
a = 0.89
b = 21.7
MRA V GENT/1-93

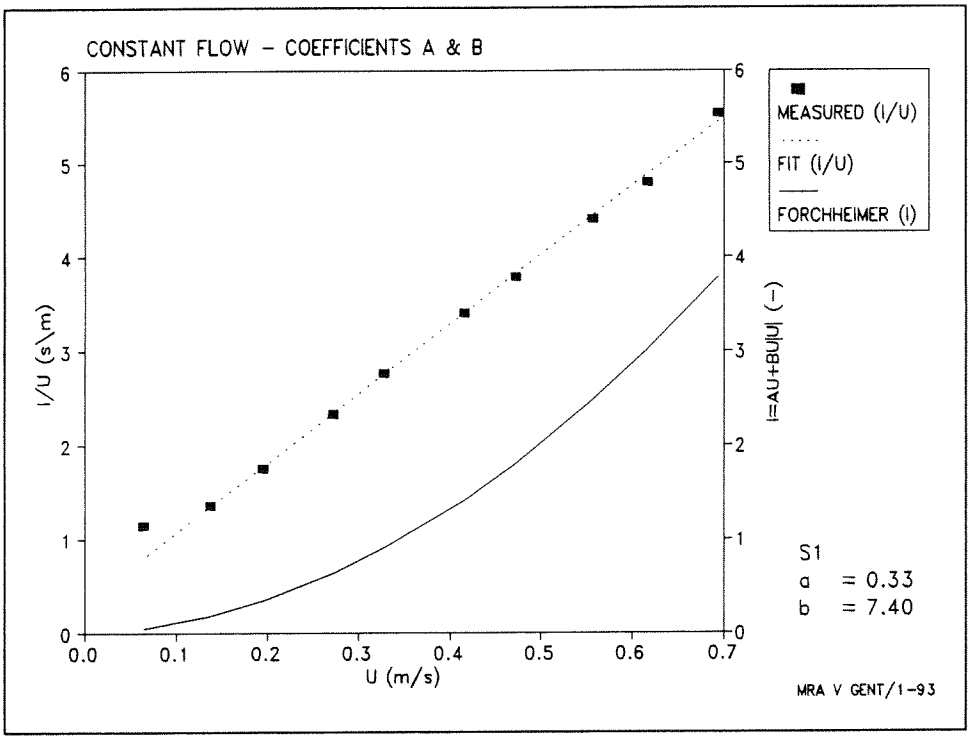
CONSTANT FLOW – COEFFICIENTS A & B
I/U (s\m)
I=AU+BU|U| (–)
U (m/s)
MEASURED (I/U)
FIT (I/U)
FORCHHEIMER (I)
S1
a = 0.33
b = 7.40
MRA V GENT/1-93

APPENDIX 2

FIGURES OSCILLATORY FLOW

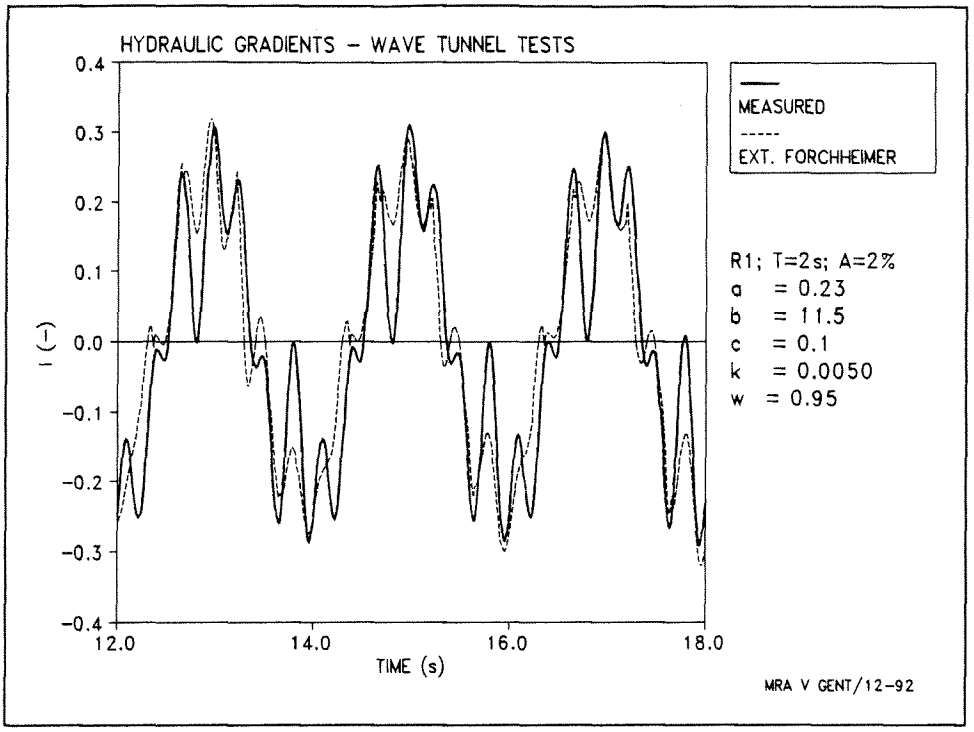
HYDRAULIC GRADIENTS – WAVE TUNNEL TESTS
0.4
0.3
0.2
0.1
0.0
-0.1
-0.2
-0.3
-0.4
I (-)
12.0
14.0
16.0
18.0
TIME (s)
MEASURED
EXT. FORCHHEIMER
R1; T=2s; A=2%
a = 0.23
b = 11.5
c = 0.1
k = 0.0050
w = 0.95
MRA V GENT/12-92

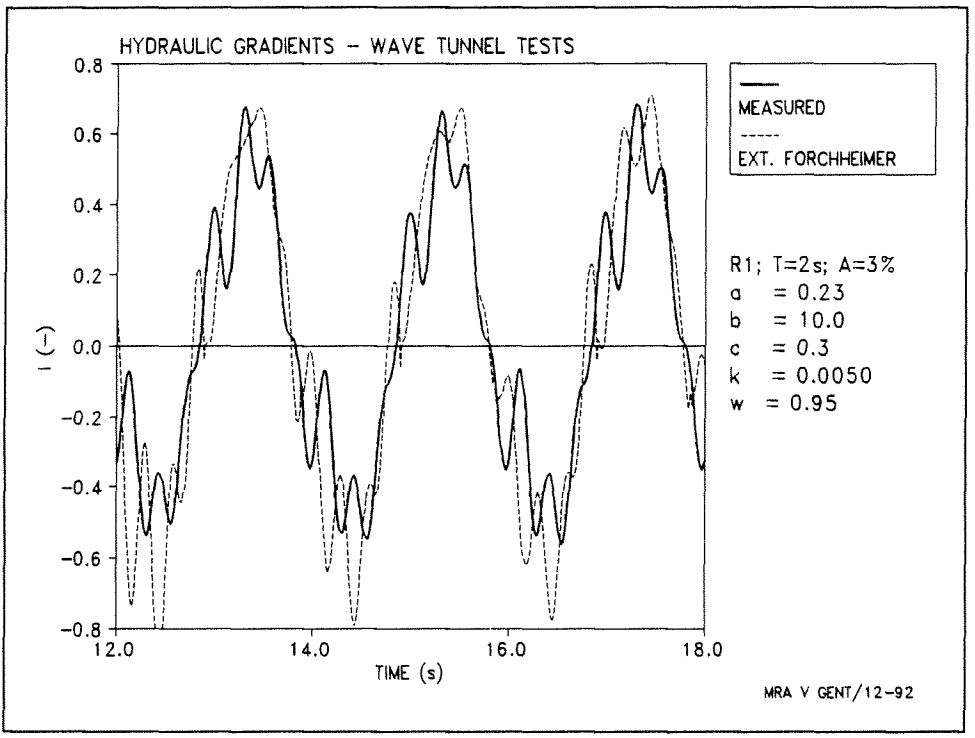
HYDRAULIC GRADIENTS – WAVE TUNNEL TESTS
0.8
0.6
0.4
0.2
0.0
-0.2
-0.4
-0.6
-0.8
I (-)
12.0
14.0
16.0
18.0
TIME (s)
MEASURED
EXT. FORCHHEIMER
R1; T=2s; A=3%
a = 0.23
b = 10.0
c = 0.3
k = 0.0050
w = 0.95
MRA V GENT/12-92

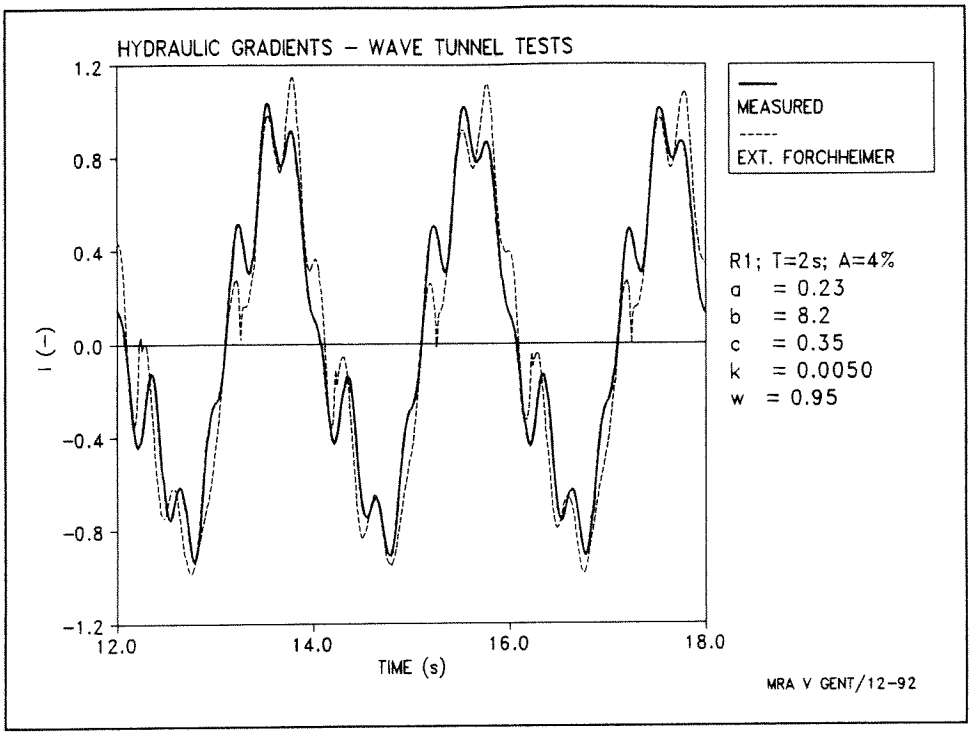
HYDRAULIC GRADIENTS – WAVE TUNNEL TESTS
1.2
0.8
0.4
0.0
-0.4
-0.8
-1.2
I (-)
12.0
14.0
16.0
18.0
TIME (s)
MEASURED
EXT. FORCHHEIMER
R1; T=2s; A=4%
a = 0.23
b = 8.2
c = 0.35
k = 0.0050
w = 0.95
MRA V GENT/12-92

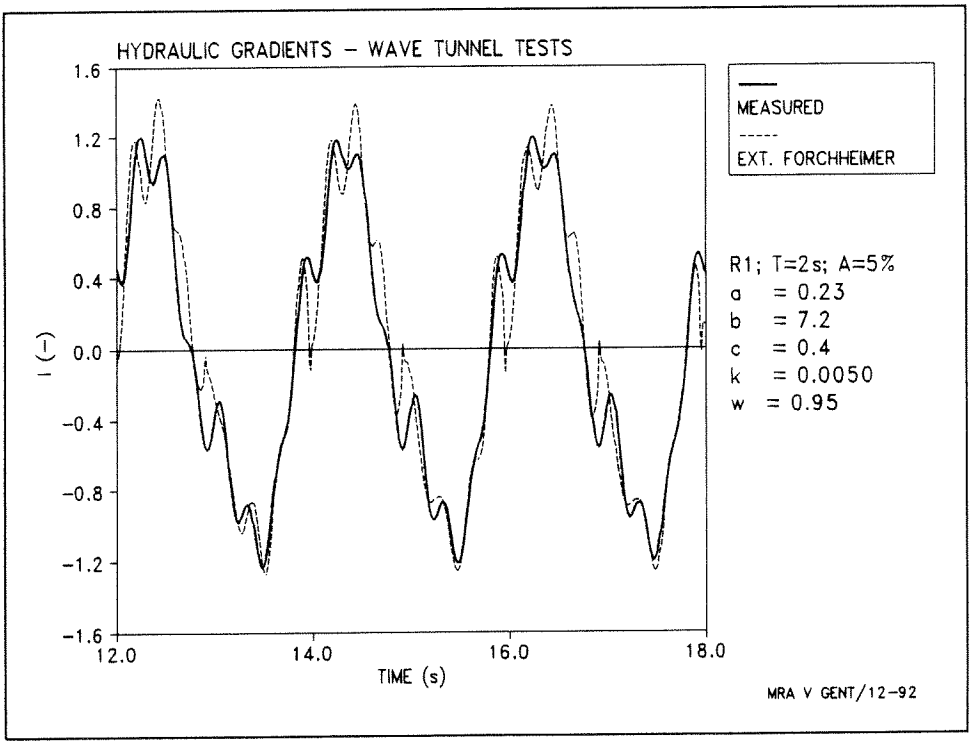
HYDRAULIC GRADIENTS – WAVE TUNNEL TESTS
1.6
1.2
0.8
0.4
0.0
-0.4
-0.8
-1.2
-1.6
I (-)
12.0
14.0
16.0
18.0
TIME (s)
MEASURED
EXT. FORCHHEIMER
R1; T=2s; A=5%
a = 0.23
b = 7.2
c = 0.4
k = 0.0050
w = 0.95
MRA V GENT/12-92

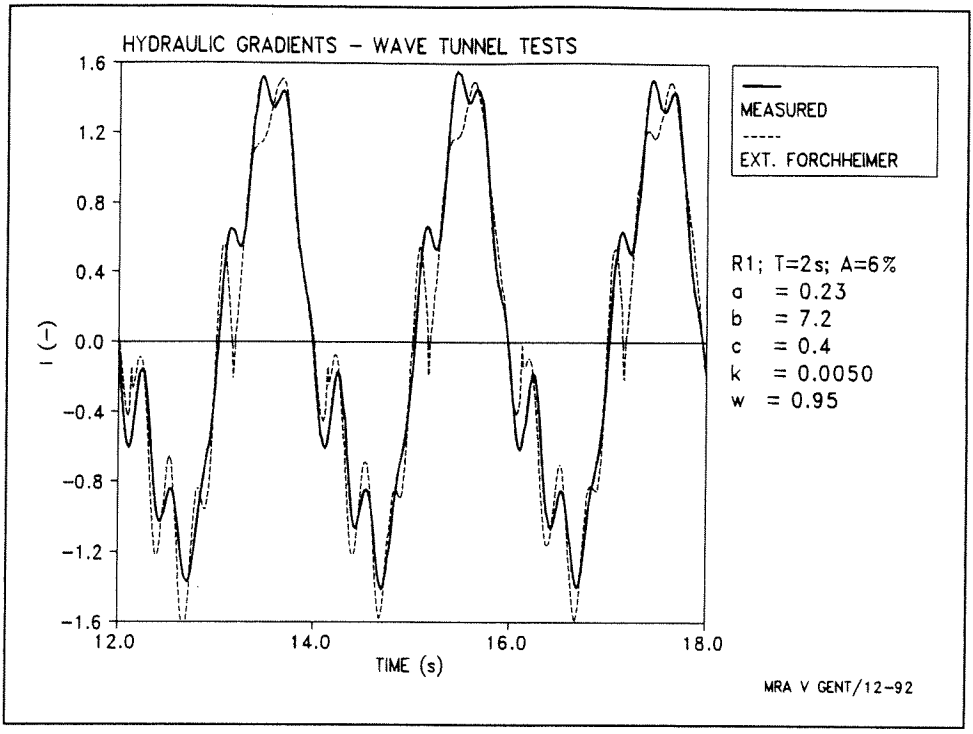
HYDRAULIC GRADIENTS – WAVE TUNNEL TESTS
1.6
1.2
0.8
0.4
0.0
-0.4
-0.8
-1.2
-1.6
I (-)
12.0
14.0
16.0
18.0
TIME (s)
MEASURED
EXT. FORCHHEIMER
R1; T=2s; A=6%
a = 0.23
b = 7.2
c = 0.4
k = 0.0050
w = 0.95
MRA V GENT/12-92

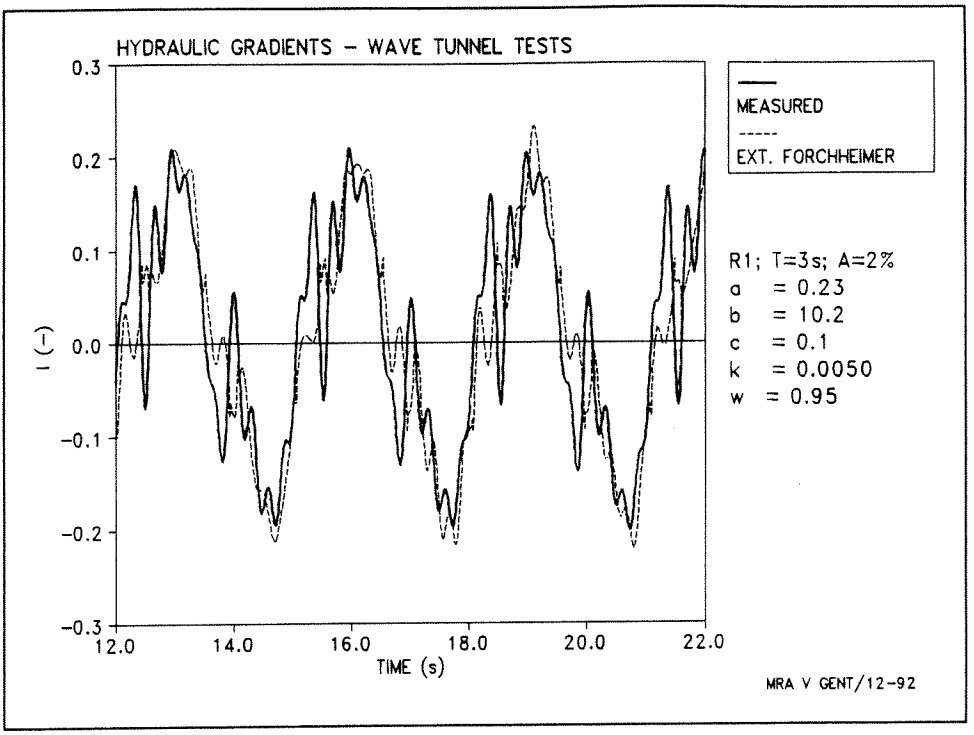
HYDRAULIC GRADIENTS – WAVE TUNNEL TESTS
0.3
0.2
0.1
0.0
−0.1
−0.2
−0.3
I (-)
12.0
14.0
16.0
18.0
20.0
22.0
TIME (s)
MEASURED
EXT. FORCHHEIMER
R1; T=3s; A=2%
a = 0.23
b = 10.2
c = 0.1
k = 0.0050
w = 0.95
MRA V GENT/12-92

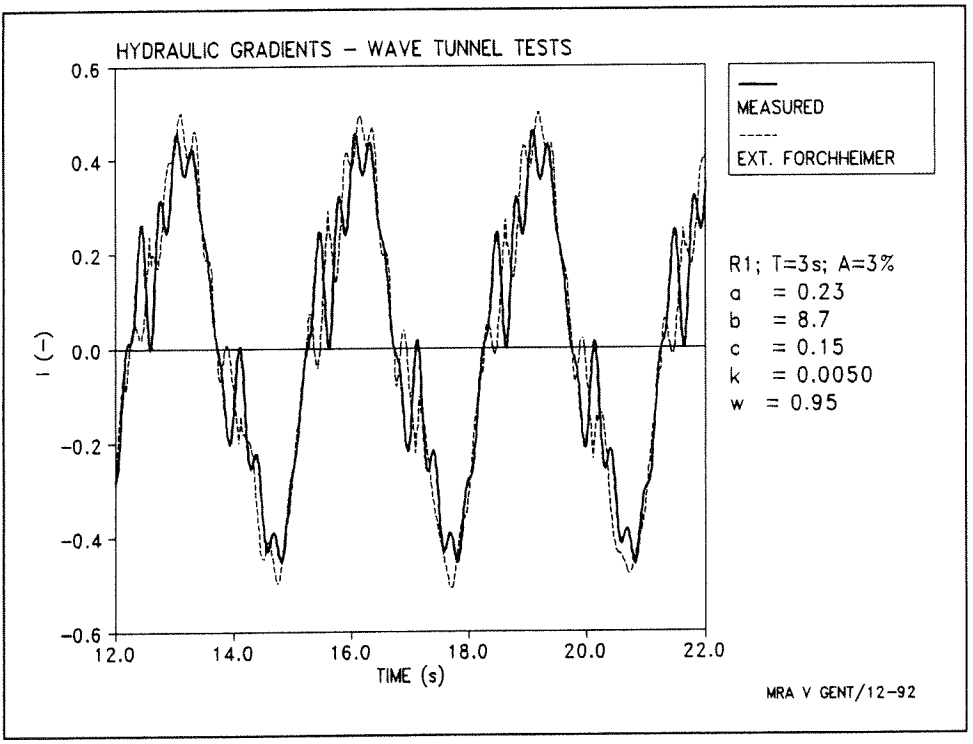
HYDRAULIC GRADIENTS – WAVE TUNNEL TESTS
0.6
0.4
0.2
0.0
−0.2
−0.4
−0.6
I (-)
12.0
14.0
16.0
18.0
20.0
22.0
TIME (s)
MEASURED
EXT. FORCHHEIMER
R1; T=3s; A=3%
a = 0.23
b = 8.7
c = 0.15
k = 0.0050
w = 0.95
MRA V GENT/12-92

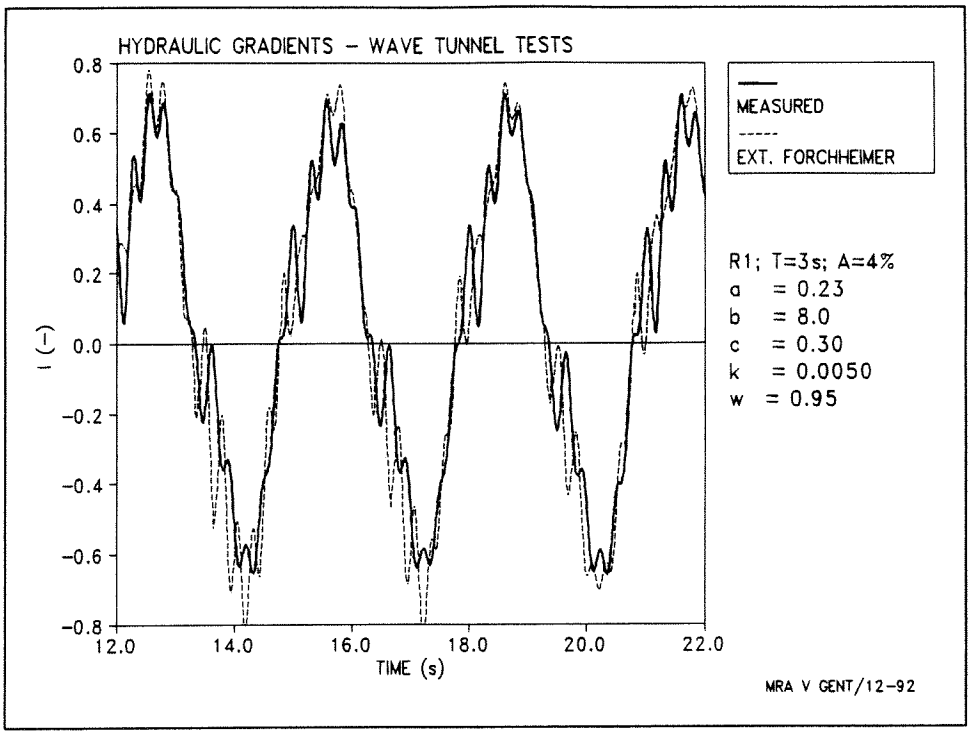
HYDRAULIC GRADIENTS – WAVE TUNNEL TESTS
0.8
0.6
0.4
0.2
0.0
-0.2
-0.4
-0.6
-0.8
I (-)
12.0
14.0
16.0
18.0
20.0
22.0
TIME (s)
MEASURED
EXT. FORCHHEIMER
R1; T=3s; A=4%
a = 0.23
b = 8.0
c = 0.30
k = 0.0050
w = 0.95
MRA V GENT/12-92

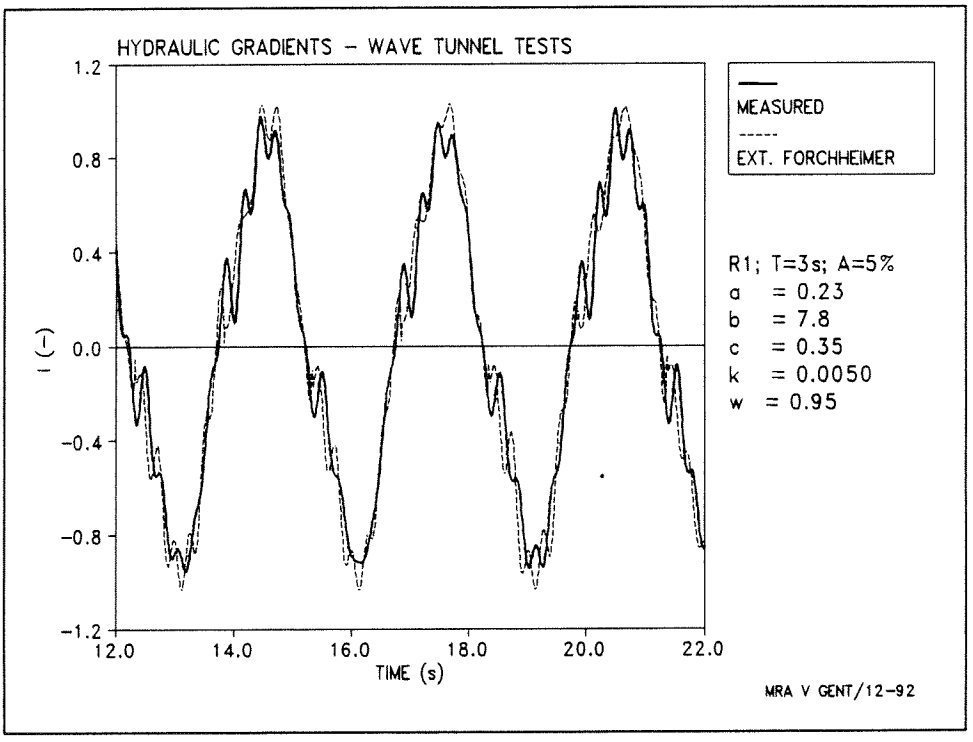
HYDRAULIC GRADIENTS – WAVE TUNNEL TESTS
1.2
0.8
0.4
0.0
-0.4
-0.8
-1.2
I (-)
12.0
14.0
16.0
18.0
20.0
22.0
TIME (s)
MEASURED
EXT. FORCHHEIMER
R1; T=3s; A=5%
a = 0.23
b = 7.8
c = 0.35
k = 0.0050
w = 0.95
MRA V GENT/12-92

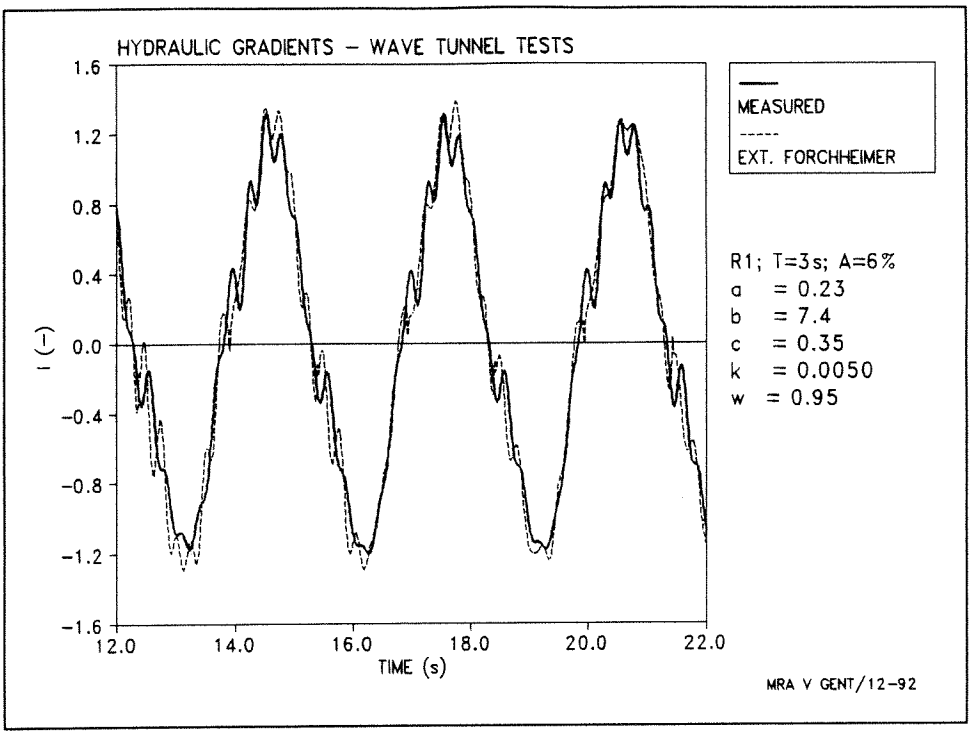
HYDRAULIC GRADIENTS – WAVE TUNNEL TESTS
1.6
1.2
0.8
0.4
0.0
-0.4
-0.8
-1.2
-1.6
I (-)
12.0
14.0
16.0
18.0
20.0
22.0
TIME (s)
MEASURED
EXT. FORCHHEIMER
R1; T=3s; A=6%
a = 0.23
b = 7.4
c = 0.35
k = 0.0050
w = 0.95
MRA V GENT/12-92

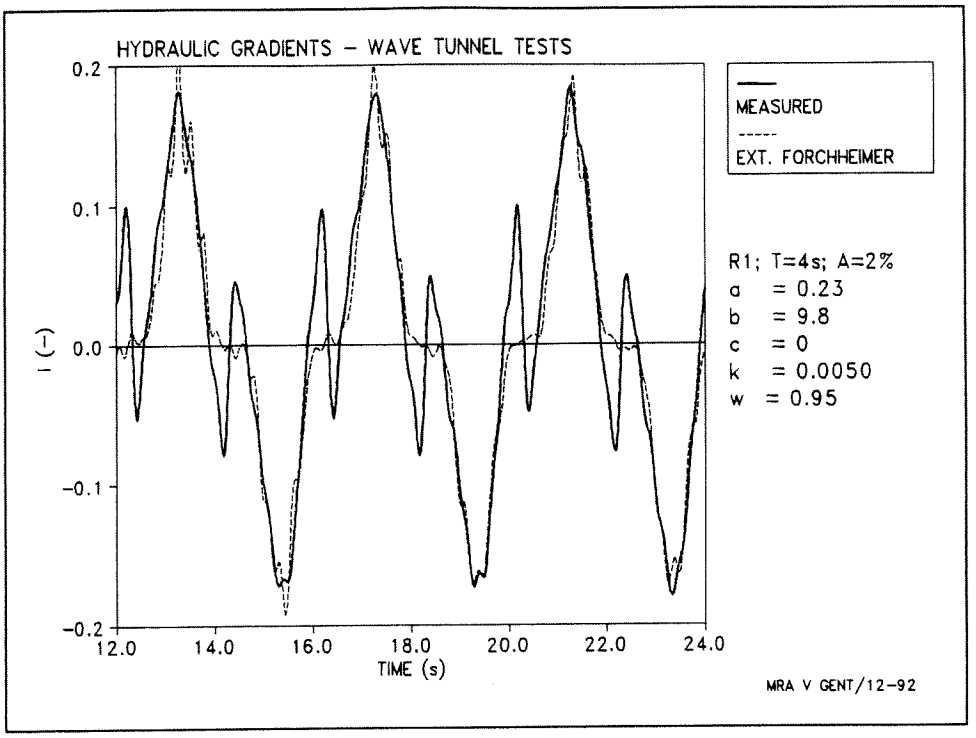
HYDRAULIC GRADIENTS – WAVE TUNNEL TESTS
0.2
0.1
0.0
-0.1
-0.2
I (-)
12.0
14.0
16.0
18.0
20.0
22.0
24.0
TIME (s)
MEASURED
EXT. FORCHHEIMER
R1; T=4s; A=2%
a = 0.23
b = 9.8
c = 0
k = 0.0050
w = 0.95
MRA V GENT/12-92

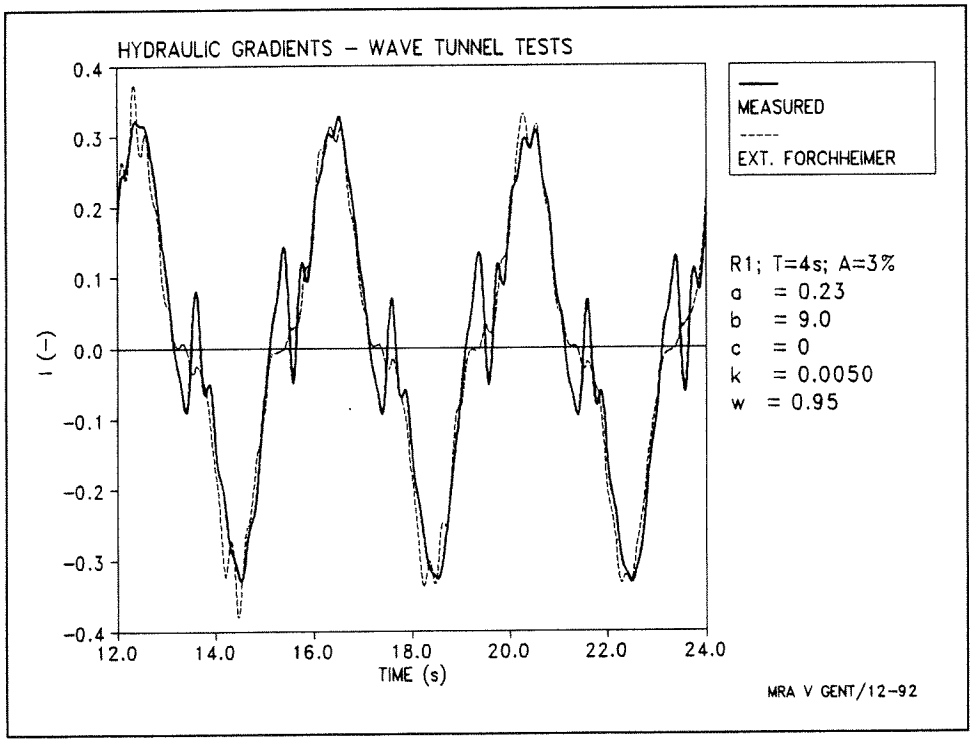
HYDRAULIC GRADIENTS – WAVE TUNNEL TESTS
0.4
0.3
0.2
0.1
0.0
-0.1
-0.2
-0.3
-0.4
I (-)
12.0
14.0
16.0
18.0
20.0
22.0
24.0
TIME (s)
MEASURED
EXT. FORCHHEIMER
R1; T=4s; A=3%
a = 0.23
b = 9.0
c = 0
k = 0.0050
w = 0.95
MRA V GENT/12-92

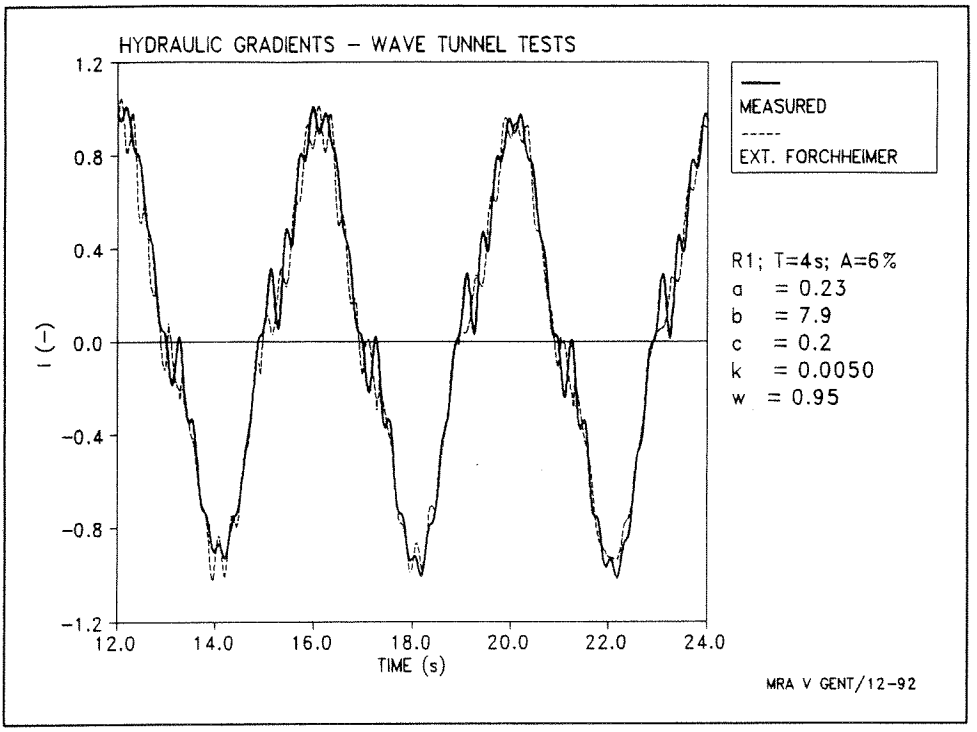
HYDRAULIC GRADIENTS – WAVE TUNNEL TESTS
I (–)
TIME (s)
MEASURED
EXT. FORCHHEIMER
R1; T=4s; A=6%
a = 0.23
b = 7.9
c = 0.2
k = 0.0050
w = 0.95
MRA V GENT/12-92

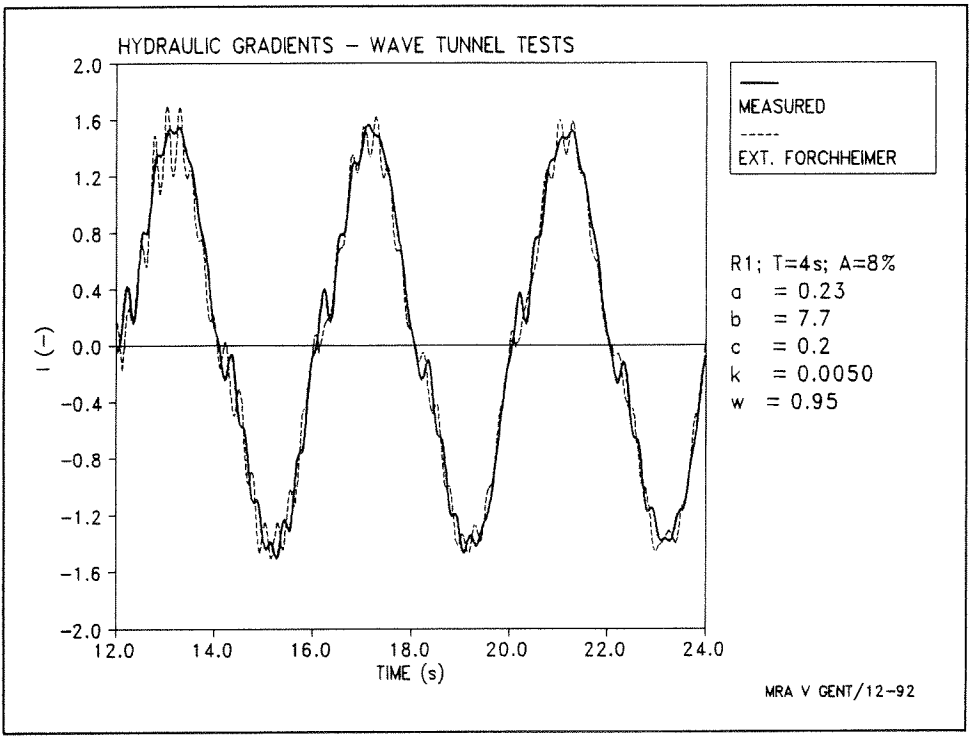
HYDRAULIC GRADIENTS – WAVE TUNNEL TESTS
I (–)
TIME (s)
MEASURED
EXT. FORCHHEIMER
R1; T=4s; A=8%
a = 0.23
b = 7.7
c = 0.2
k = 0.0050
w = 0.95
MRA V GENT/12-92

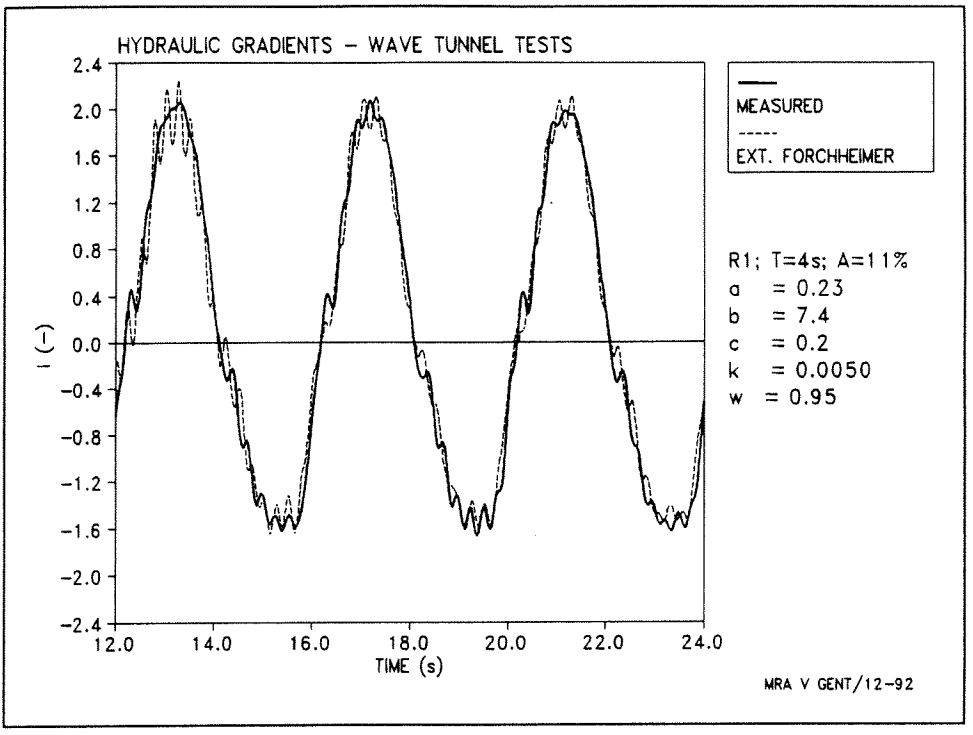
HYDRAULIC GRADIENTS – WAVE TUNNEL TESTS
2.4
2.0
1.6
1.2
0.8
0.4
0.0
-0.4
-0.8
-1.2
-1.6
-2.0
-2.4
I (-)
12.0
14.0
16.0
18.0
20.0
22.0
24.0
TIME (s)
MEASURED
EXT. FORCHHEIMER
R1; T=4s; A=11%
a = 0.23
b = 7.4
c = 0.2
k = 0.0050
w = 0.95
MRA V GENT/12-92

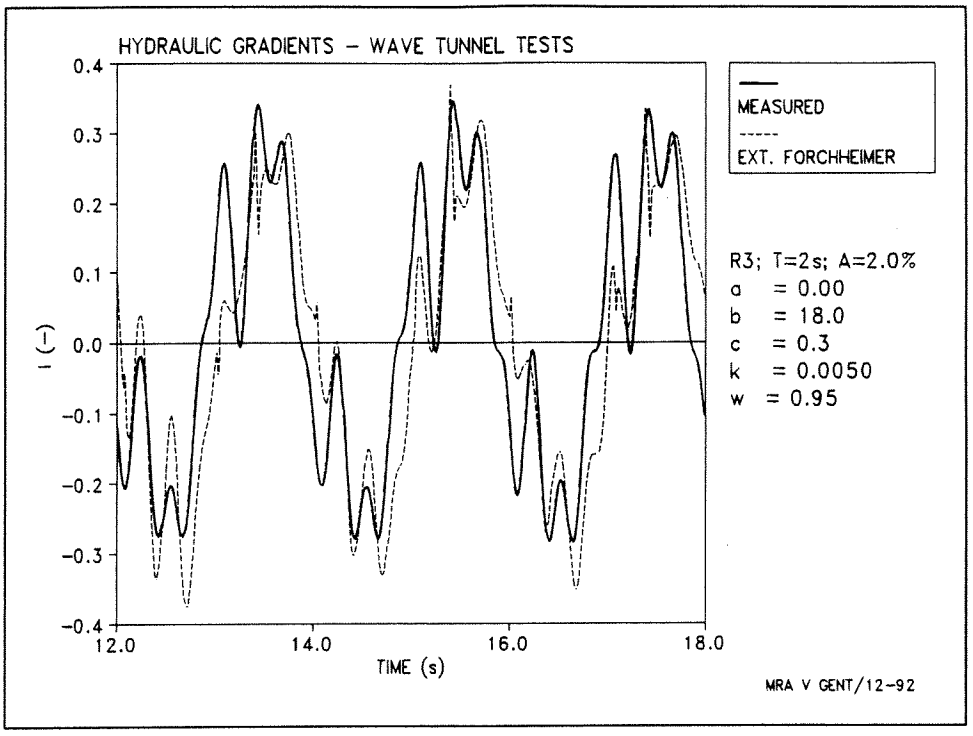
HYDRAULIC GRADIENTS – WAVE TUNNEL TESTS
I (-)
TIME (s)
MEASURED
EXT. FORCHHEIMER
R3; T=2s; A=2.0%
a = 0.00
b = 18.0
c = 0.3
k = 0.0050
w = 0.95
MRA V GENT/12-92

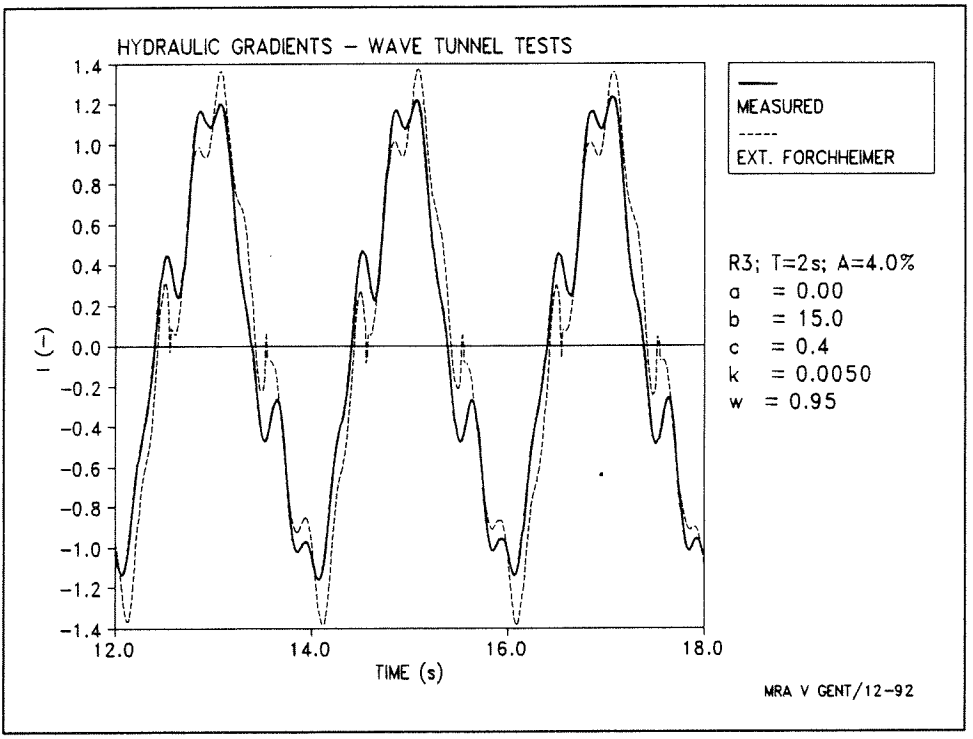
HYDRAULIC GRADIENTS – WAVE TUNNEL TESTS
I (-)
TIME (s)
MEASURED
EXT. FORCHHEIMER
R3; T=2s; A=4.0%
a = 0.00
b = 15.0
c = 0.4
k = 0.0050
w = 0.95
MRA V GENT/12-92

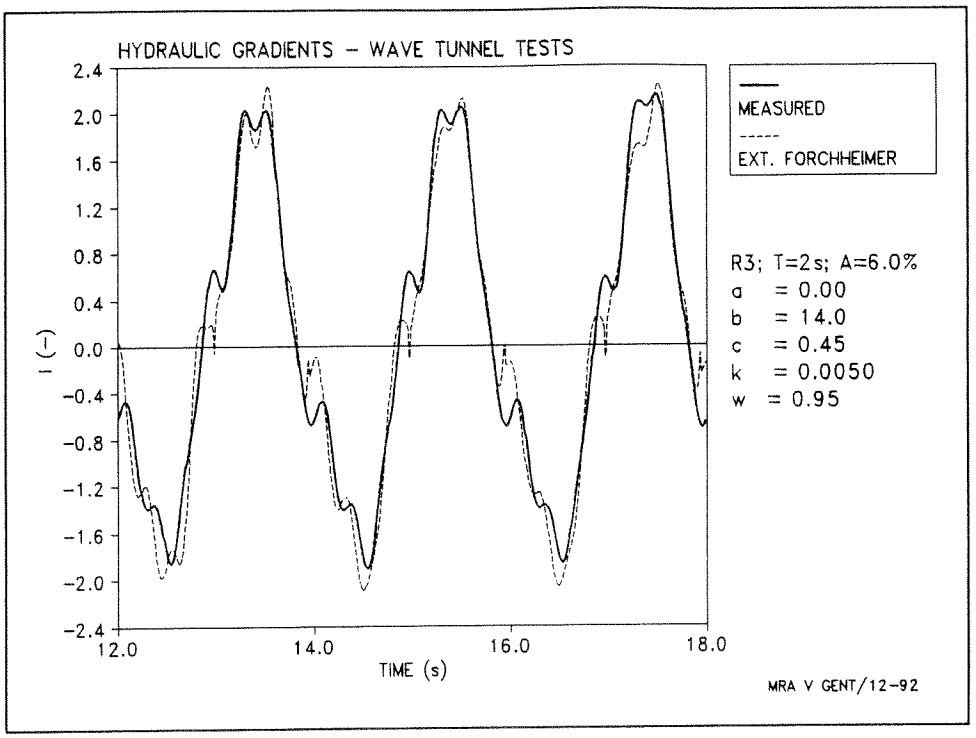
HYDRAULIC GRADIENTS – WAVE TUNNEL TESTS
2.4
2.0
1.6
1.2
0.8
0.4
0.0
-0.4
-0.8
-1.2
-1.6
-2.0
-2.4
I (-)
12.0
14.0
16.0
18.0
TIME (s)
MEASURED
EXT. FORCHHEIMER
R3; T=2s; A=6.0%
a = 0.00
b = 14.0
c = 0.45
k = 0.0050
w = 0.95
MRA V GENT/12-92

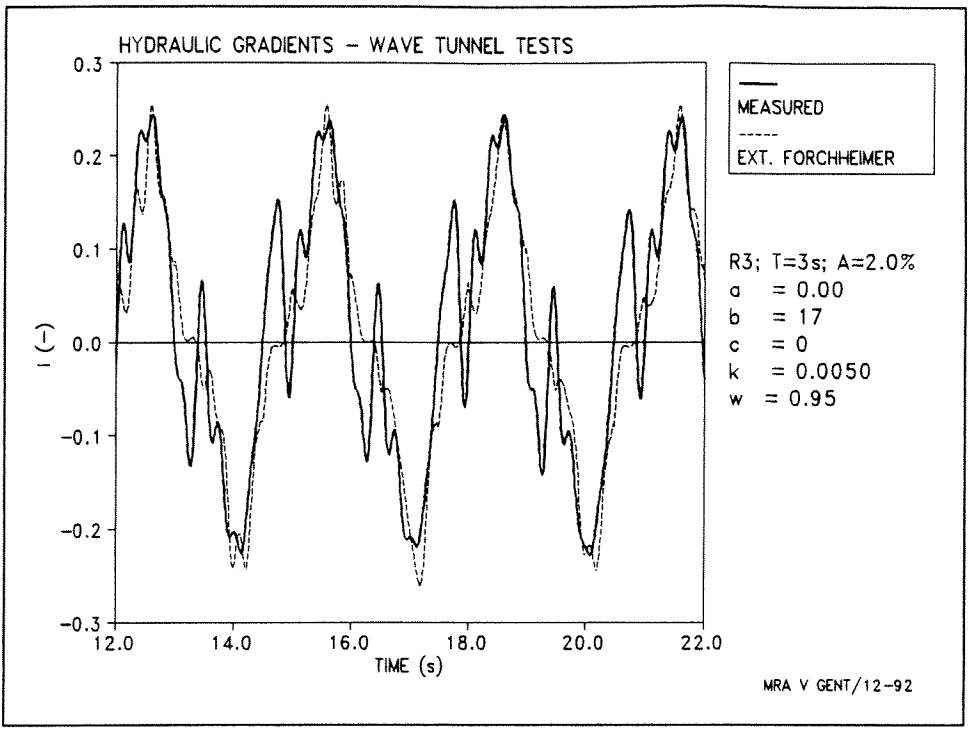
HYDRAULIC GRADIENTS – WAVE TUNNEL TESTS
MEASURED
EXT. FORCHHEIMER
R3; T=3s; A=2.0%
a = 0.00
b = 17
c = 0
k = 0.0050
w = 0.95
I (-)
TIME (s)
MRA V GENT/12-92

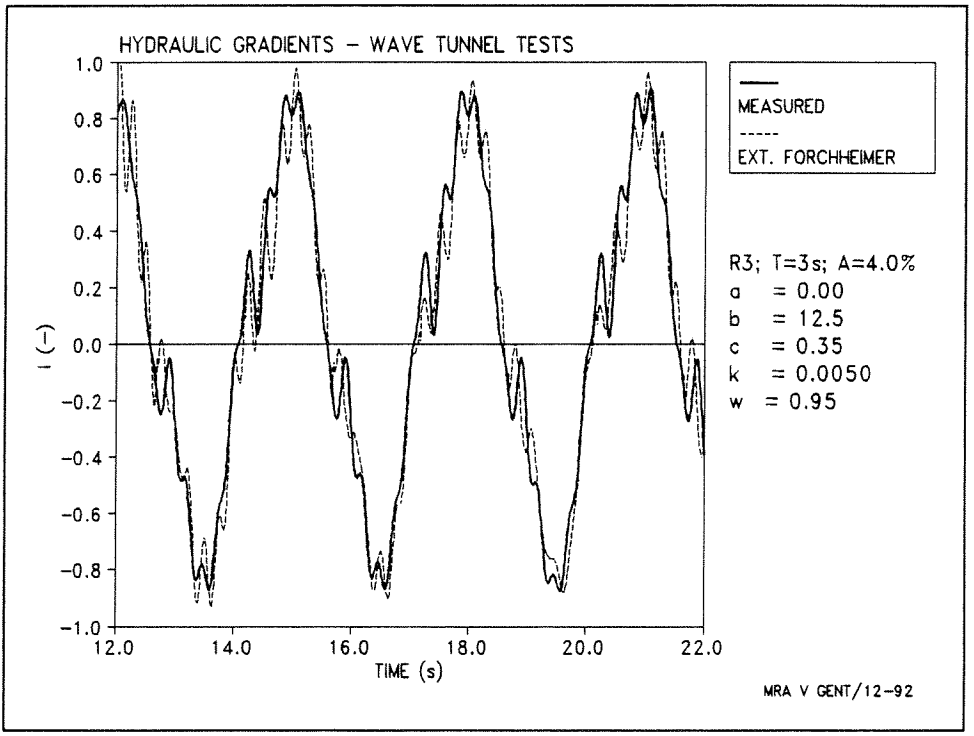
HYDRAULIC GRADIENTS – WAVE TUNNEL TESTS
MEASURED
EXT. FORCHHEIMER
R3; T=3s; A=4.0%
a = 0.00
b = 12.5
c = 0.35
k = 0.0050
w = 0.95
I (-)
TIME (s)
MRA V GENT/12-92

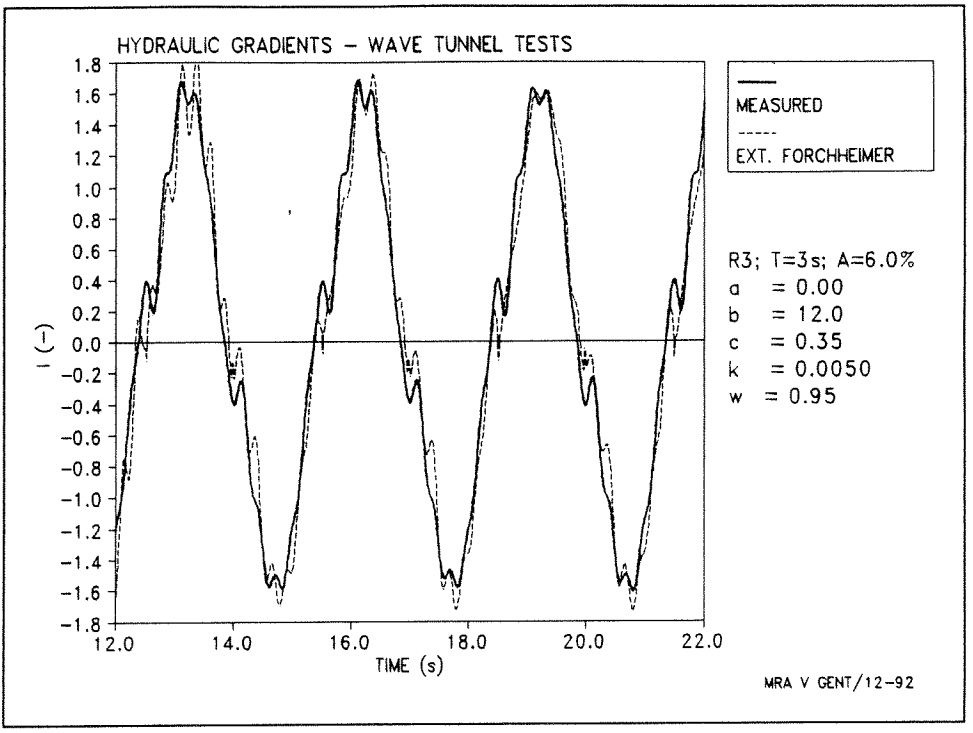
HYDRAULIC GRADIENTS – WAVE TUNNEL TESTS
I (-)
TIME (s)
MEASURED
EXT. FORCHHEIMER
R3; T=3s; A=6.0%
a = 0.00
b = 12.0
c = 0.35
k = 0.0050
w = 0.95
MRA V GENT/12-92

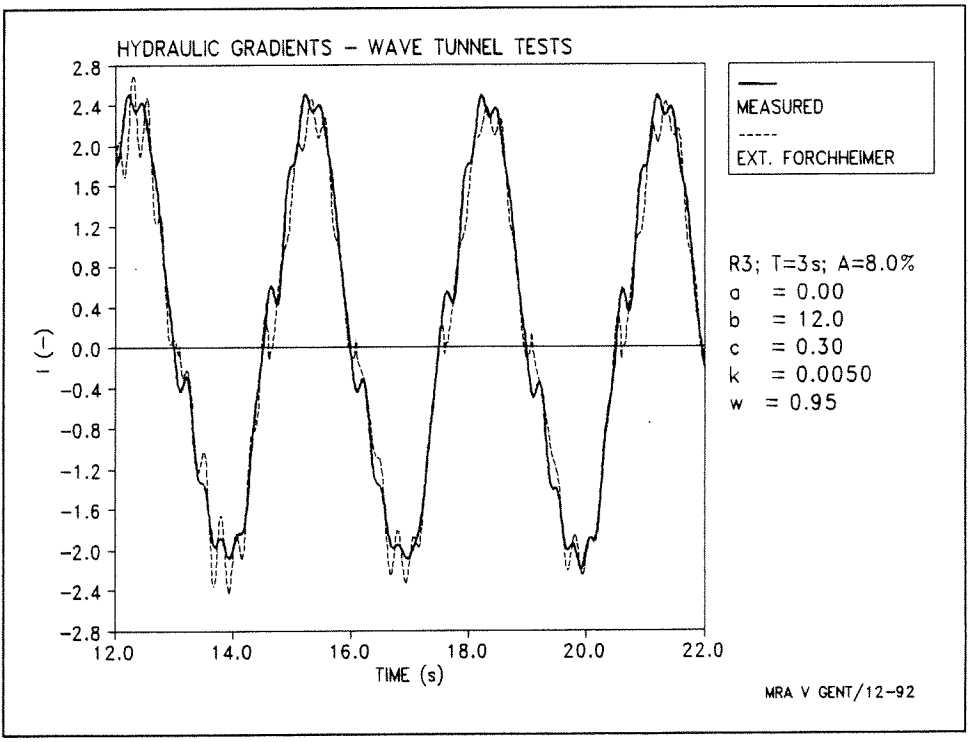
HYDRAULIC GRADIENTS – WAVE TUNNEL TESTS
I (-)
TIME (s)
MEASURED
EXT. FORCHHEIMER
R3; T=3s; A=8.0%
a = 0.00
b = 12.0
c = 0.30
k = 0.0050
w = 0.95
MRA V GENT/12-92

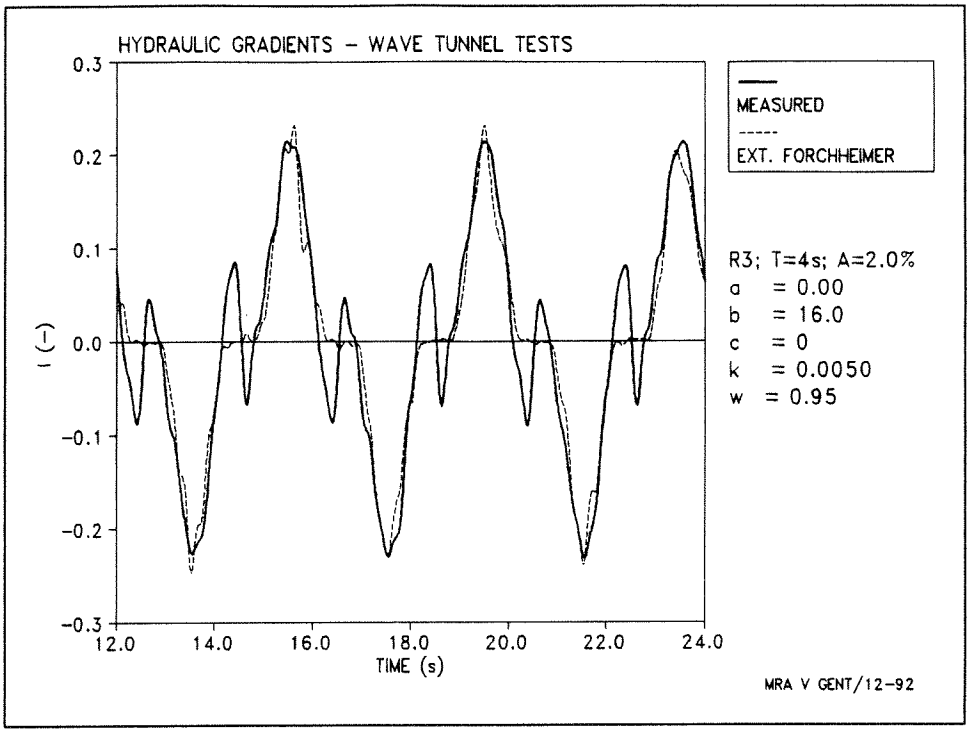
HYDRAULIC GRADIENTS – WAVE TUNNEL TESTS
I (–)
TIME (s)
MEASURED
EXT. FORCHHEIMER
R3; T=4s; A=2.0%
a = 0.00
b = 16.0
c = 0
k = 0.0050
w = 0.95
MRA V GENT/12-92

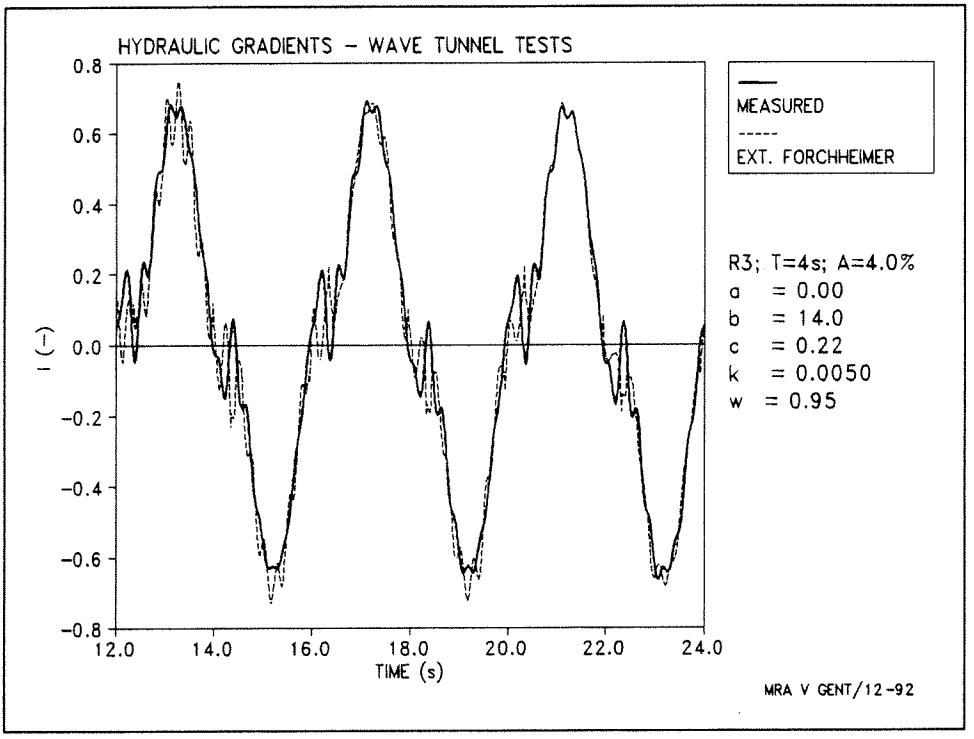
HYDRAULIC GRADIENTS – WAVE TUNNEL TESTS
I (–)
TIME (s)
MEASURED
EXT. FORCHHEIMER
R3; T=4s; A=4.0%
a = 0.00
b = 14.0
c = 0.22
k = 0.0050
w = 0.95
MRA V GENT/12-92

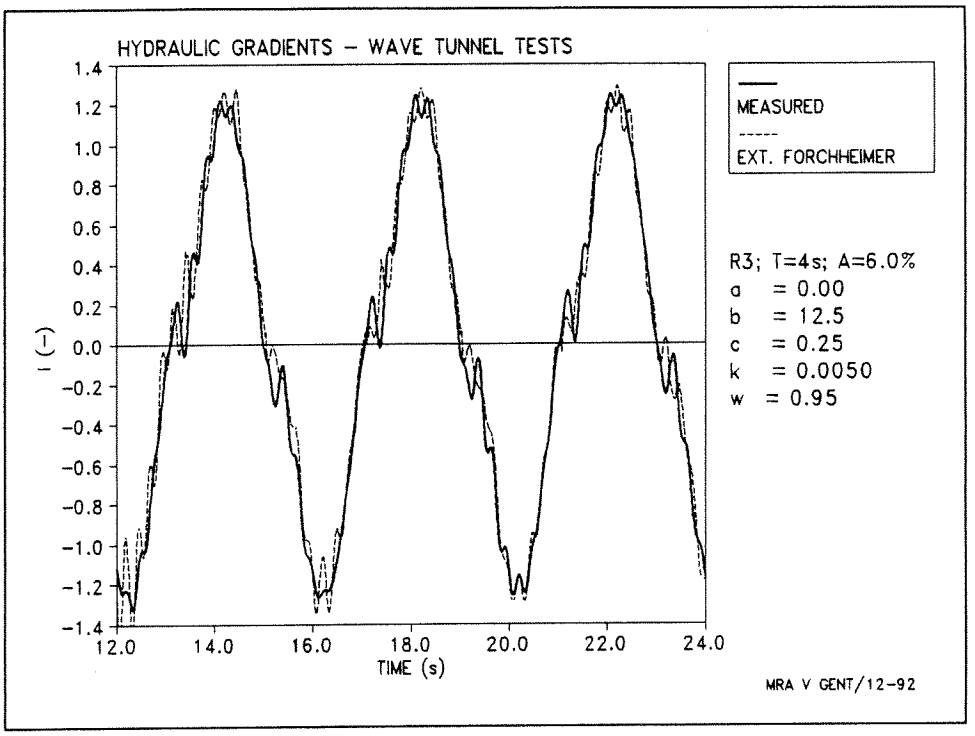
HYDRAULIC GRADIENTS – WAVE TUNNEL TESTS
I (-)
TIME (s)
MEASURED
EXT. FORCHHEIMER
R3; T=4s; A=6.0%
a = 0.00
b = 12.5
c = 0.25
k = 0.0050
w = 0.95
MRA V GENT/12-92

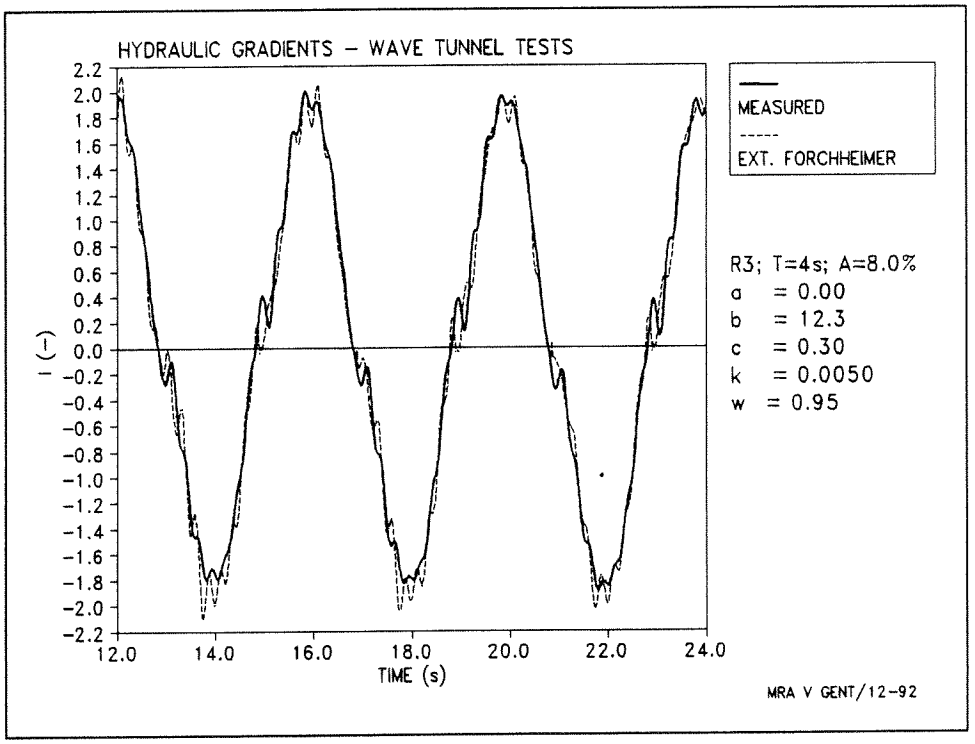
HYDRAULIC GRADIENTS – WAVE TUNNEL TESTS
I (-)
TIME (s)
MEASURED
EXT. FORCHHEIMER
R3; T=4s; A=8.0%
a = 0.00
b = 12.3
c = 0.30
k = 0.0050
w = 0.95
MRA V GENT/12-92

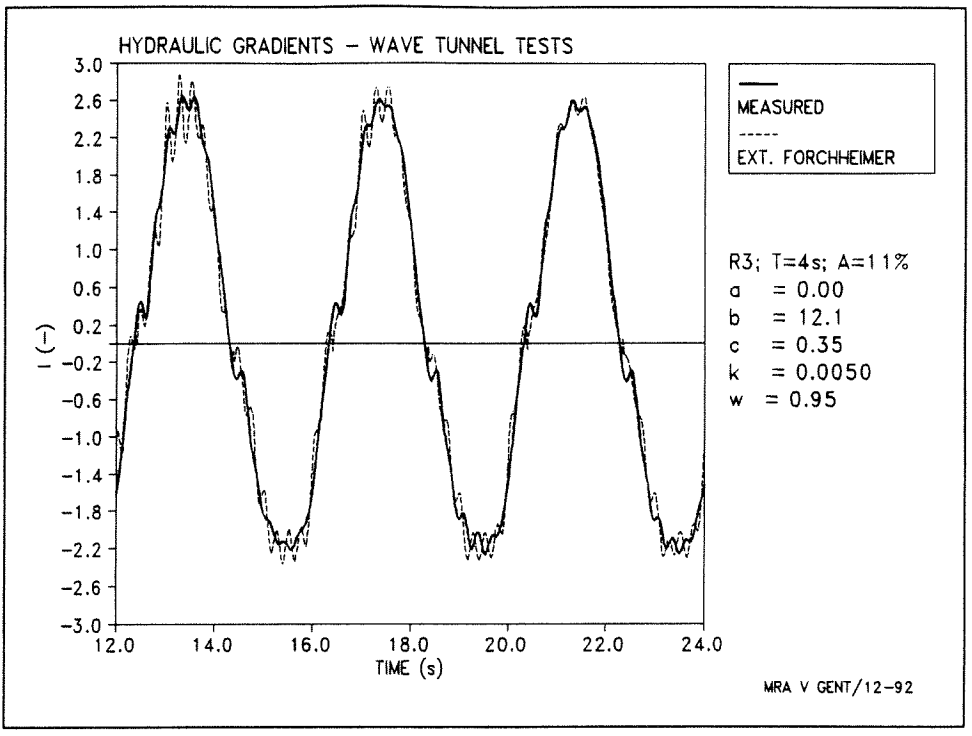
HYDRAULIC GRADIENTS – WAVE TUNNEL TESTS
3.0
2.6
2.2
1.8
1.4
1.0
0.6
0.2
-0.2
-0.6
-1.0
-1.4
-1.8
-2.2
-2.6
-3.0
I (-)
12.0
14.0
16.0
18.0
20.0
22.0
24.0
TIME (s)
MEASURED
EXT. FORCHHEIMER
R3; T=4s; A=11%
a = 0.00
b = 12.1
c = 0.35
k = 0.0050
w = 0.95
MRA V GENT/12-92

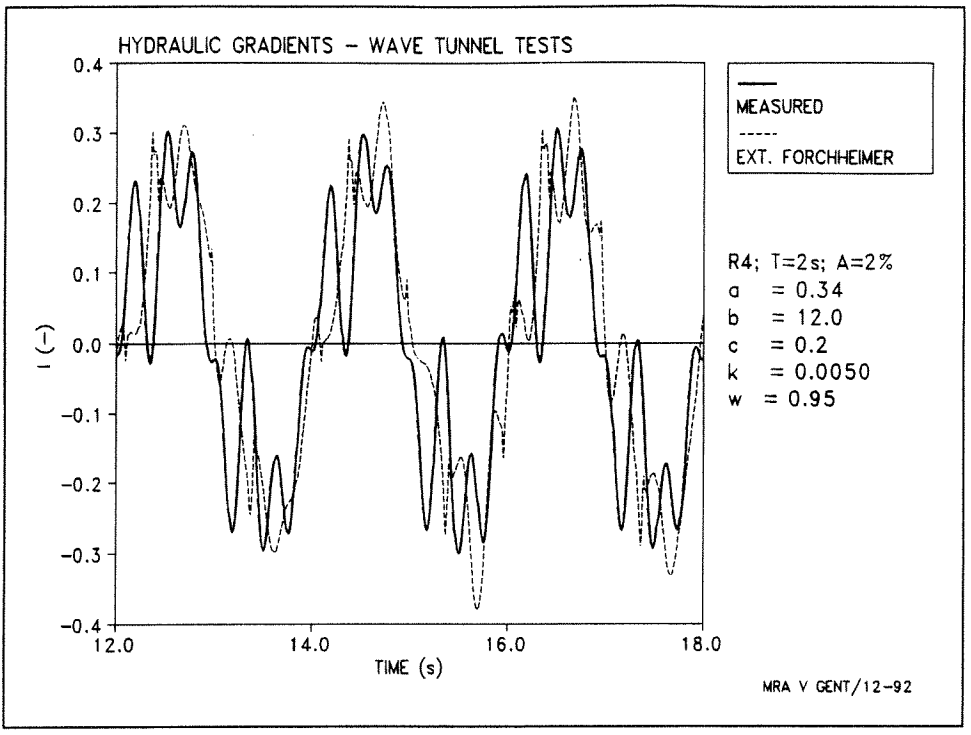
HYDRAULIC GRADIENTS - WAVE TUNNEL TESTS
MEASURED
EXT. FORCHHEIMER
R4; T=2s; A=2%
a = 0.34
b = 12.0
c = 0.2
k = 0.0050
w = 0.95
I (-)
TIME (s)
MRA V GENT/12-92

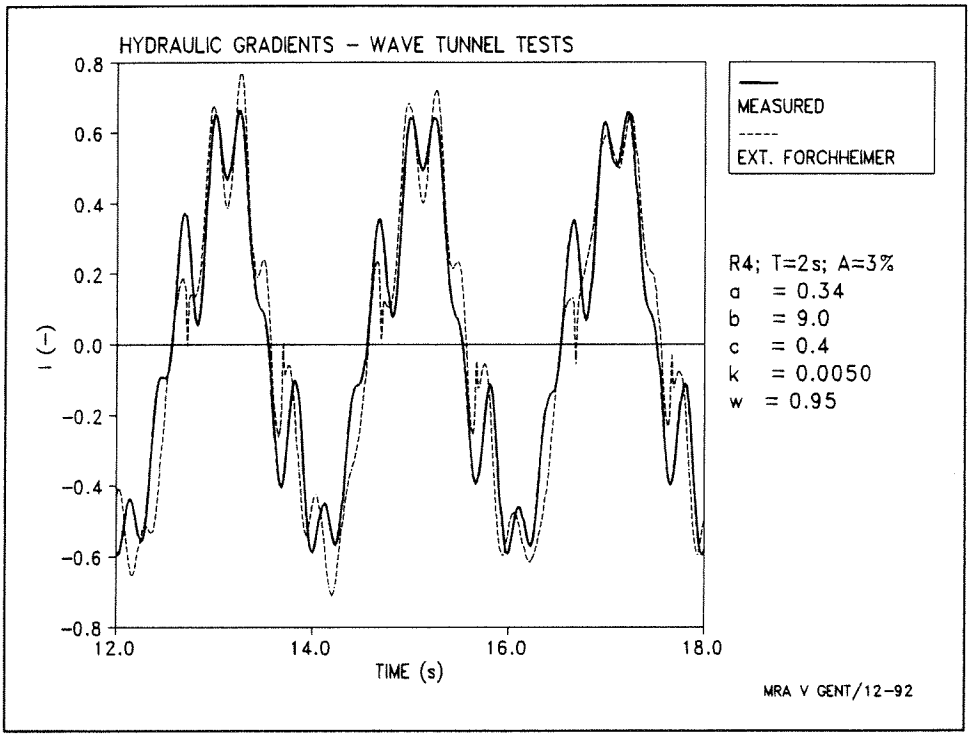
HYDRAULIC GRADIENTS - WAVE TUNNEL TESTS
MEASURED
EXT. FORCHHEIMER
R4; T=2s; A=3%
a = 0.34
b = 9.0
c = 0.4
k = 0.0050
w = 0.95
I (-)
TIME (s)
MRA V GENT/12-92

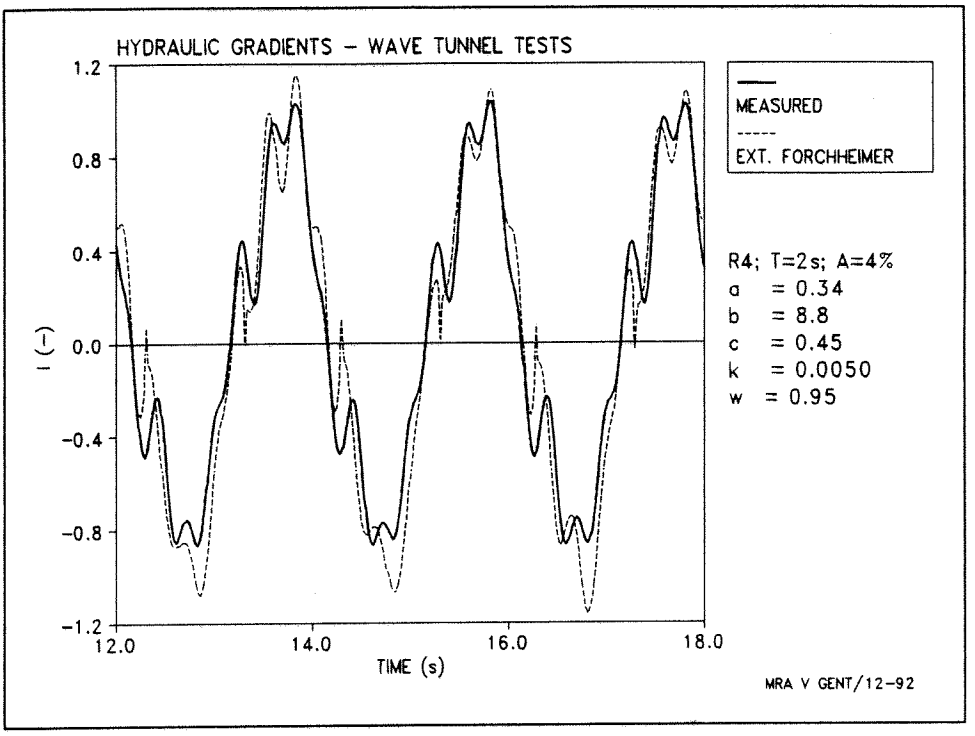
HYDRAULIC GRADIENTS – WAVE TUNNEL TESTS
1.2
0.8
0.4
0.0
-0.4
-0.8
-1.2
I (-)
12.0
14.0
16.0
18.0
TIME (s)
MEASURED
EXT. FORCHHEIMER
R4; T=2s; A=4%
a = 0.34
b = 8.8
c = 0.45
k = 0.0050
w = 0.95
MRA V GENT/12-92

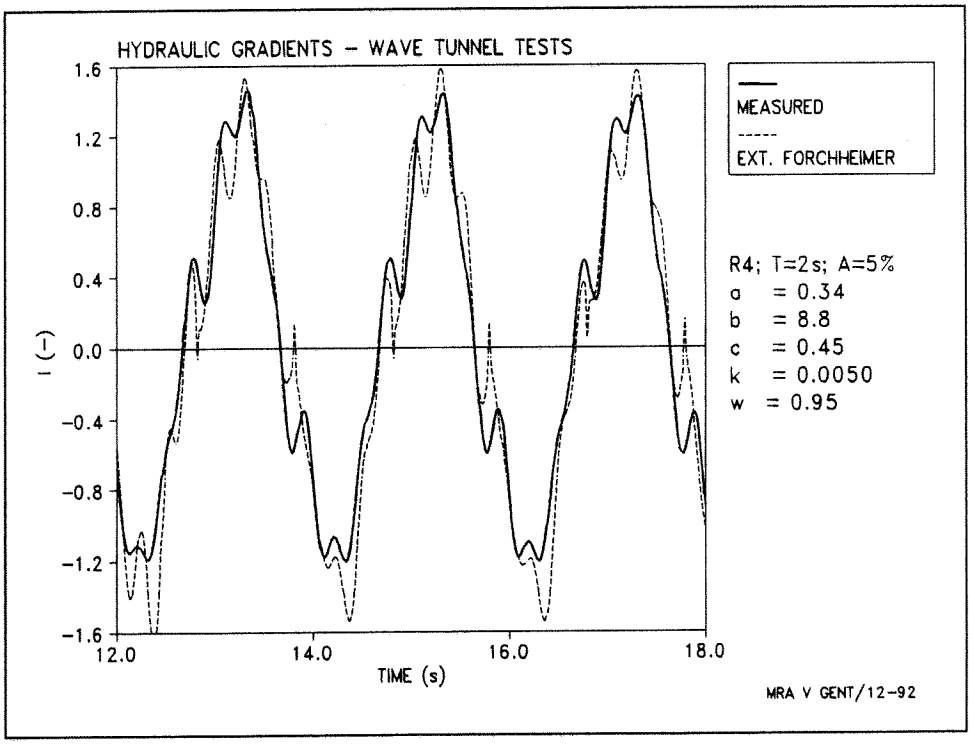
HYDRAULIC GRADIENTS – WAVE TUNNEL TESTS
1.6
1.2
0.8
0.4
0.0
-0.4
-0.8
-1.2
-1.6
I (-)
12.0
14.0
16.0
18.0
TIME (s)
MEASURED
EXT. FORCHHEIMER
R4; T=2s; A=5%
a = 0.34
b = 8.8
c = 0.45
k = 0.0050
w = 0.95
MRA V GENT/12-92

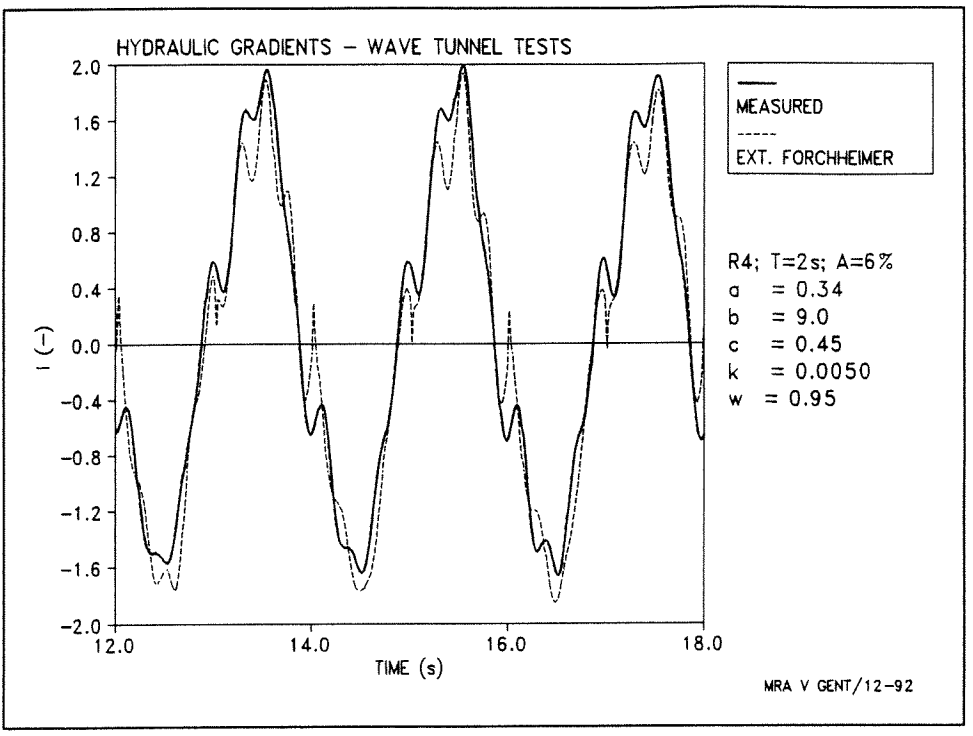
HYDRAULIC GRADIENTS – WAVE TUNNEL TESTS
2.0
1.6
1.2
0.8
0.4
0.0
-0.4
-0.8
-1.2
-1.6
-2.0
I (-)
12.0
14.0
16.0
18.0
TIME (s)
MEASURED
EXT. FORCHHEIMER
R4; T=2s; A=6%
a = 0.34
b = 9.0
c = 0.45
k = 0.0050
w = 0.95
MRA V GENT/12-92

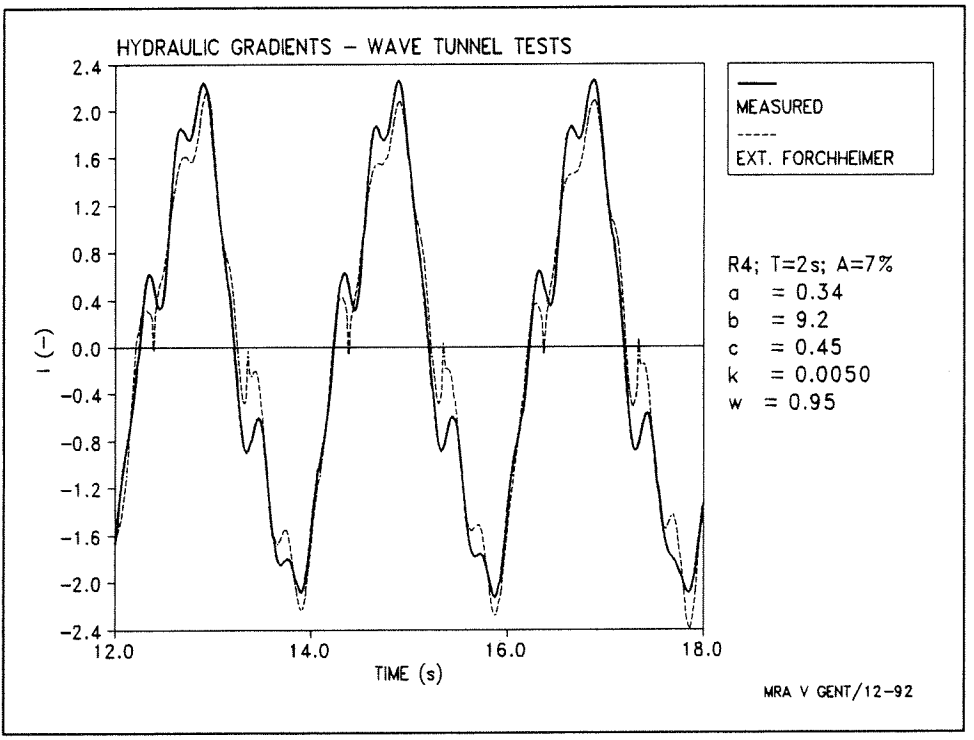
HYDRAULIC GRADIENTS – WAVE TUNNEL TESTS
2.4
2.0
1.6
1.2
0.8
0.4
0.0
-0.4
-0.8
-1.2
-1.6
-2.0
-2.4
I (-)
12.0
14.0
16.0
18.0
TIME (s)
MEASURED
EXT. FORCHHEIMER
R4; T=2s; A=7%
a = 0.34
b = 9.2
c = 0.45
k = 0.0050
w = 0.95
MRA V GENT/12-92

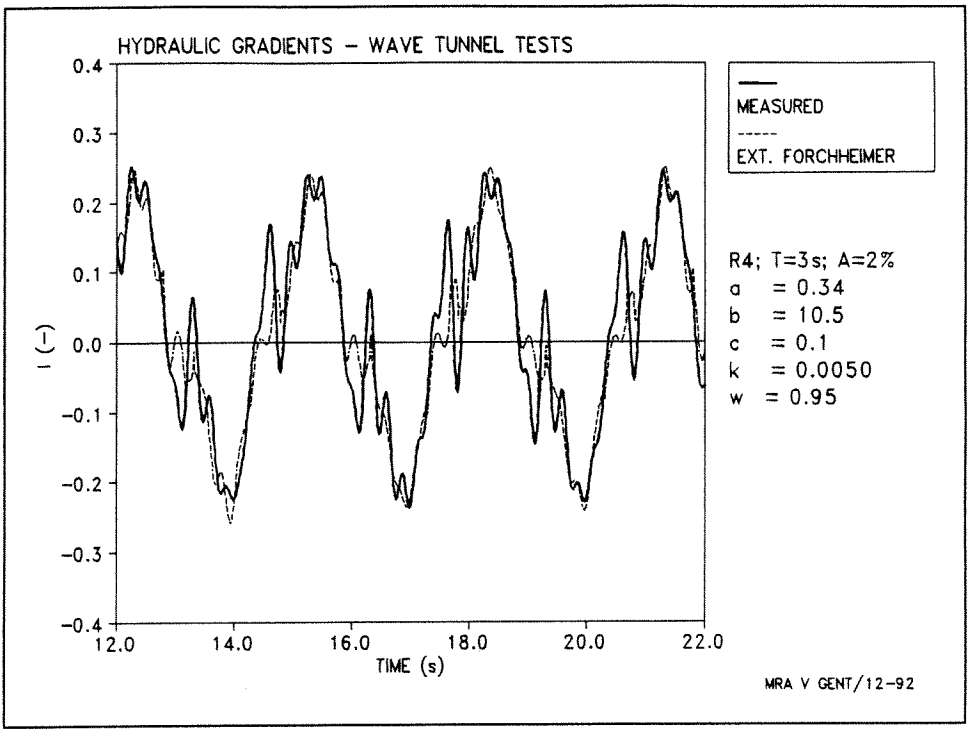
HYDRAULIC GRADIENTS – WAVE TUNNEL TESTS
0.4
0.3
0.2
0.1
0.0
−0.1
−0.2
−0.3
−0.4
I (-)
12.0
14.0
16.0
18.0
20.0
22.0
TIME (s)
MEASURED
EXT. FORCHHEIMER
R4; T=3s; A=2%
a = 0.34
b = 10.5
c = 0.1
k = 0.0050
w = 0.95
MRA V GENT/12-92

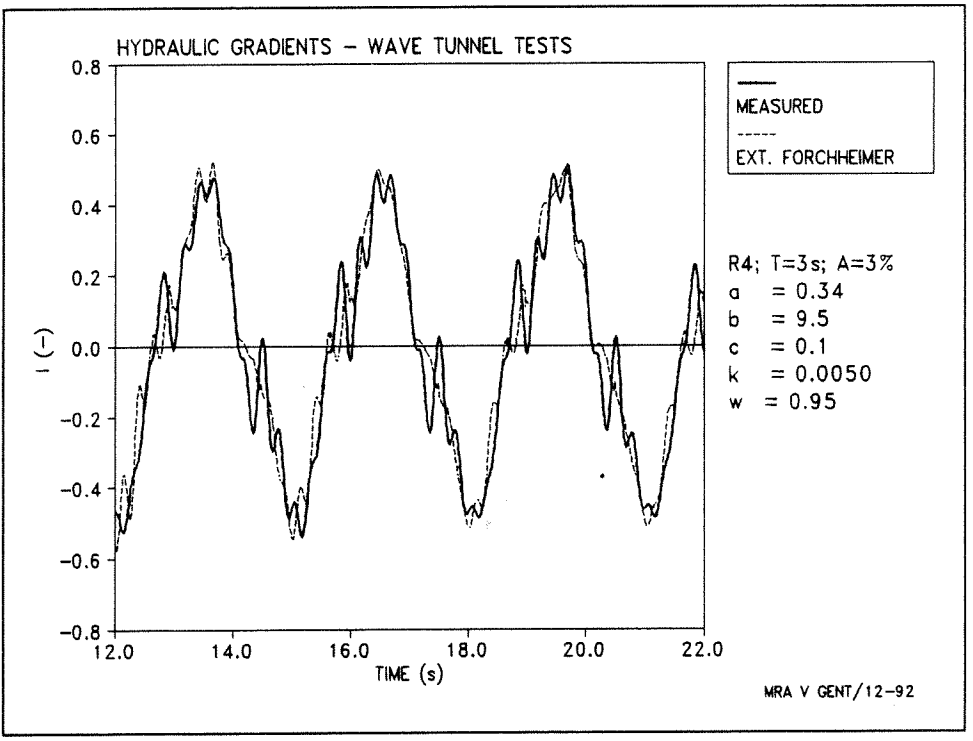
HYDRAULIC GRADIENTS – WAVE TUNNEL TESTS
0.8
0.6
0.4
0.2
0.0
−0.2
−0.4
−0.6
−0.8
I (-)
12.0
14.0
16.0
18.0
20.0
22.0
TIME (s)
MEASURED
EXT. FORCHHEIMER
R4; T=3s; A=3%
a = 0.34
b = 9.5
c = 0.1
k = 0.0050
w = 0.95
MRA V GENT/12-92

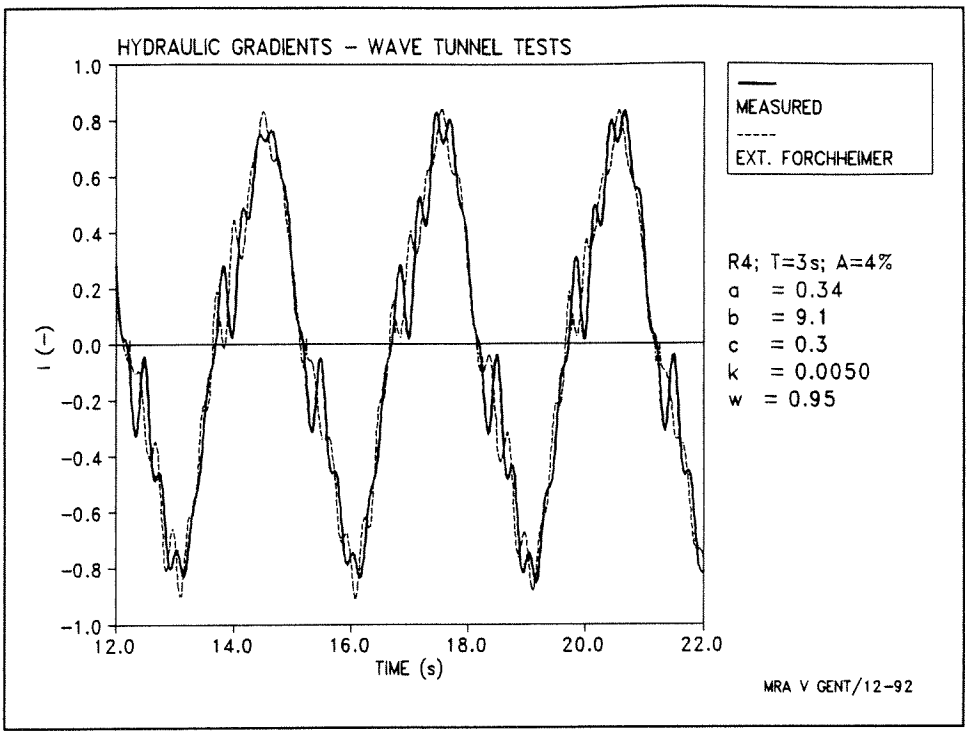
HYDRAULIC GRADIENTS – WAVE TUNNEL TESTS
1.0
0.8
0.6
0.4
0.2
0.0
-0.2
-0.4
-0.6
-0.8
-1.0
I (-)
12.0
14.0
16.0
18.0
20.0
22.0
TIME (s)
MEASURED
EXT. FORCHHEIMER
R4; T=3s; A=4%
a = 0.34
b = 9.1
c = 0.3
k = 0.0050
w = 0.95
MRA V GENT/12-92

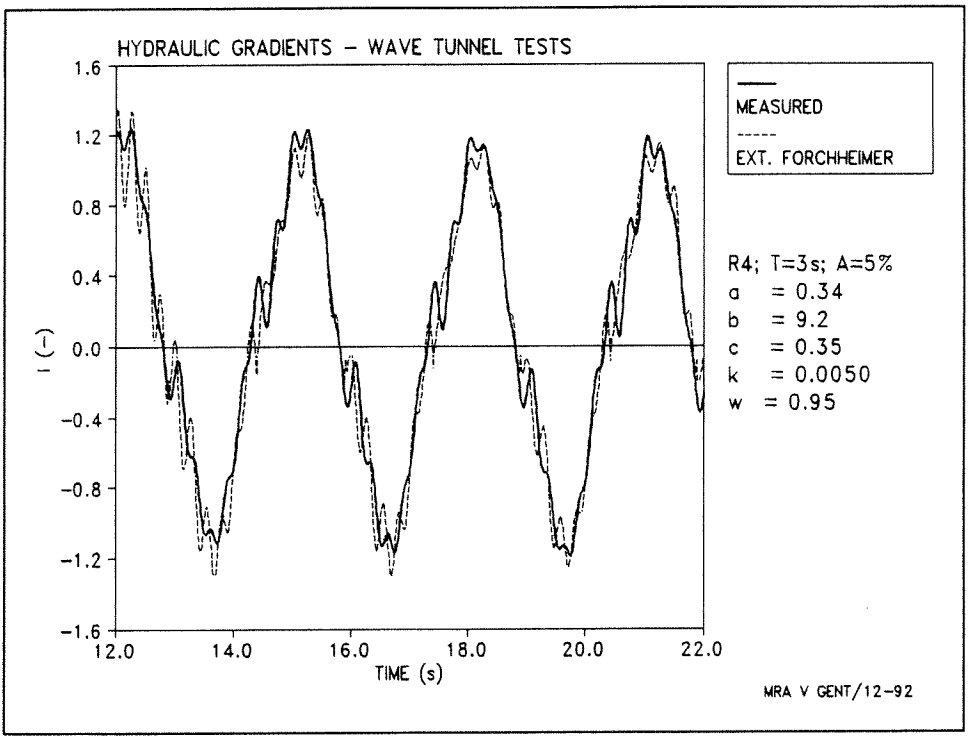
HYDRAULIC GRADIENTS – WAVE TUNNEL TESTS
1.6
1.2
0.8
0.4
0.0
-0.4
-0.8
-1.2
-1.6
I (-)
12.0
14.0
16.0
18.0
20.0
22.0
TIME (s)
MEASURED
EXT. FORCHHEIMER
R4; T=3s; A=5%
a = 0.34
b = 9.2
c = 0.35
k = 0.0050
w = 0.95
MRA V GENT/12-92

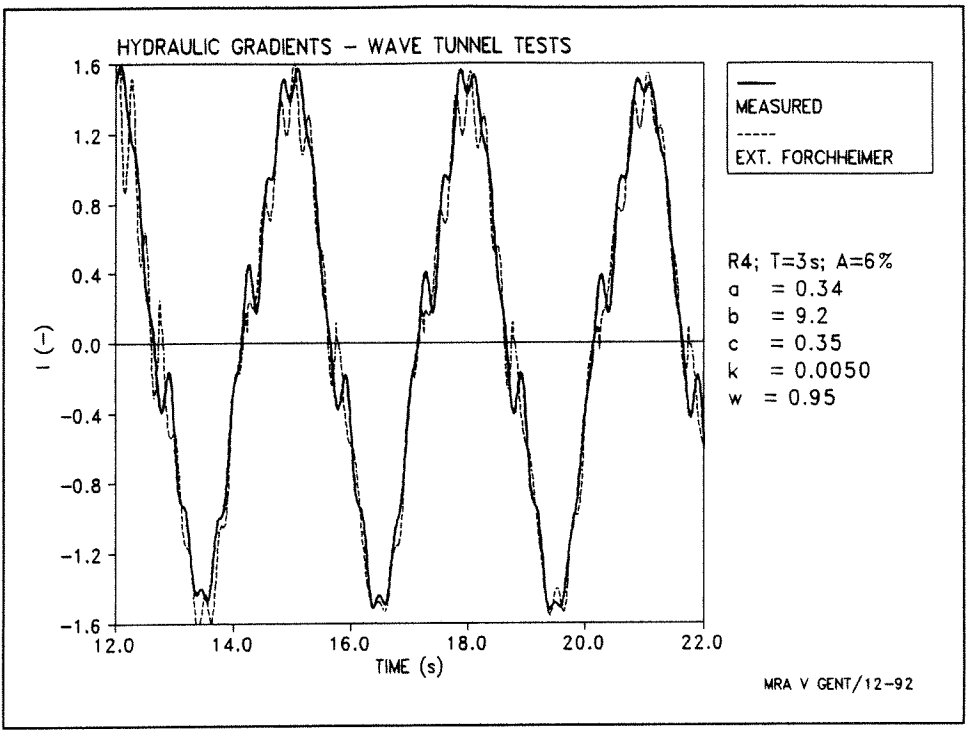
HYDRAULIC GRADIENTS – WAVE TUNNEL TESTS
I (-)
TIME (s)
MEASURED
EXT. FORCHHEIMER
R4; T=3s; A=6%
a = 0.34
b = 9.2
c = 0.35
k = 0.0050
w = 0.95
MRA V GENT/12-92

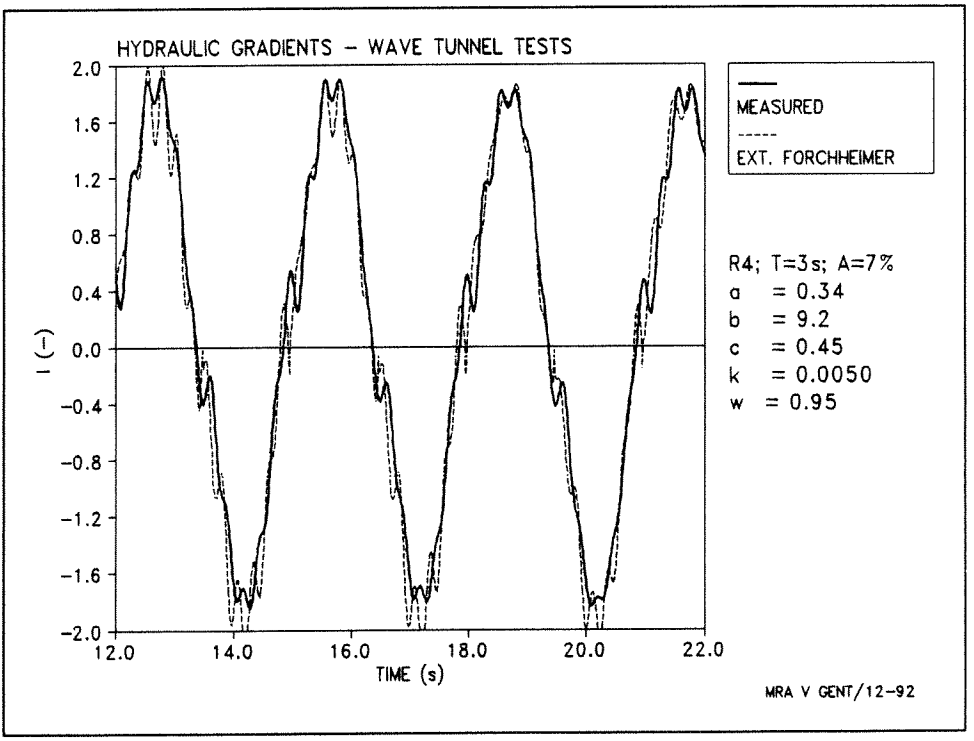
HYDRAULIC GRADIENTS – WAVE TUNNEL TESTS
I (-)
TIME (s)
MEASURED
EXT. FORCHHEIMER
R4; T=3s; A=7%
a = 0.34
b = 9.2
c = 0.45
k = 0.0050
w = 0.95
MRA V GENT/12-92

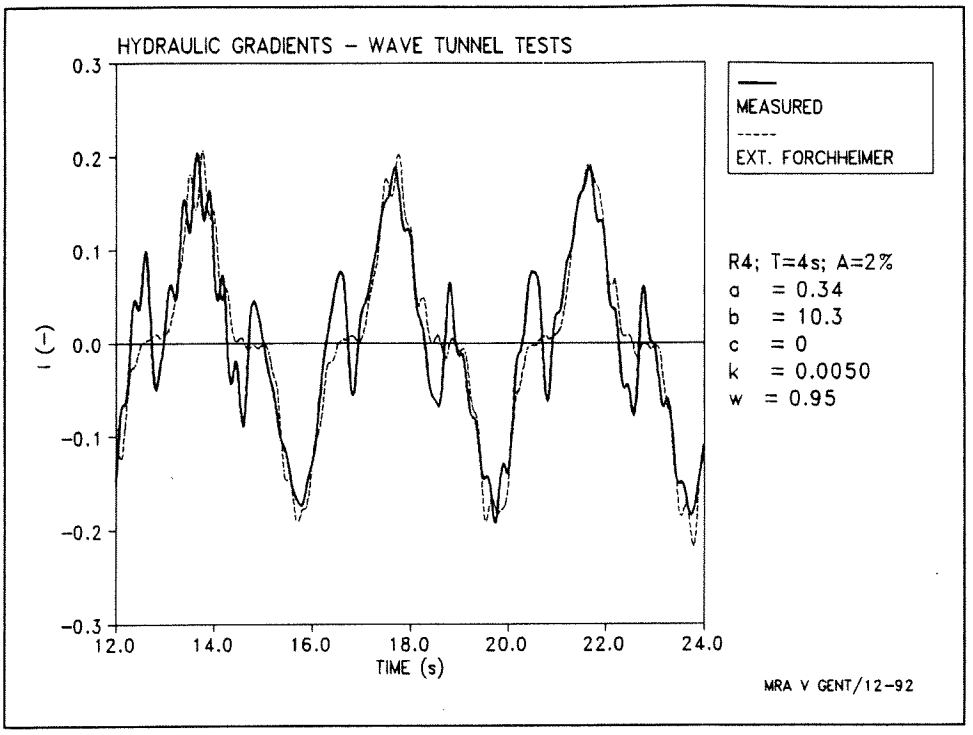
HYDRAULIC GRADIENTS – WAVE TUNNEL TESTS
I (-)
TIME (s)
MEASURED
EXT. FORCHHEIMER
R4; T=4s; A=2%
a = 0.34
b = 10.3
c = 0
k = 0.0050
w = 0.95
MRA V GENT/12-92

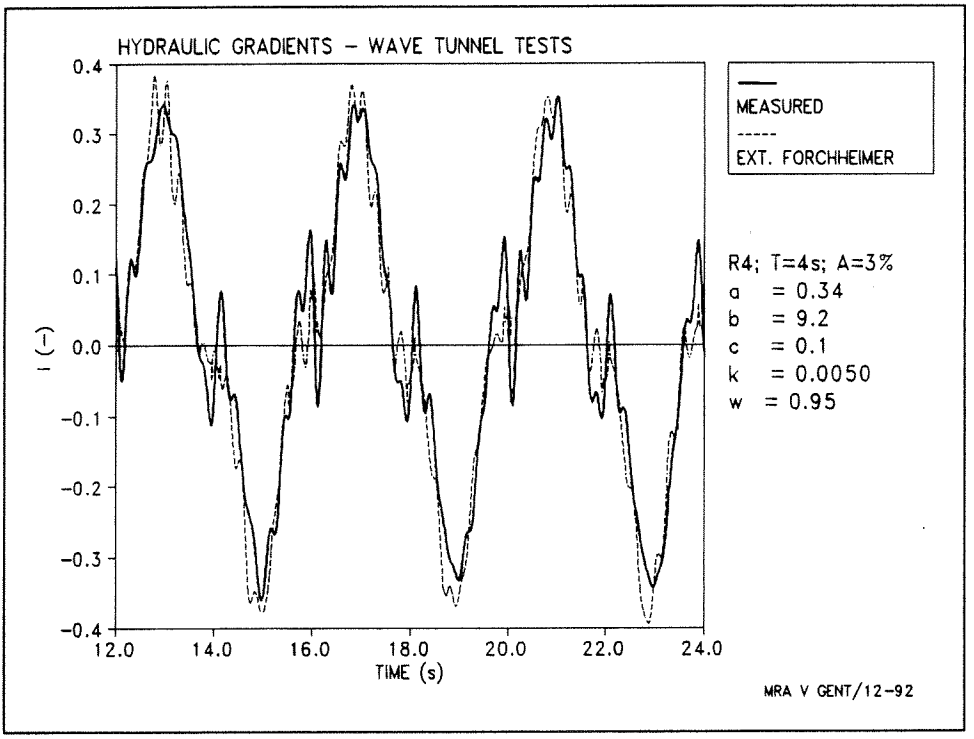
HYDRAULIC GRADIENTS – WAVE TUNNEL TESTS
I (-)
TIME (s)
MEASURED
EXT. FORCHHEIMER
R4; T=4s; A=3%
a = 0.34
b = 9.2
c = 0.1
k = 0.0050
w = 0.95
MRA V GENT/12-92

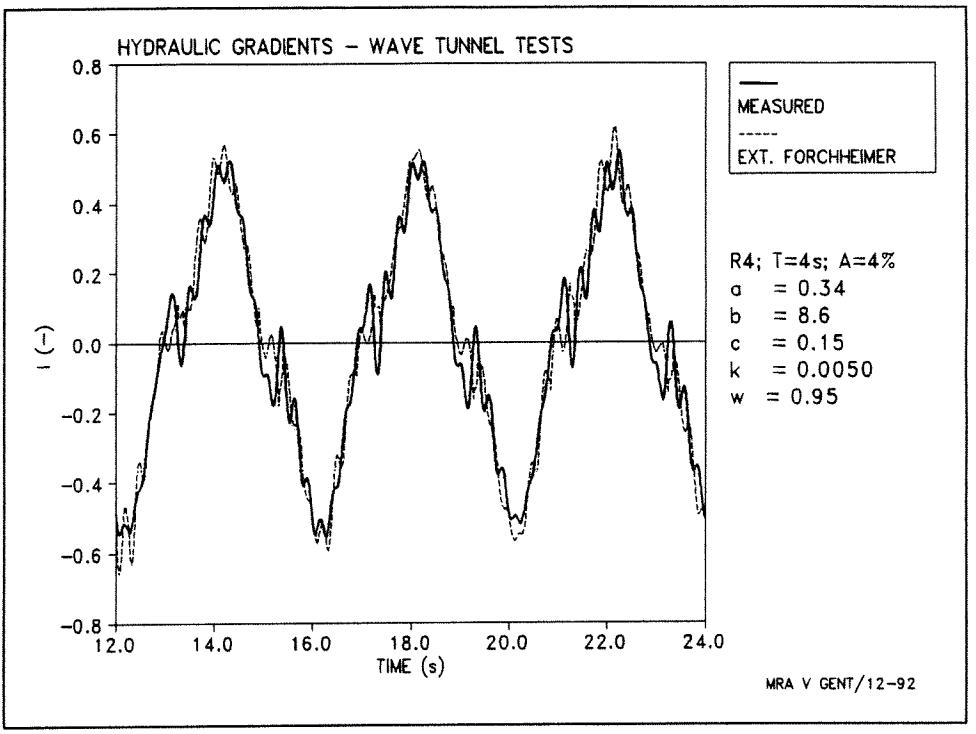
HYDRAULIC GRADIENTS – WAVE TUNNEL TESTS
i (-)
TIME (s)
MEASURED
EXT. FORCHHEIMER
R4; T=4s; A=4%
a = 0.34
b = 8.6
c = 0.15
k = 0.0050
w = 0.95
MRA V GENT/12-92

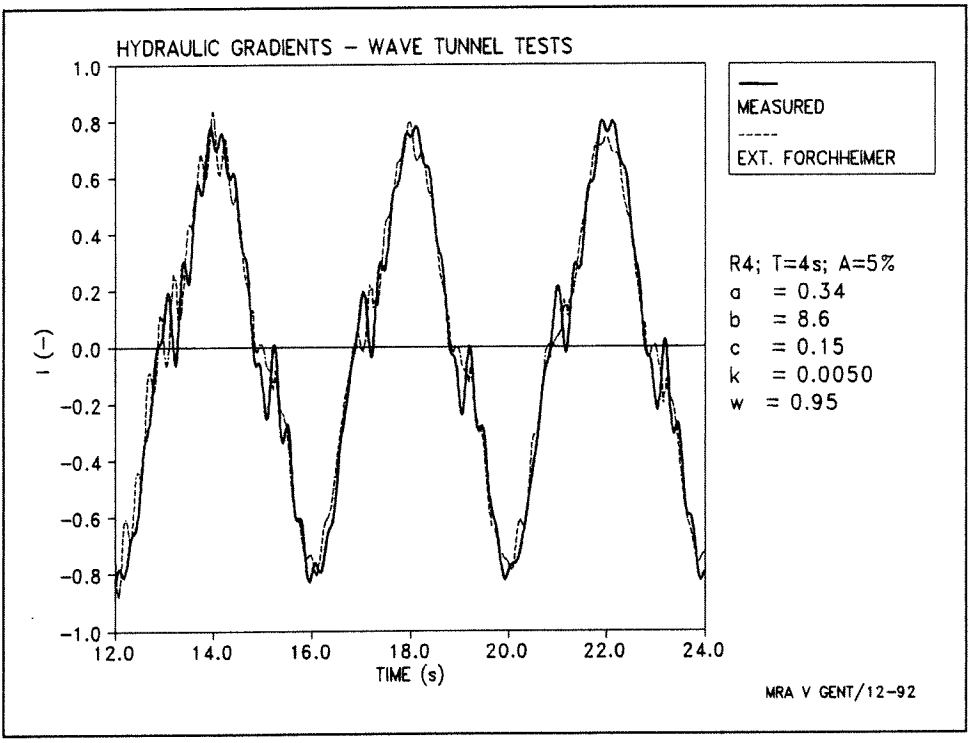
HYDRAULIC GRADIENTS – WAVE TUNNEL TESTS
i (-)
TIME (s)
MEASURED
EXT. FORCHHEIMER
R4; T=4s; A=5%
a = 0.34
b = 8.6
c = 0.15
k = 0.0050
w = 0.95
MRA V GENT/12-92

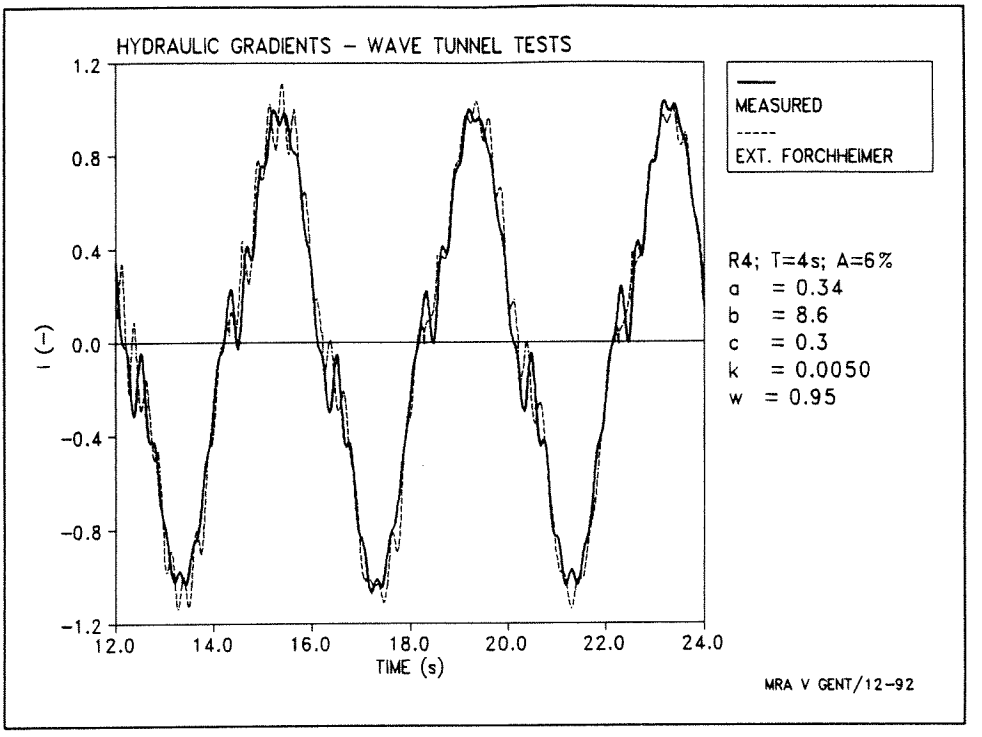
HYDRAULIC GRADIENTS – WAVE TUNNEL TESTS
1.2
0.8
0.4
0.0
-0.4
-0.8
-1.2
I (-)
12.0
14.0
16.0
18.0
20.0
22.0
24.0
TIME (s)
MEASURED
EXT. FORCHHEIMER
R4; T=4s; A=6%
a = 0.34
b = 8.6
c = 0.3
k = 0.0050
w = 0.95
MRA V GENT/12-92

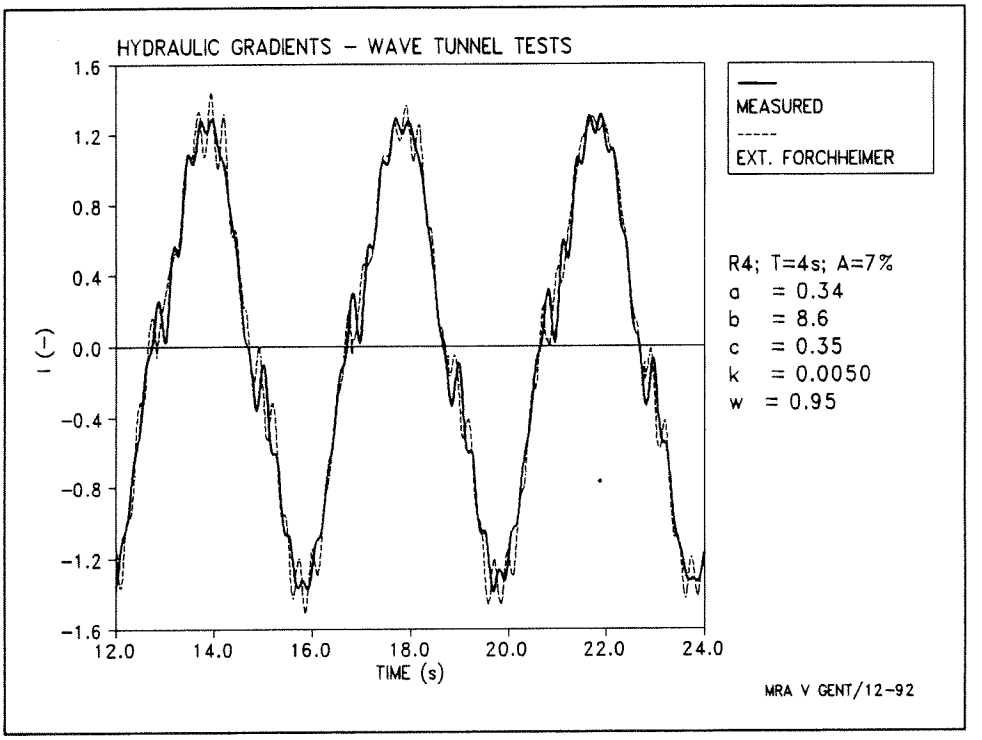
HYDRAULIC GRADIENTS – WAVE TUNNEL TESTS
1.6
1.2
0.8
0.4
0.0
-0.4
-0.8
-1.2
-1.6
I (-)
12.0
14.0
16.0
18.0
20.0
22.0
24.0
TIME (s)
MEASURED
EXT. FORCHHEIMER
R4; T=4s; A=7%
a = 0.34
b = 8.6
c = 0.35
k = 0.0050
w = 0.95
MRA V GENT/12-92

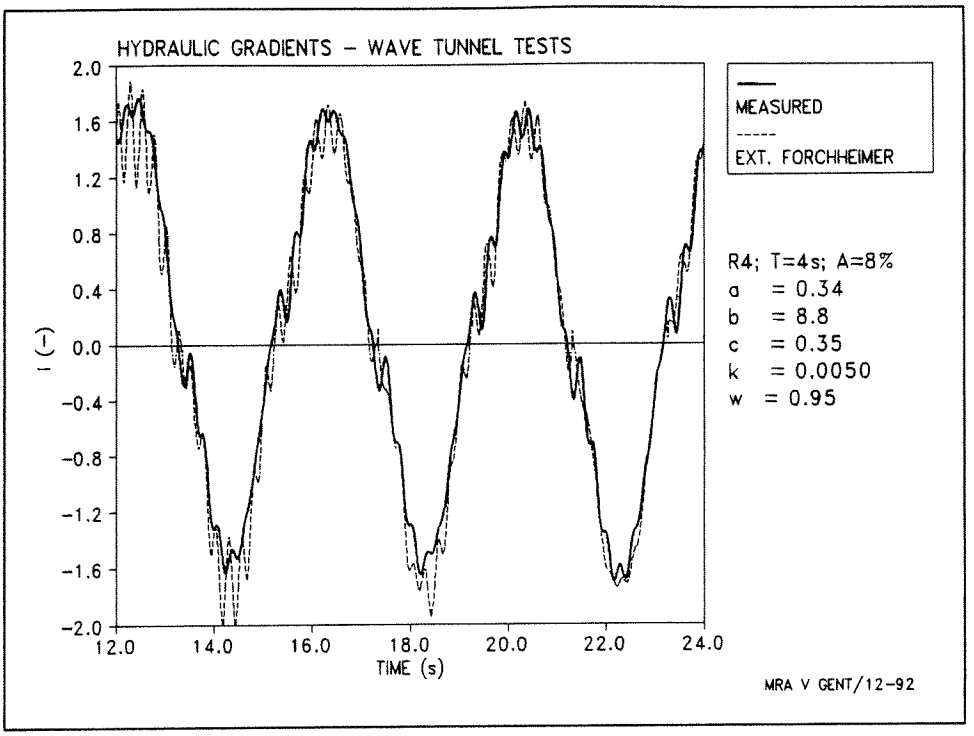
HYDRAULIC GRADIENTS – WAVE TUNNEL TESTS
I (-)
TIME (s)
MEASURED
EXT. FORCHHEIMER
R4; T=4s; A=8%
a = 0.34
b = 8.8
c = 0.35
k = 0.0050
w = 0.95
MRA V GENT/12-92

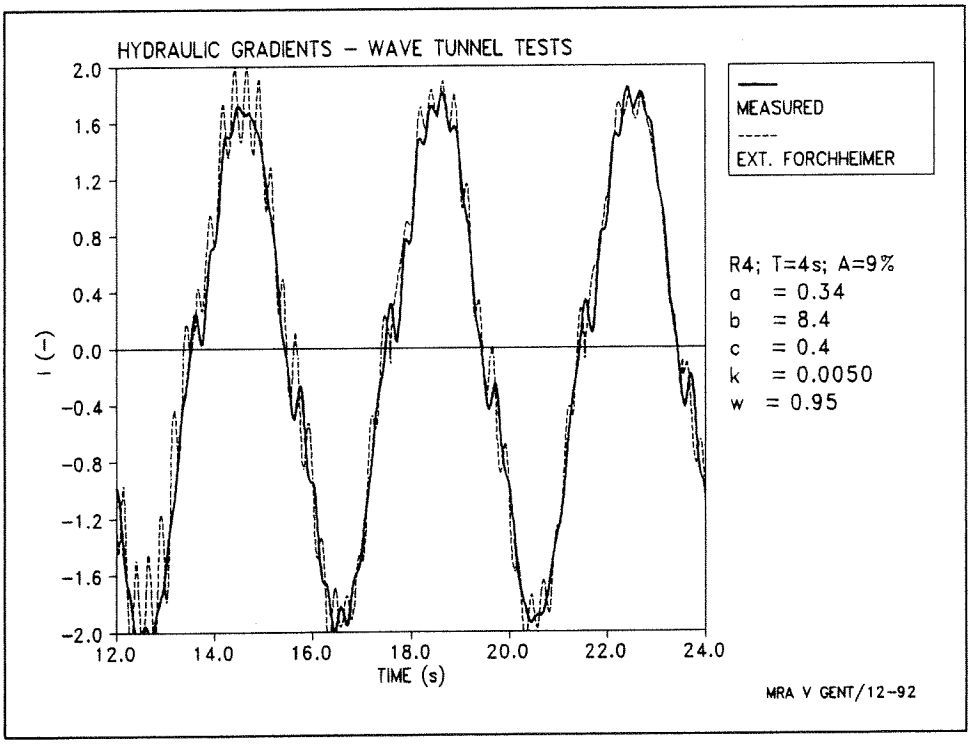
HYDRAULIC GRADIENTS – WAVE TUNNEL TESTS
I (-)
TIME (s)
MEASURED
EXT. FORCHHEIMER
R4; T=4s; A=9%
a = 0.34
b = 8.4
c = 0.4
k = 0.0050
w = 0.95
MRA V GENT/12-92

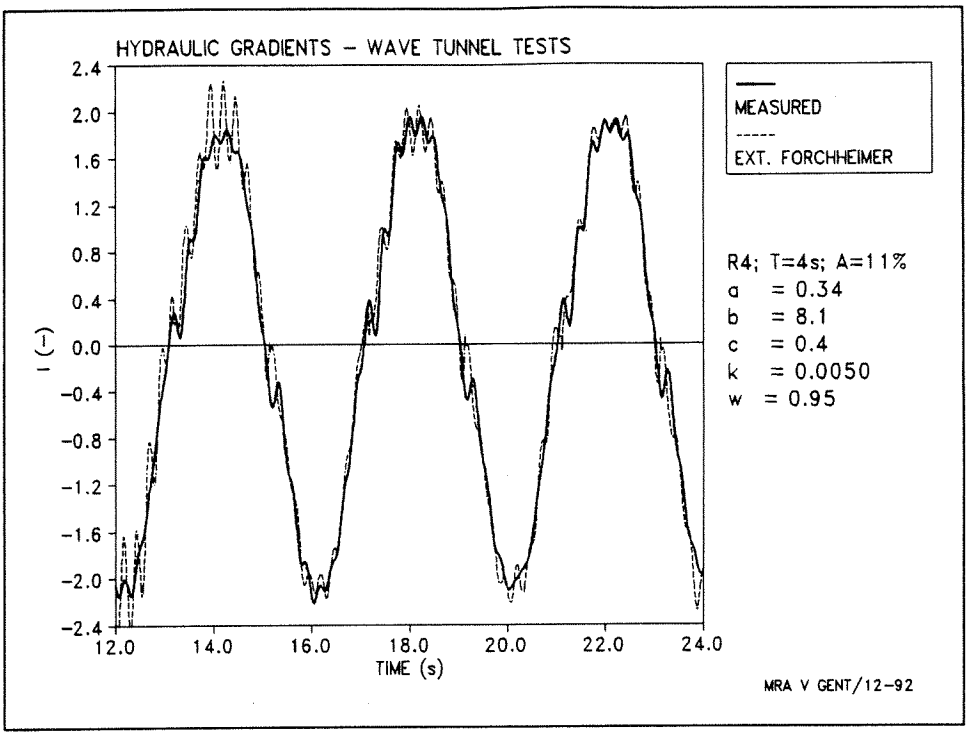
HYDRAULIC GRADIENTS – WAVE TUNNEL TESTS
I (-)
TIME (s)
MEASURED
EXT. FORCHHEIMER
R4; T=4s; A=11%
a = 0.34
b = 8.1
c = 0.4
k = 0.0050
w = 0.95
MRA V GENT/12-92

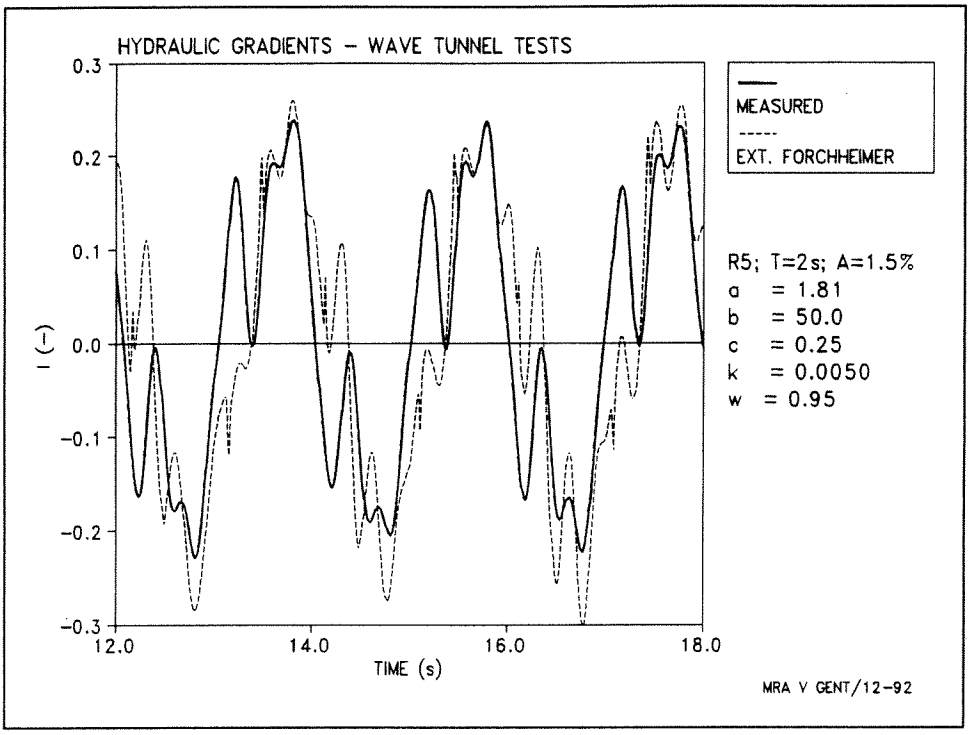
HYDRAULIC GRADIENTS – WAVE TUNNEL TESTS
0.3
0.2
0.1
0.0
-0.1
-0.2
-0.3
I (-)
12.0
14.0
16.0
18.0
TIME (s)
MEASURED
EXT. FORCHHEIMER
R5; T=2s; A=1.5%
a = 1.81
b = 50.0
c = 0.25
k = 0.0050
w = 0.95
MRA V GENT/12-92

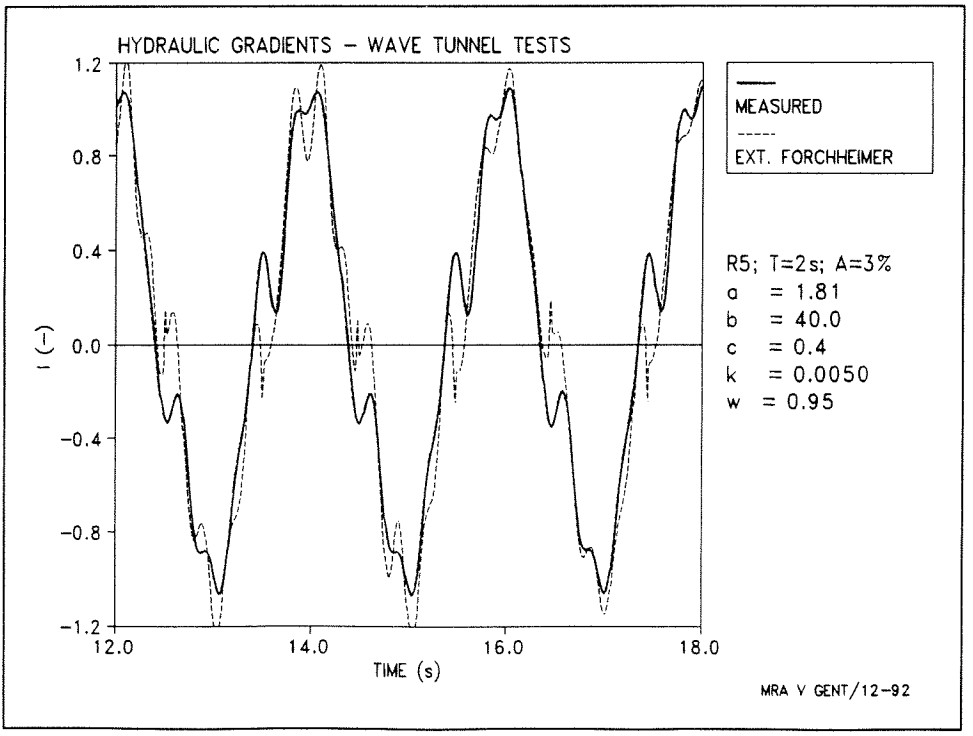
HYDRAULIC GRADIENTS – WAVE TUNNEL TESTS
1.2
0.8
0.4
0.0
-0.4
-0.8
-1.2
I (-)
12.0
14.0
16.0
18.0
TIME (s)
MEASURED
EXT. FORCHHEIMER
R5; T=2s; A=3%
a = 1.81
b = 40.0
c = 0.4
k = 0.0050
w = 0.95
MRA V GENT/12-92

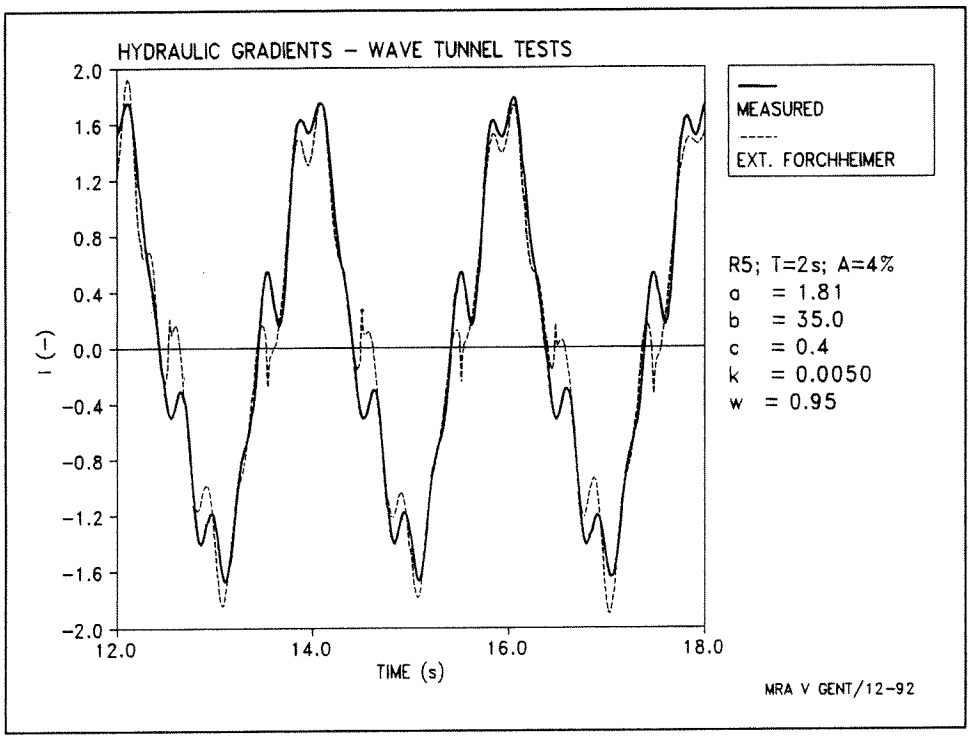
HYDRAULIC GRADIENTS – WAVE TUNNEL TESTS
2.0
1.6
1.2
0.8
0.4
0.0
-0.4
-0.8
-1.2
-1.6
-2.0
i (-)
12.0
14.0
16.0
18.0
TIME (s)
MEASURED
EXT. FORCHHEIMER
R5; T=2s; A=4%
a = 1.81
b = 35.0
c = 0.4
k = 0.0050
w = 0.95
MRA V GENT/12-92

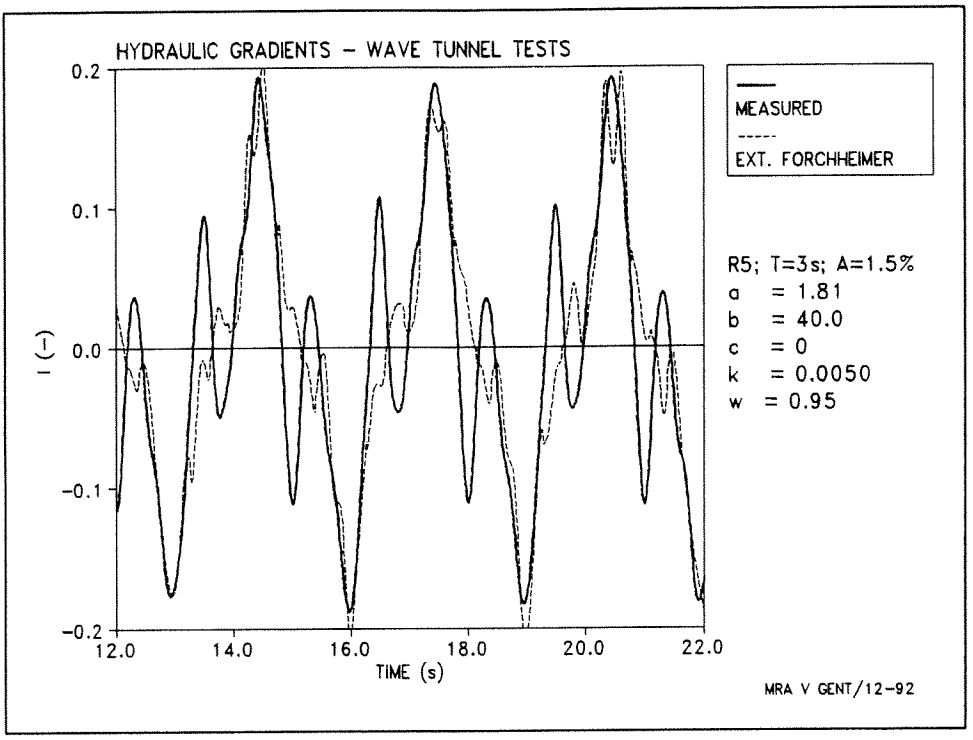
HYDRAULIC GRADIENTS – WAVE TUNNEL TESTS
0.2
0.1
0.0
-0.1
-0.2
I (-)
12.0
14.0
16.0
18.0
20.0
22.0
TIME (s)
MEASURED
EXT. FORCHHEIMER
R5; T=3s; A=1.5%
a = 1.81
b = 40.0
c = 0
k = 0.0050
w = 0.95
MRA V GENT/12-92

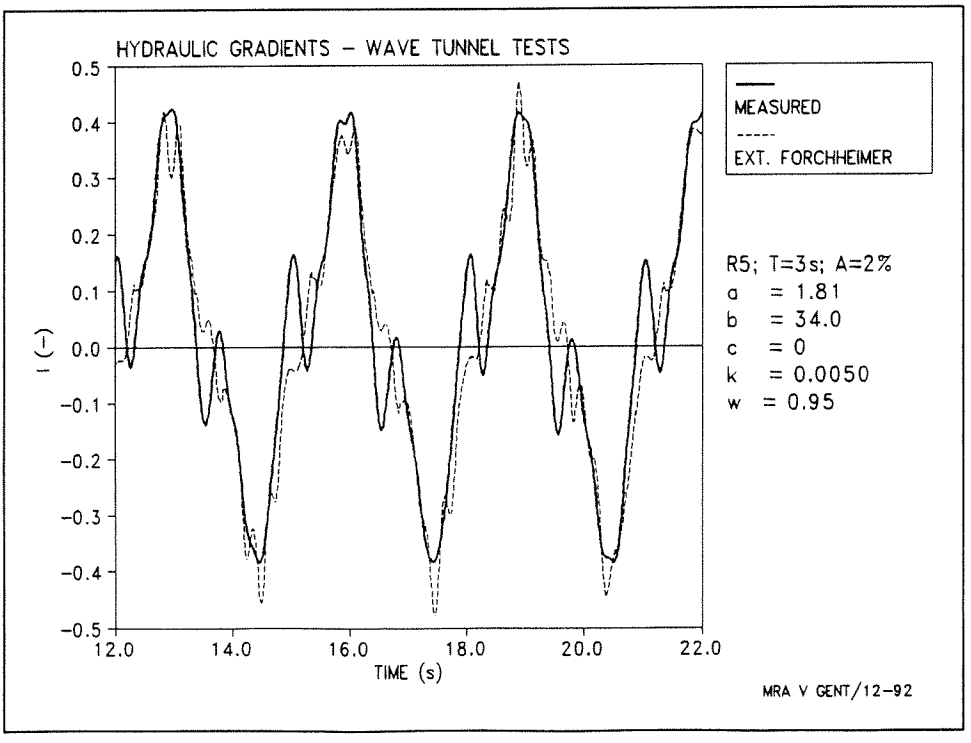
HYDRAULIC GRADIENTS – WAVE TUNNEL TESTS
0.5
0.4
0.3
0.2
0.1
0.0
-0.1
-0.2
-0.3
-0.4
-0.5
I (-)
12.0
14.0
16.0
18.0
20.0
22.0
TIME (s)
MEASURED
EXT. FORCHHEIMER
R5; T=3s; A=2%
a = 1.81
b = 34.0
c = 0
k = 0.0050
w = 0.95
MRA V GENT/12-92

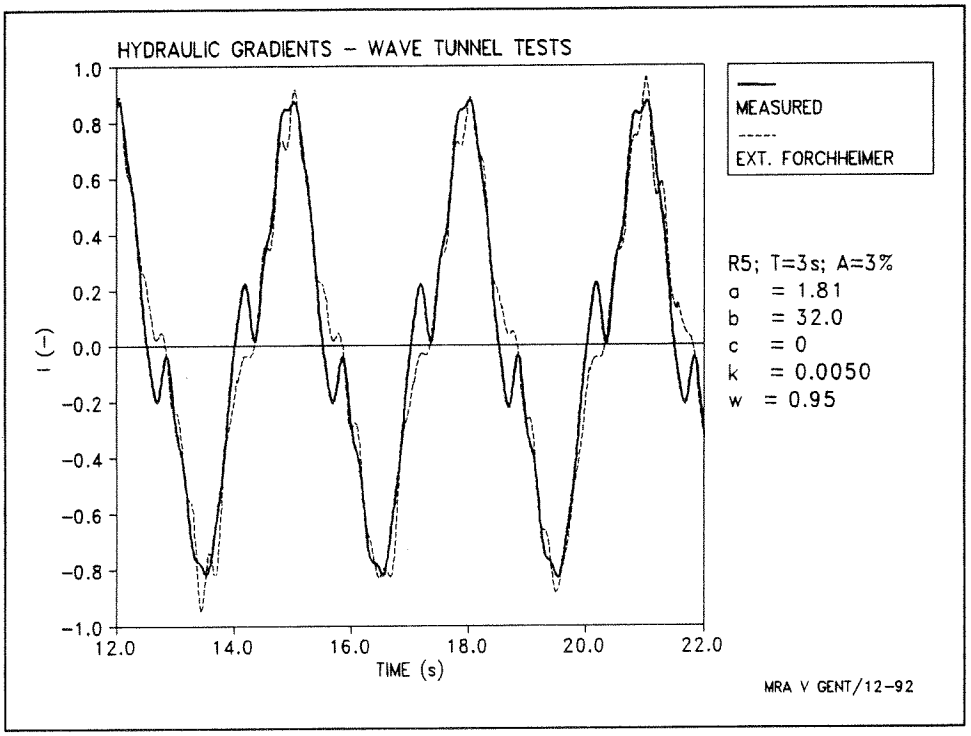
HYDRAULIC GRADIENTS – WAVE TUNNEL TESTS
1.0
0.8
0.6
0.4
0.2
0.0
-0.2
-0.4
-0.6
-0.8
-1.0
i (-)
12.0
14.0
16.0
18.0
20.0
22.0
TIME (s)
MEASURED
EXT. FORCHHEIMER
R5; T=3s; A=3%
a = 1.81
b = 32.0
c = 0
k = 0.0050
w = 0.95
MRA V GENT/12-92

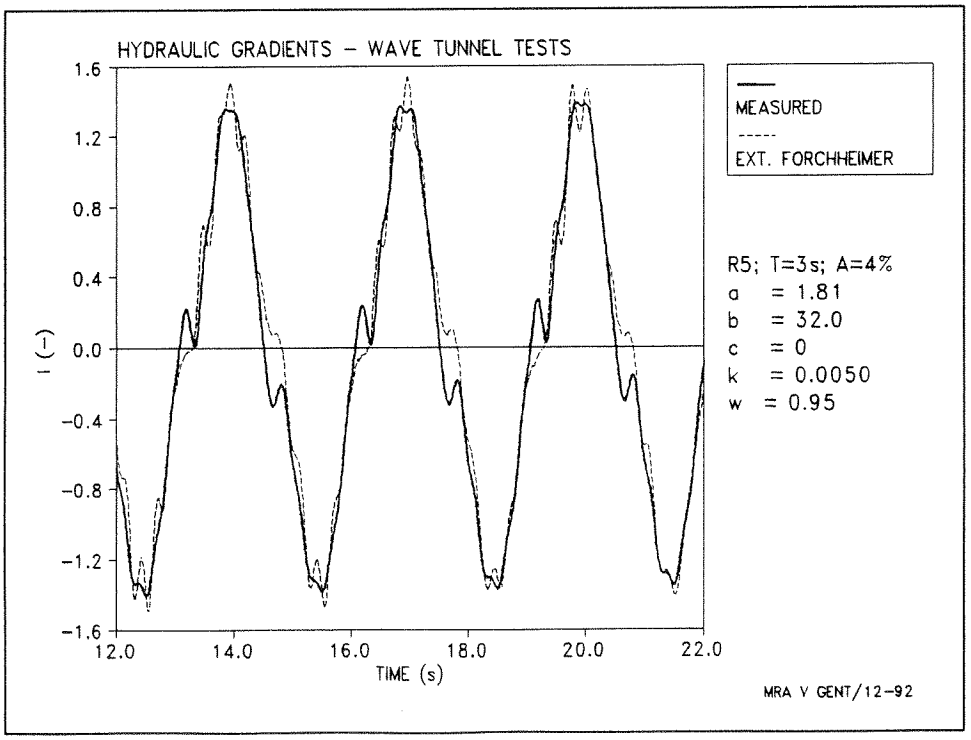
HYDRAULIC GRADIENTS – WAVE TUNNEL TESTS
1.6
1.2
0.8
0.4
0.0
-0.4
-0.8
-1.2
-1.6
i (-)
12.0
14.0
16.0
18.0
20.0
22.0
TIME (s)
MEASURED
EXT. FORCHHEIMER
R5; T=3s; A=4%
a = 1.81
b = 32.0
c = 0
k = 0.0050
w = 0.95
MRA V GENT/12-92

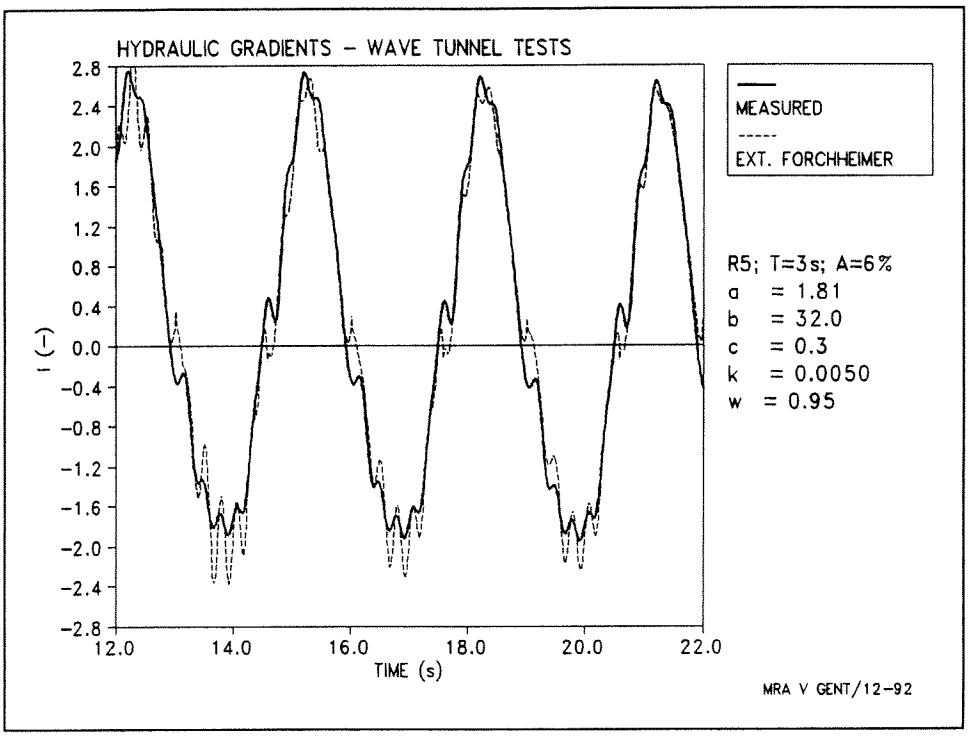
HYDRAULIC GRADIENTS - WAVE TUNNEL TESTS
i (-)
2.8
2.4
2.0
1.6
1.2
0.8
0.4
0.0
-0.4
-0.8
-1.2
-1.6
-2.0
-2.4
-2.8
12.0
14.0
16.0
18.0
20.0
22.0
TIME (s)
MEASURED
EXT. FORCHHEIMER
R5; T=3s; A=6%
a = 1.81
b = 32.0
c = 0.3
k = 0.0050
w = 0.95
MRA V GENT/12-92

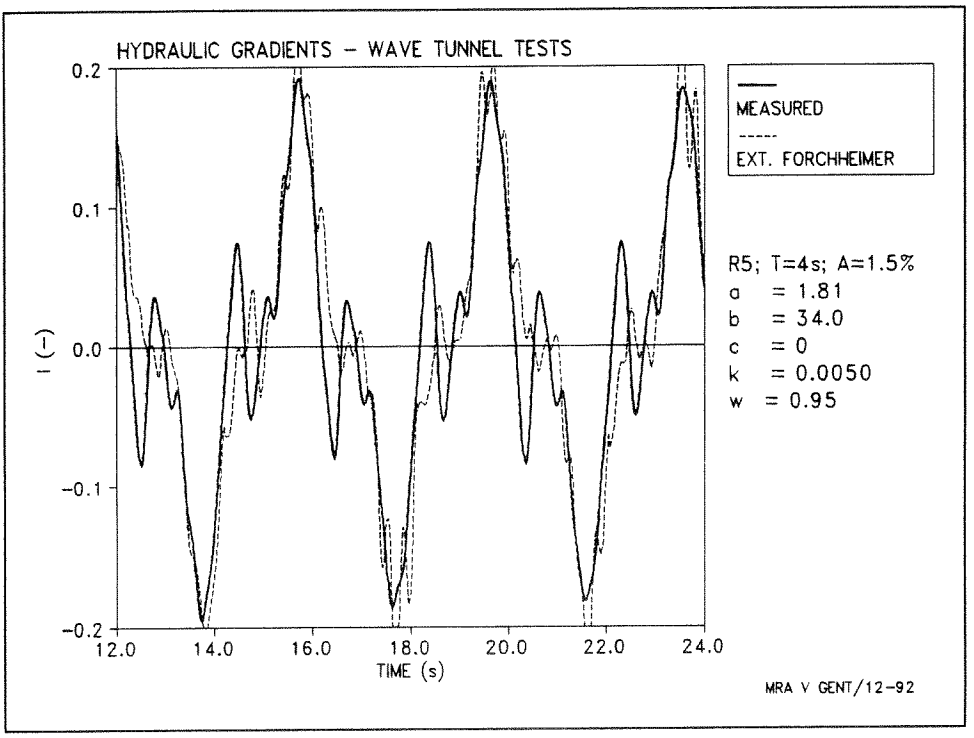
HYDRAULIC GRADIENTS – WAVE TUNNEL TESTS
0.2
0.1
0.0
-0.1
-0.2
I (-)
12.0
14.0
16.0
18.0
20.0
22.0
24.0
TIME (s)
MEASURED
EXT. FORCHHEIMER
R5; T=4s; A=1.5%
a = 1.81
b = 34.0
c = 0
k = 0.0050
w = 0.95
MRA V GENT/12-92

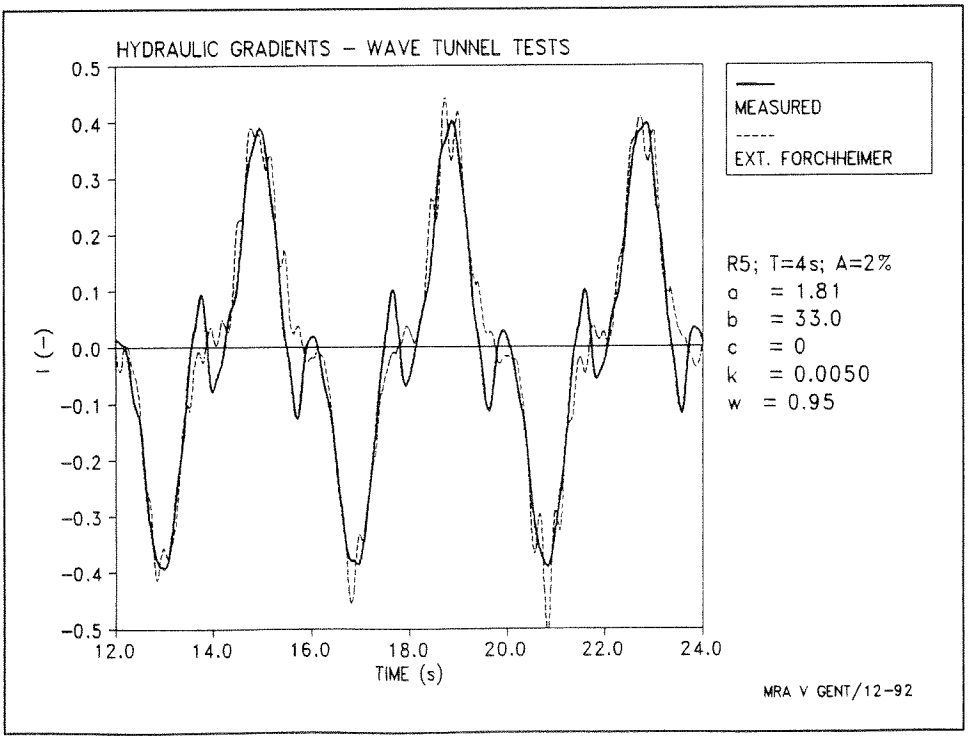
HYDRAULIC GRADIENTS – WAVE TUNNEL TESTS
0.5
0.4
0.3
0.2
0.1
0.0
-0.1
-0.2
-0.3
-0.4
-0.5
I (-)
12.0
14.0
16.0
18.0
20.0
22.0
24.0
TIME (s)
MEASURED
EXT. FORCHHEIMER
R5; T=4s; A=2%
a = 1.81
b = 33.0
c = 0
k = 0.0050
w = 0.95
MRA V GENT/12-92

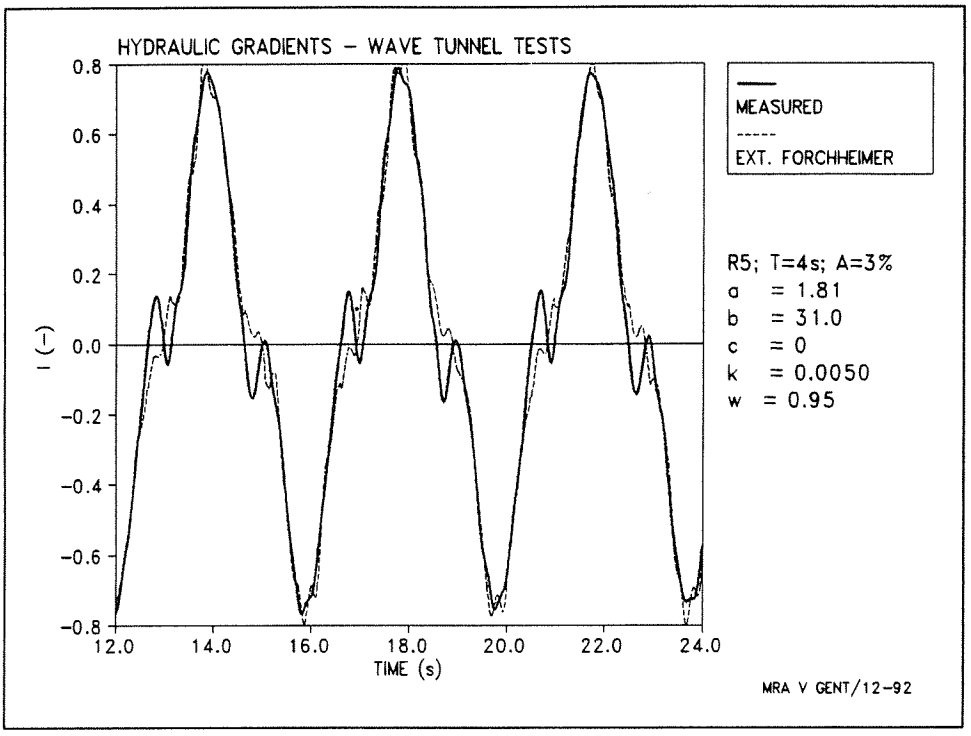
HYDRAULIC GRADIENTS – WAVE TUNNEL TESTS
I (–)
TIME (s)
MEASURED
EXT. FORCHHEIMER
R5; T=4s; A=3%
a = 1.81
b = 31.0
c = 0
k = 0.0050
w = 0.95
MRA V GENT/12-92

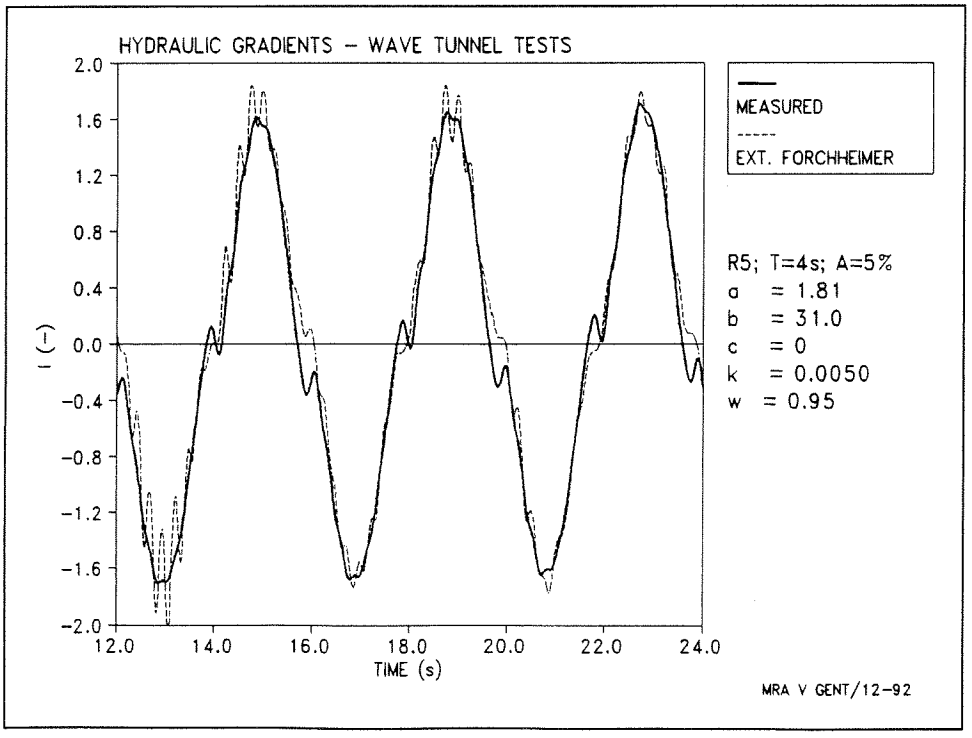
HYDRAULIC GRADIENTS – WAVE TUNNEL TESTS
I (–)
TIME (s)
MEASURED
EXT. FORCHHEIMER
R5; T=4s; A=5%
a = 1.81
b = 31.0
c = 0
k = 0.0050
w = 0.95
MRA V GENT/12-92

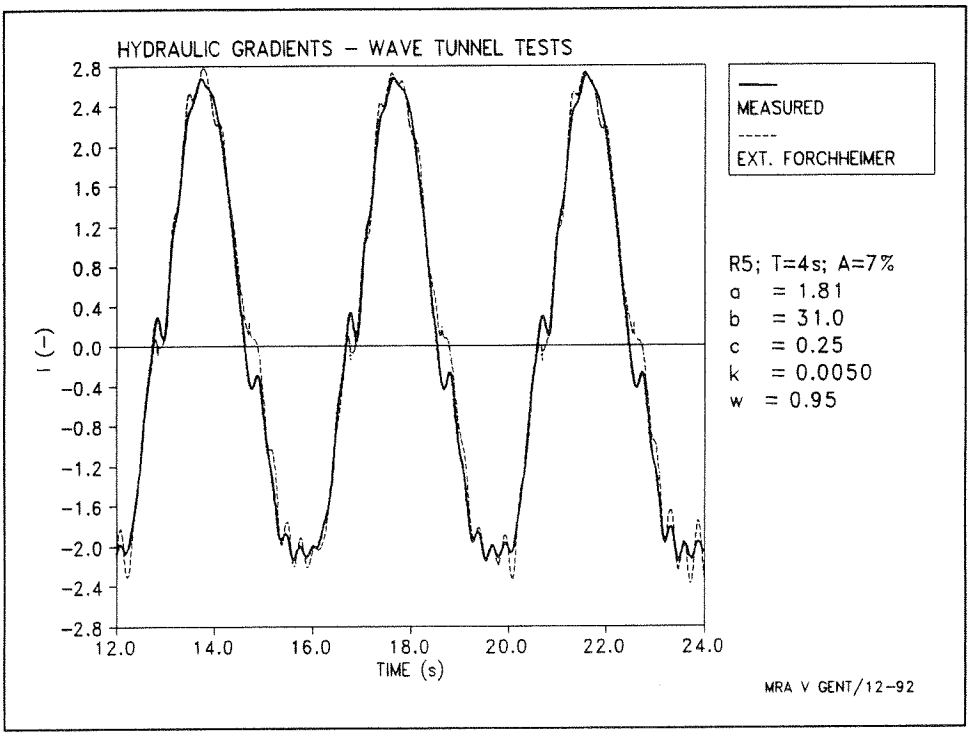
HYDRAULIC GRADIENTS – WAVE TUNNEL TESTS
I (-)
TIME (s)
MEASURED
EXT. FORCHHEIMER
R5; T=4s; A=7%
a = 1.81
b = 31.0
c = 0.25
k = 0.0050
w = 0.95
MRA V GENT/12-92

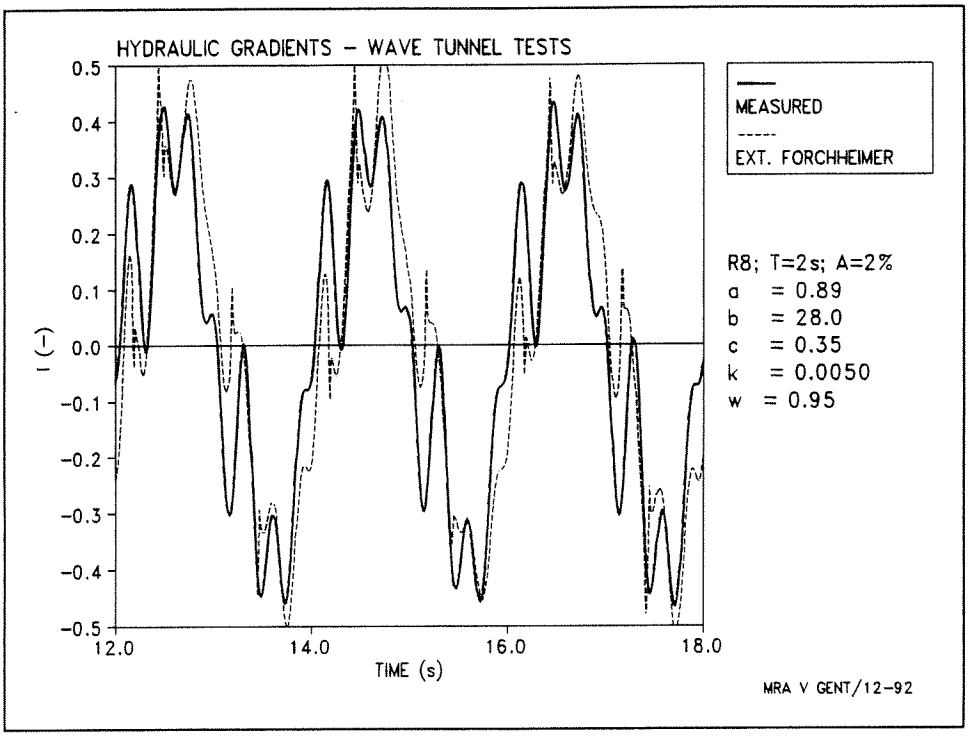
HYDRAULIC GRADIENTS – WAVE TUNNEL TESTS
0.5
0.4
0.3
0.2
0.1
0.0
-0.1
-0.2
-0.3
-0.4
-0.5
I (-)
12.0
14.0
16.0
18.0
TIME (s)
MEASURED
EXT. FORCHHEIMER
R8; T=2s; A=2%
a = 0.89
b = 28.0
c = 0.35
k = 0.0050
w = 0.95
MRA V GENT/12-92

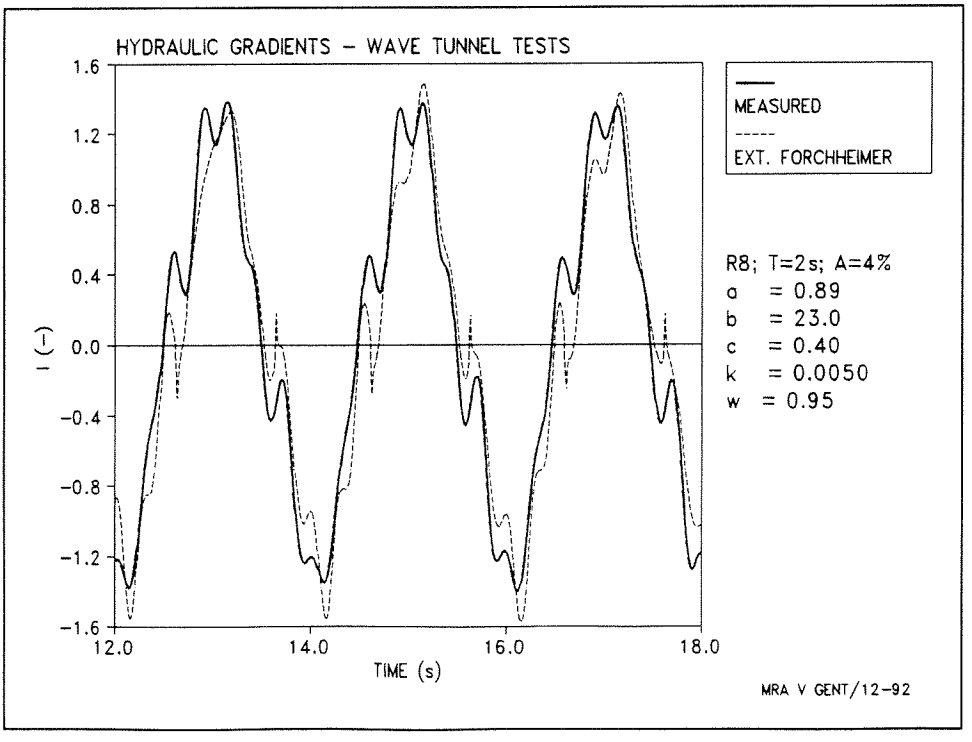
HYDRAULIC GRADIENTS – WAVE TUNNEL TESTS
1.6
1.2
0.8
0.4
0.0
-0.4
-0.8
-1.2
-1.6
I (-)
12.0
14.0
16.0
18.0
TIME (s)
MEASURED
EXT. FORCHHEIMER
R8; T=2s; A=4%
a = 0.89
b = 23.0
c = 0.40
k = 0.0050
w = 0.95
MRA V GENT/12-92

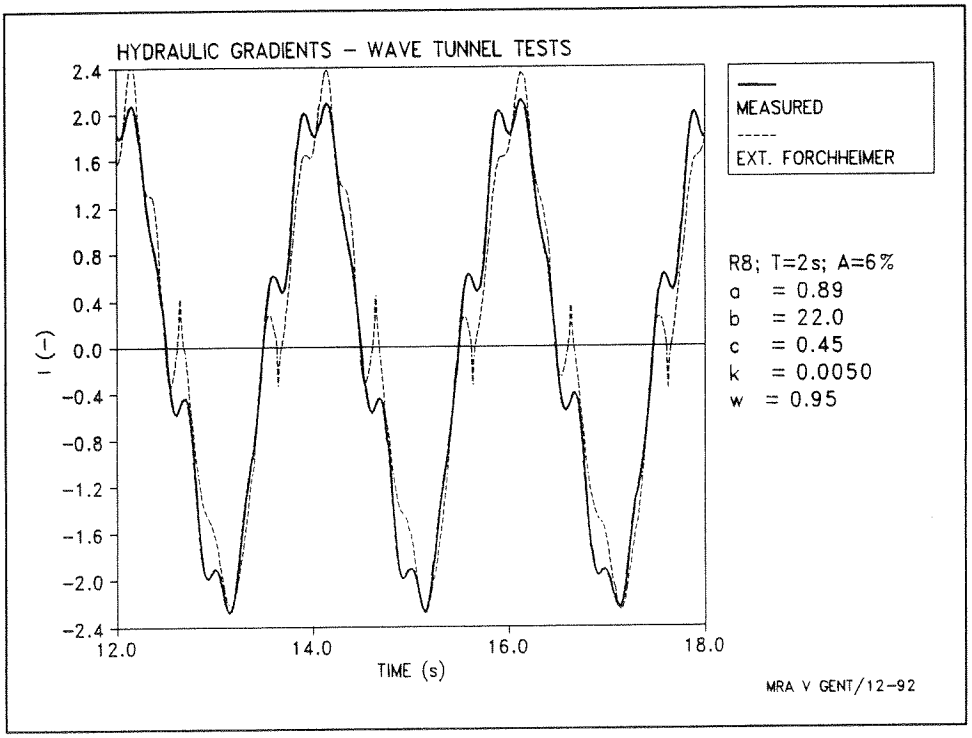
HYDRAULIC GRADIENTS – WAVE TUNNEL TESTS
2.4
2.0
1.6
1.2
0.8
0.4
0.0
-0.4
-0.8
-1.2
-1.6
-2.0
-2.4
I (-)
12.0
14.0
16.0
18.0
TIME (s)
MEASURED
EXT. FORCHHEIMER
R8; T=2s; A=6%
a = 0.89
b = 22.0
c = 0.45
k = 0.0050
w = 0.95
MRA V GENT/12-92

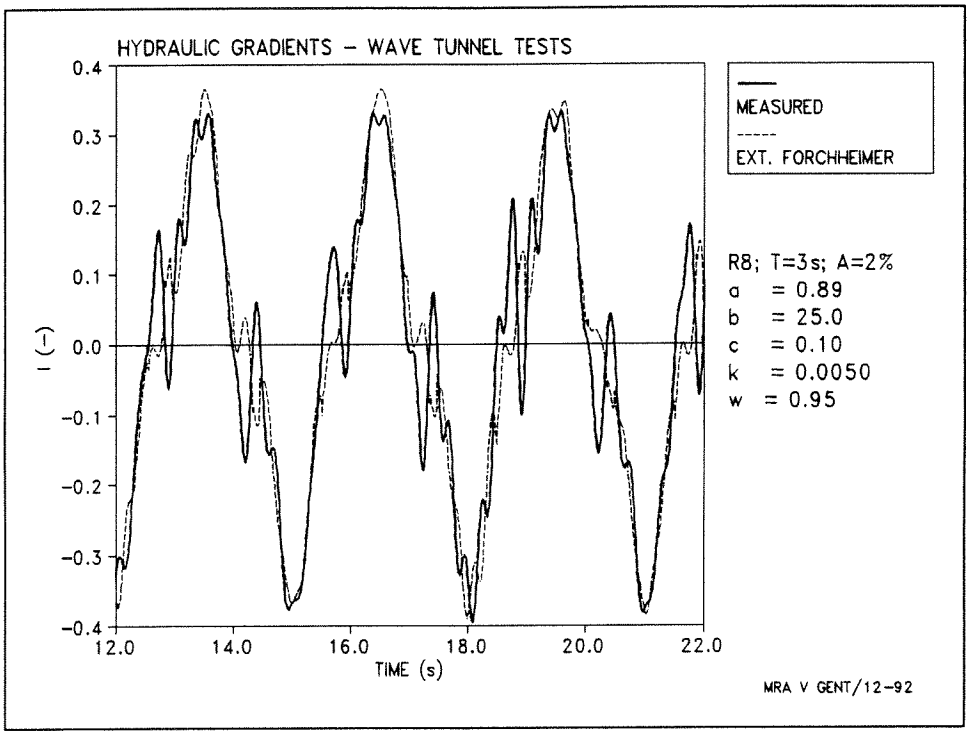
HYDRAULIC GRADIENTS – WAVE TUNNEL TESTS
MEASURED
EXT. FORCHHEIMER
R8; T=3s; A=2%
a = 0.89
b = 25.0
c = 0.10
k = 0.0050
w = 0.95
I (-)
TIME (s)
MRA V GENT/12-92

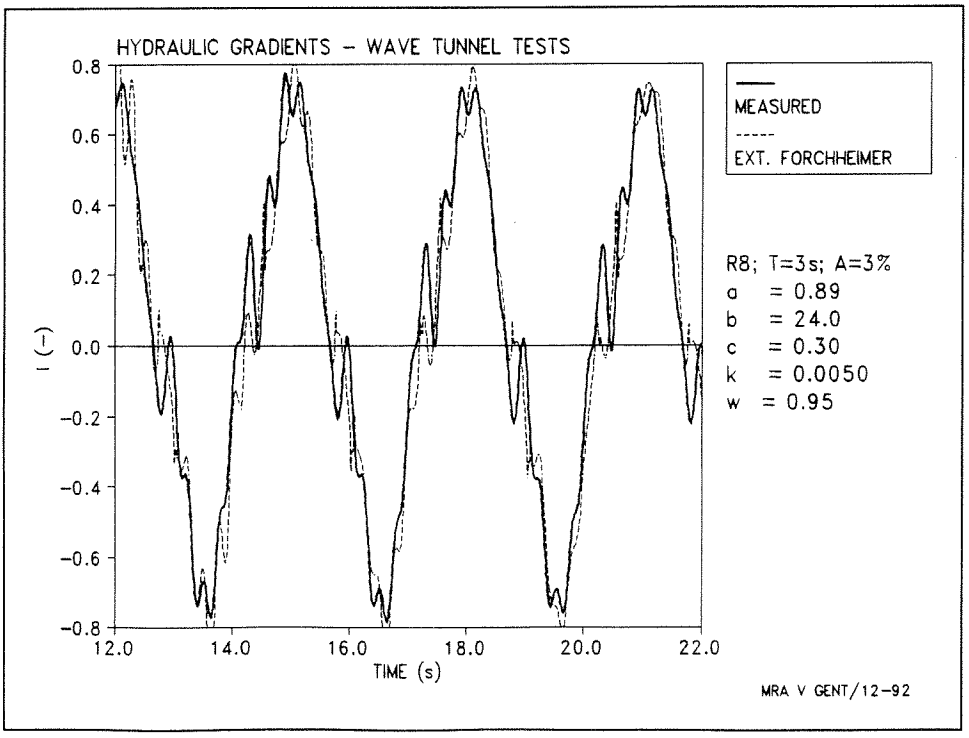
HYDRAULIC GRADIENTS – WAVE TUNNEL TESTS
MEASURED
EXT. FORCHHEIMER
R8; T=3s; A=3%
a = 0.89
b = 24.0
c = 0.30
k = 0.0050
w = 0.95
I (-)
TIME (s)
MRA V GENT/12-92

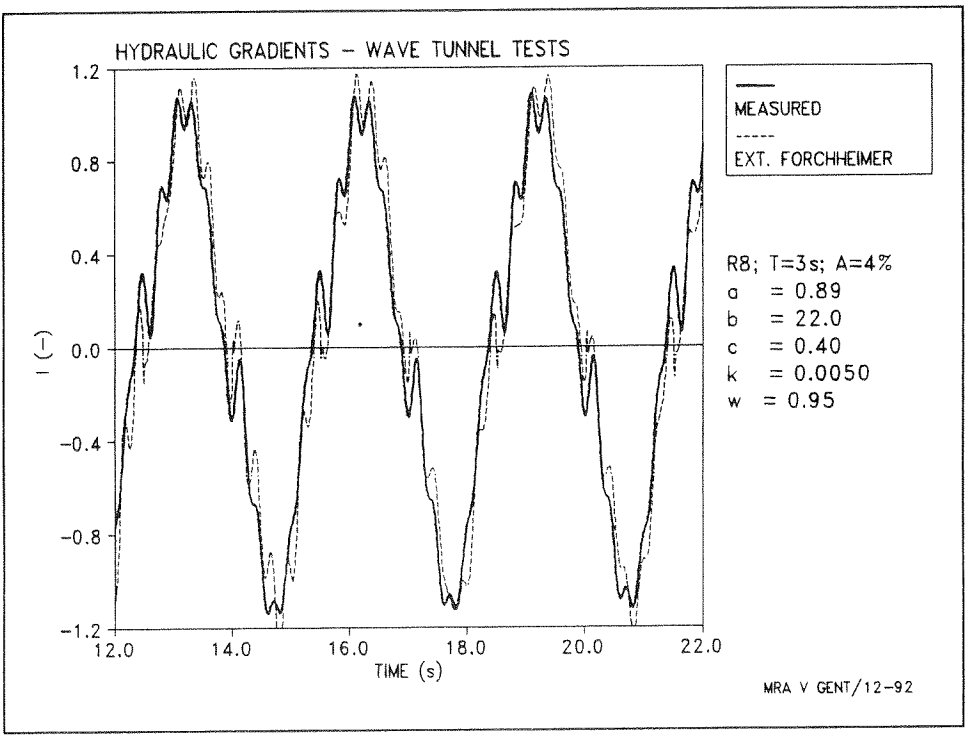
HYDRAULIC GRADIENTS – WAVE TUNNEL TESTS
1.2
0.8
0.4
0.0
-0.4
-0.8
-1.2
I (-)
12.0
14.0
16.0
18.0
20.0
22.0
TIME (s)
MEASURED
EXT. FORCHHEIMER
R8; T=3s; A=4%
a = 0.89
b = 22.0
c = 0.40
k = 0.0050
w = 0.95
MRA V GENT/12-92

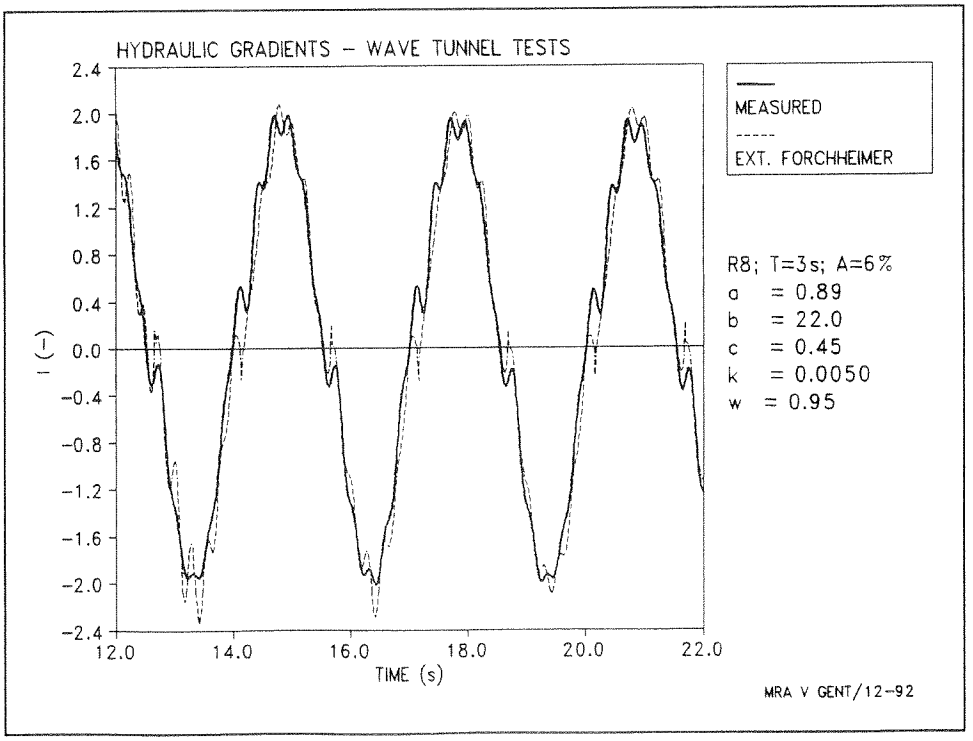
HYDRAULIC GRADIENTS – WAVE TUNNEL TESTS
2.4
2.0
1.6
1.2
0.8
0.4
0.0
-0.4
-0.8
-1.2
-1.6
-2.0
-2.4
I (-)
12.0
14.0
16.0
18.0
20.0
22.0
TIME (s)
MEASURED
EXT. FORCHHEIMER
R8; T=3s; A=6%
a = 0.89
b = 22.0
c = 0.45
k = 0.0050
w = 0.95
MRA V GENT/12-92

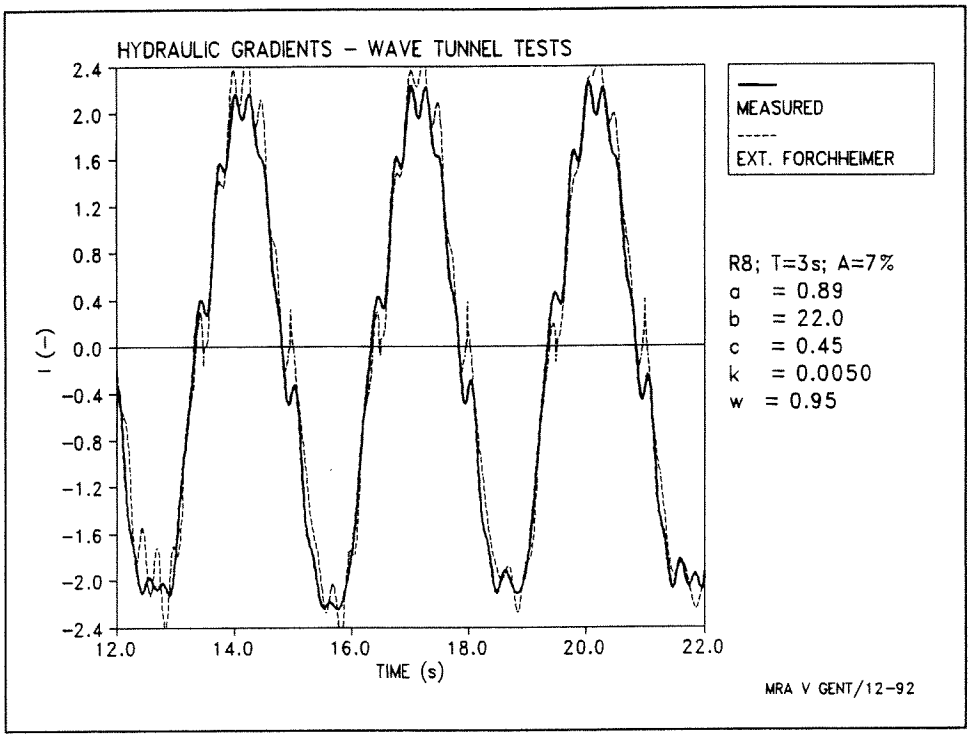
HYDRAULIC GRADIENTS – WAVE TUNNEL TESTS
I (-)
TIME (s)
MEASURED
EXT. FORCHHEIMER
R8; T=3s; A=7%
a = 0.89
b = 22.0
c = 0.45
k = 0.0050
w = 0.95
MRA V GENT/12-92

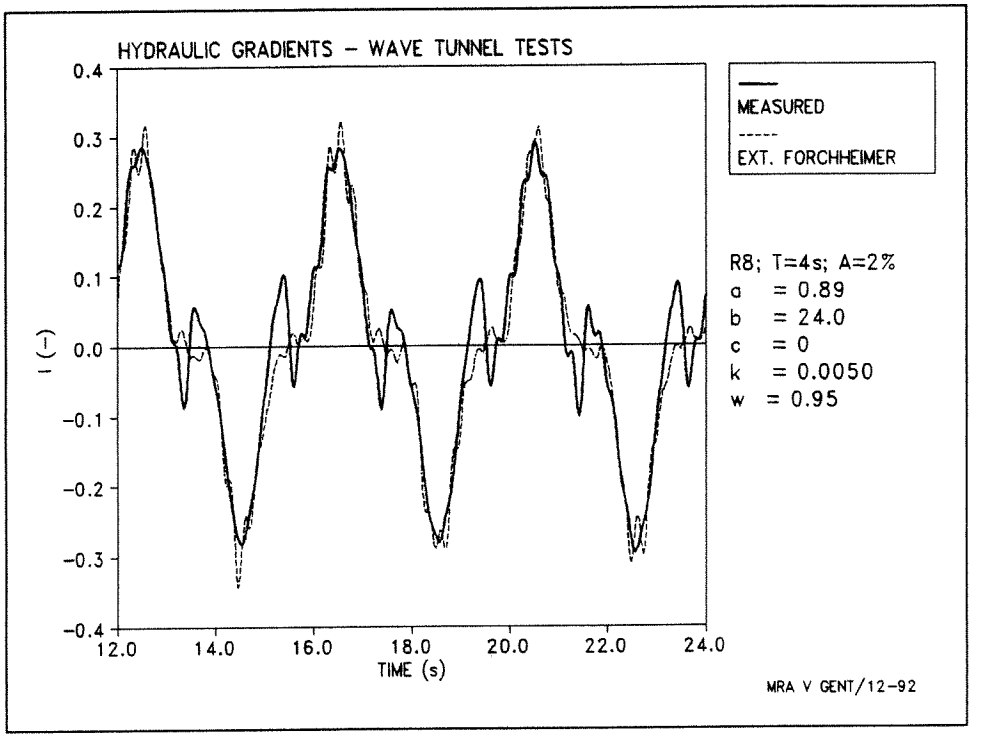
HYDRAULIC GRADIENTS – WAVE TUNNEL TESTS
I (-)
TIME (s)
MEASURED
EXT. FORCHHEIMER
R8; T=4s; A=2%
a = 0.89
b = 24.0
c = 0
k = 0.0050
w = 0.95
MRA V GENT/12-92

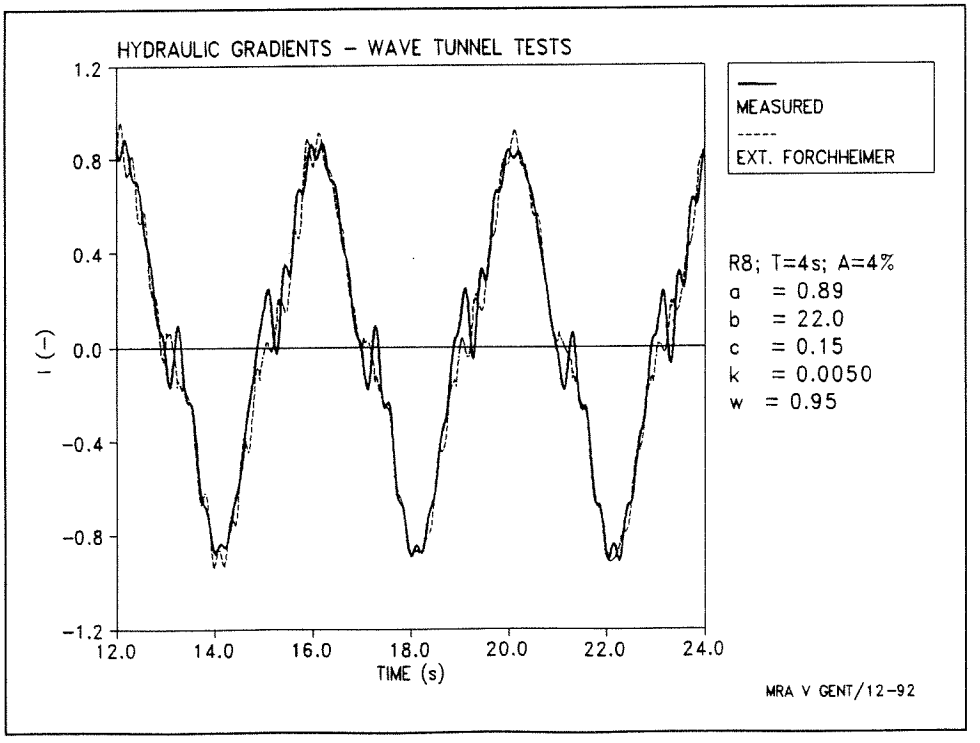
HYDRAULIC GRADIENTS – WAVE TUNNEL TESTS
I (-)
TIME (s)
MEASURED
EXT. FORCHHEIMER
R8; T=4s; A=4%
a = 0.89
b = 22.0
c = 0.15
k = 0.0050
w = 0.95
MRA V GENT/12-92

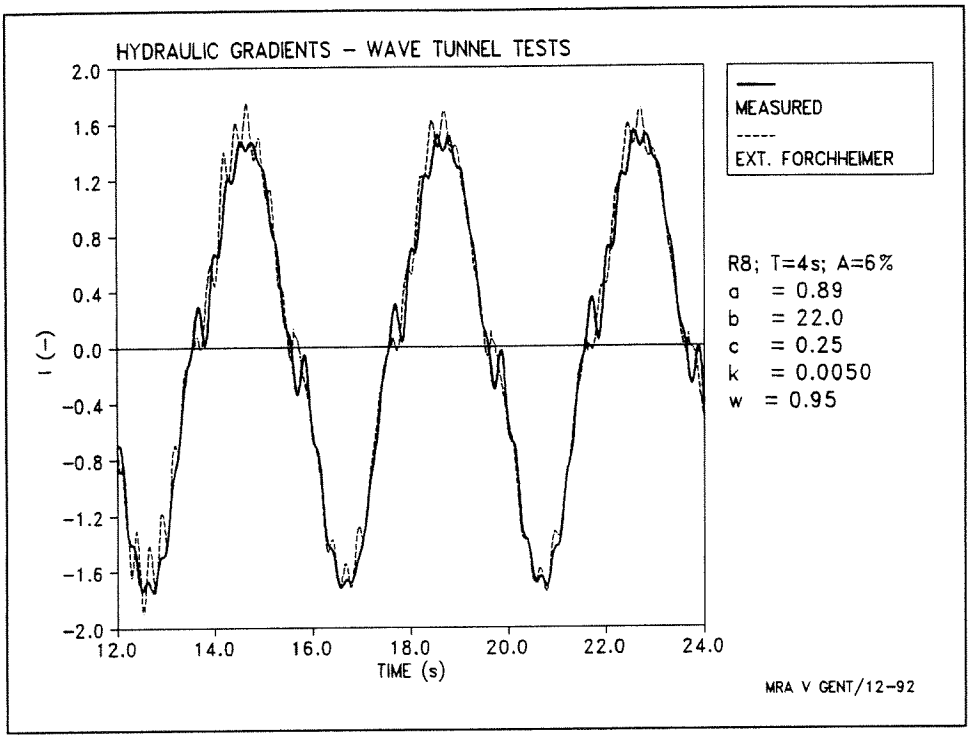
HYDRAULIC GRADIENTS – WAVE TUNNEL TESTS
I (-)
TIME (s)
MEASURED
EXT. FORCHHEIMER
R8; T=4s; A=6%
a = 0.89
b = 22.0
c = 0.25
k = 0.0050
w = 0.95
MRA V GENT/12-92

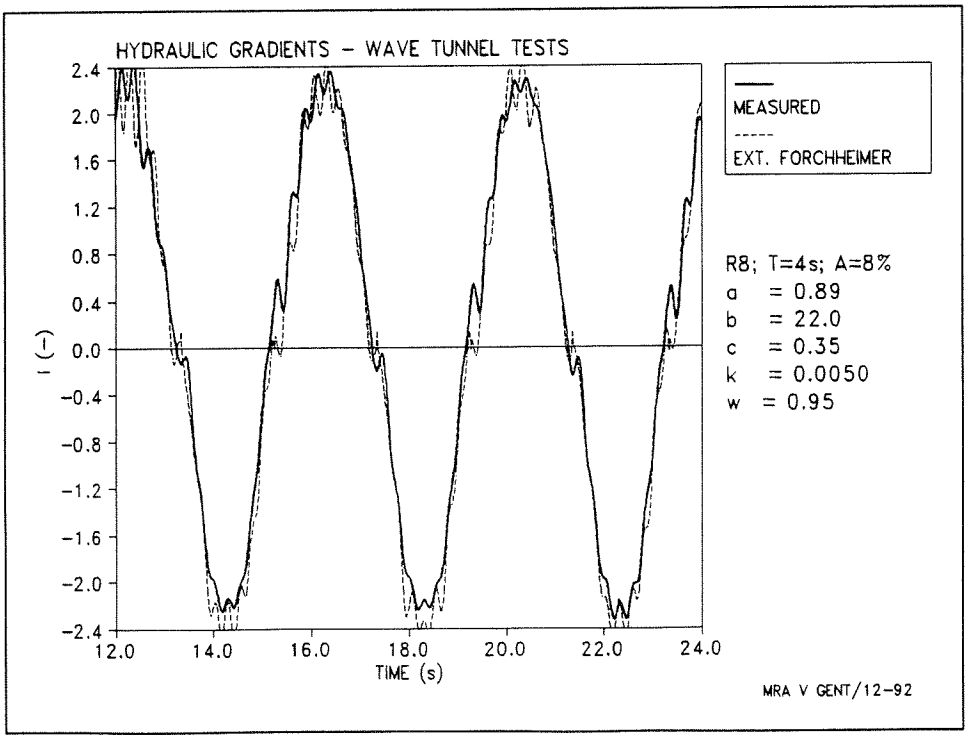
HYDRAULIC GRADIENTS – WAVE TUNNEL TESTS
I (-)
TIME (s)
MEASURED
EXT. FORCHHEIMER
R8; T=4s; A=8%
a = 0.89
b = 22.0
c = 0.35
k = 0.0050
w = 0.95
MRA V GENT/12-92

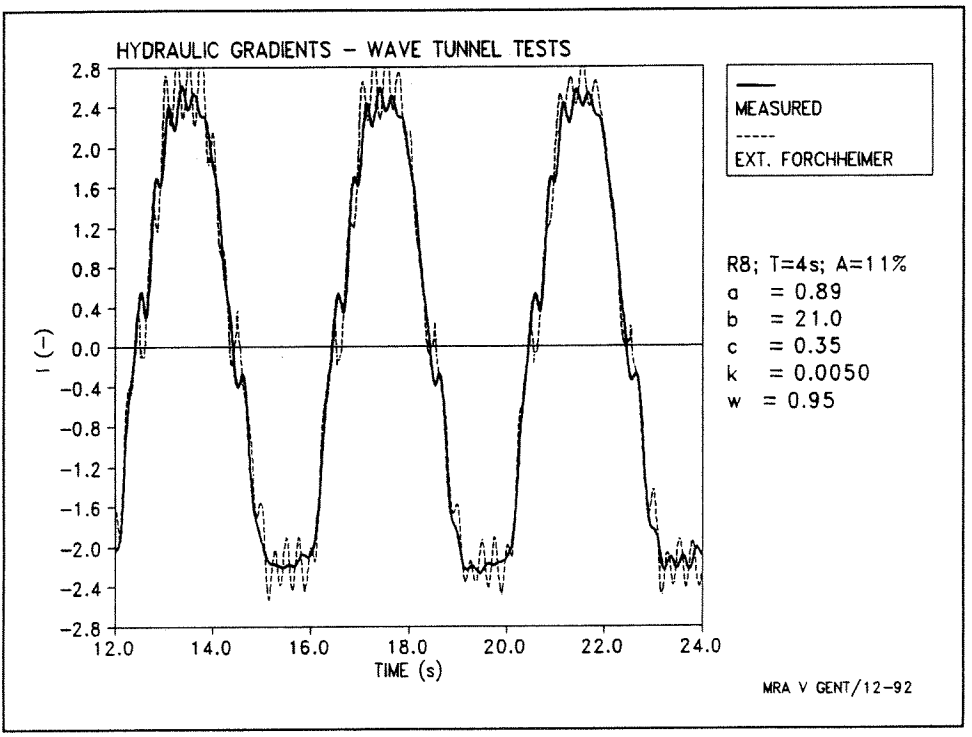
HYDRAULIC GRADIENTS – WAVE TUNNEL TESTS
I (-)
TIME (s)
MEASURED
EXT. FORCHHEIMER
R8; T=4s; A=11%
a = 0.89
b = 21.0
c = 0.35
k = 0.0050
w = 0.95
MRA V GENT/12-92

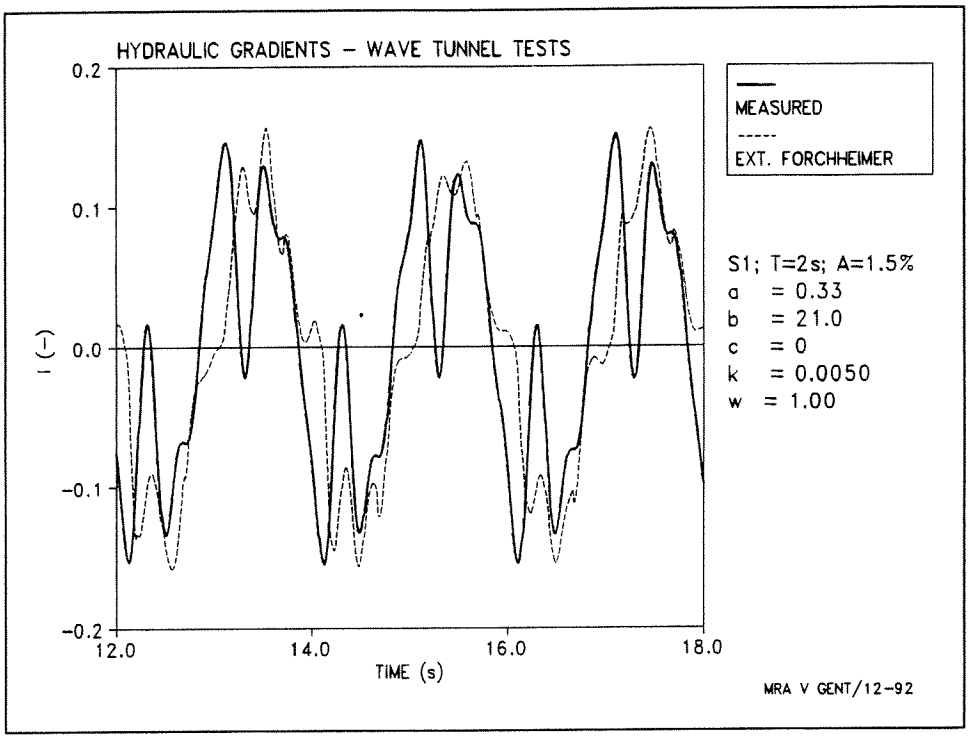
HYDRAULIC GRADIENTS – WAVE TUNNEL TESTS
0.2
0.1
0.0
-0.1
-0.2
I (-)
12.0
14.0
16.0
18.0
TIME (s)
MEASURED
EXT. FORCHHEIMER
S1; T=2s; A=1.5%
a = 0.33
b = 21.0
c = 0
k = 0.0050
w = 1.00
MRA V GENT/12-92

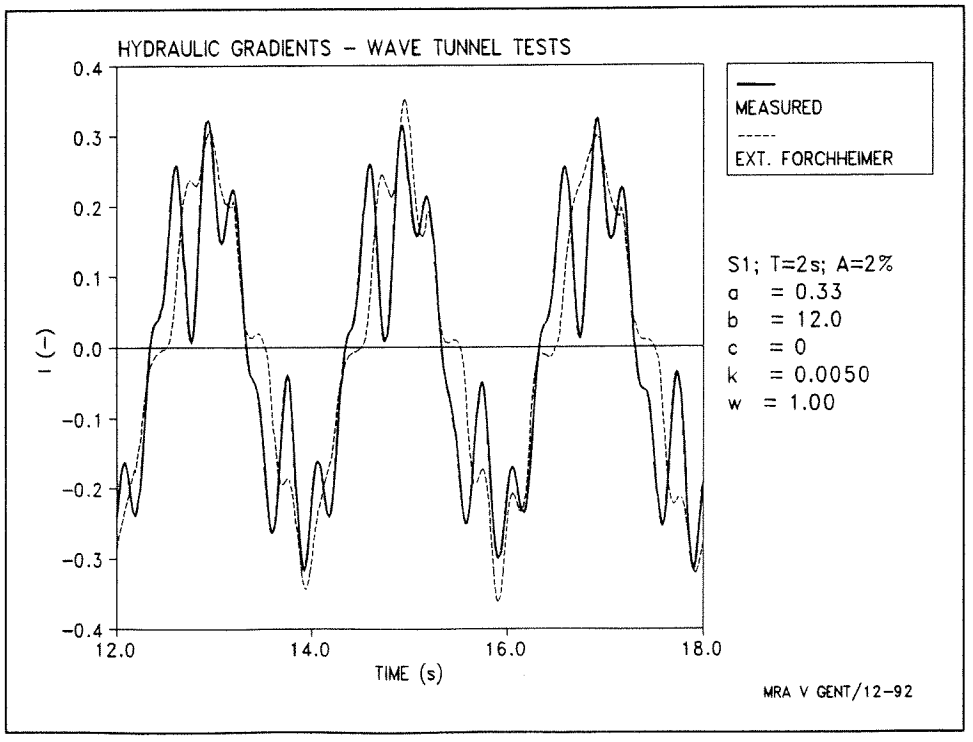
HYDRAULIC GRADIENTS – WAVE TUNNEL TESTS
0.4
0.3
0.2
0.1
0.0
-0.1
-0.2
-0.3
-0.4
I (-)
12.0
14.0
16.0
18.0
TIME (s)
MEASURED
EXT. FORCHHEIMER
S1; T=2s; A=2%
a = 0.33
b = 12.0
c = 0
k = 0.0050
w = 1.00
MRA V GENT/12-92

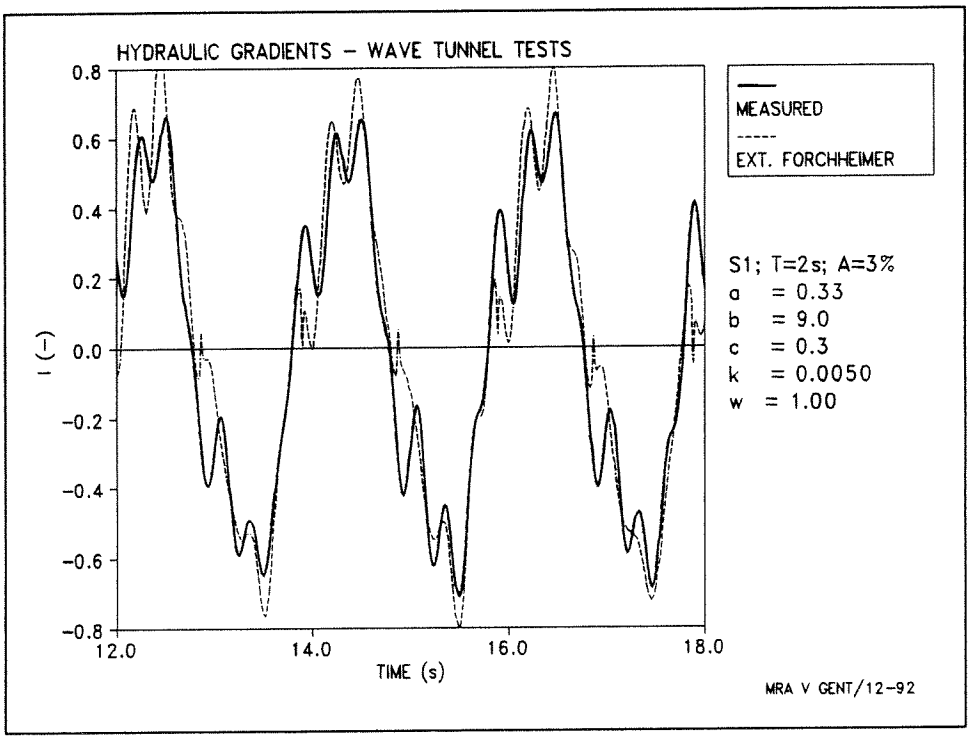
HYDRAULIC GRADIENTS – WAVE TUNNEL TESTS
I (-)
TIME (s)
MEASURED
EXT. FORCHHEIMER
S1; T=2s; A=3%
a = 0.33
b = 9.0
c = 0.3
k = 0.0050
w = 1.00
MRA V GENT/12-92

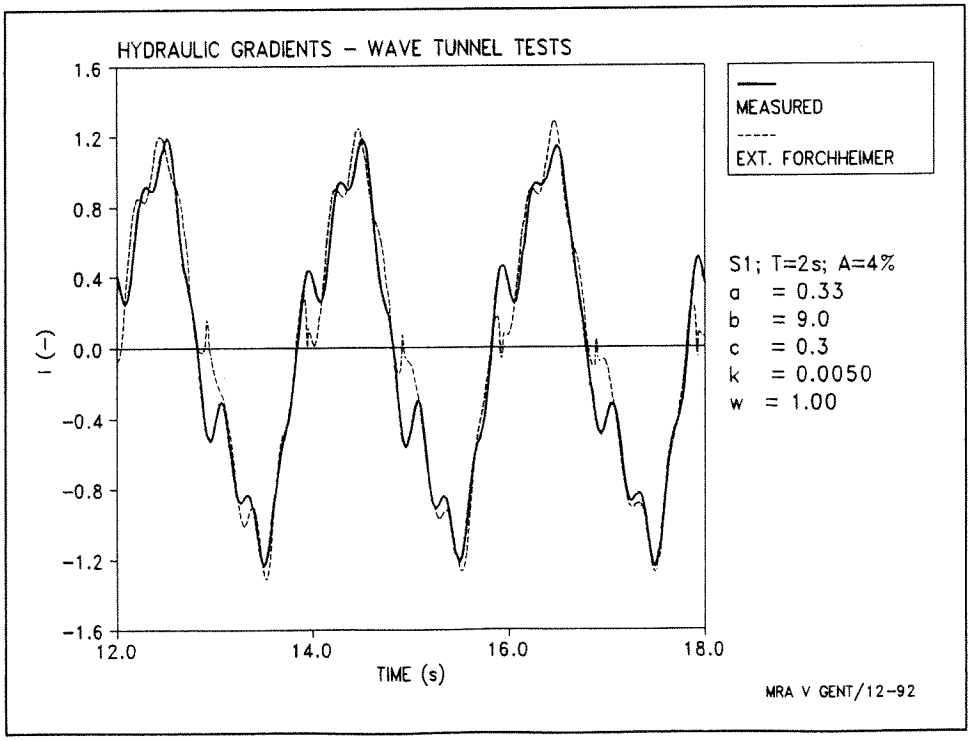
HYDRAULIC GRADIENTS – WAVE TUNNEL TESTS
I (-)
TIME (s)
MEASURED
EXT. FORCHHEIMER
S1; T=2s; A=4%
a = 0.33
b = 9.0
c = 0.3
k = 0.0050
w = 1.00
MRA V GENT/12-92

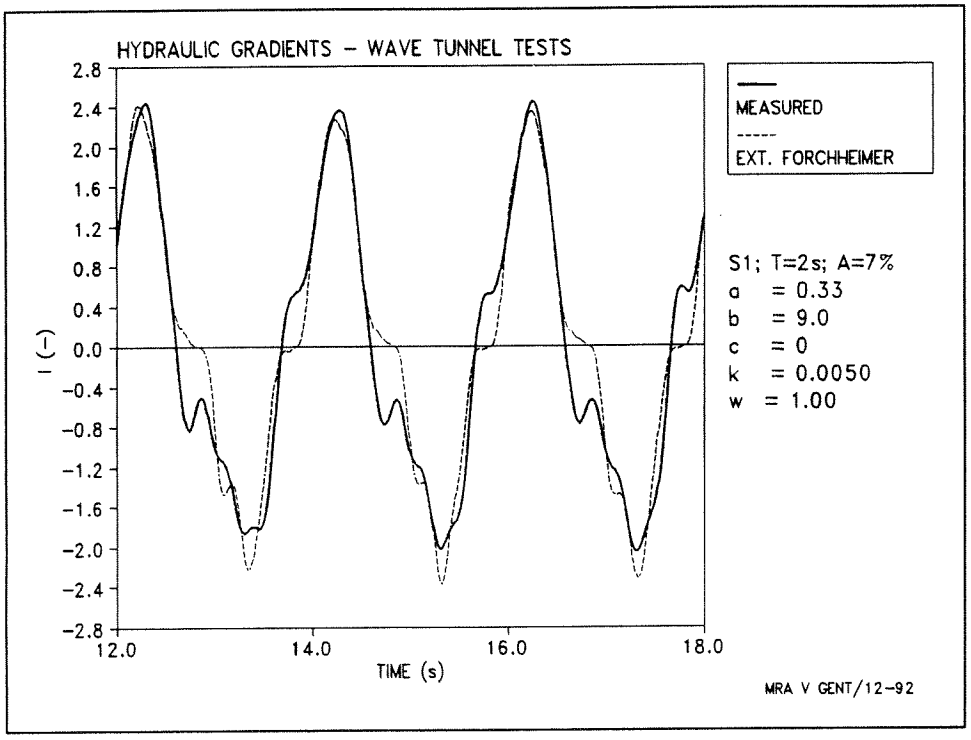
HYDRAULIC GRADIENTS – WAVE TUNNEL TESTS
2.8
2.4
2.0
1.6
1.2
0.8
0.4
0.0
-0.4
-0.8
-1.2
-1.6
-2.0
-2.4
-2.8
I (-)
12.0
14.0
16.0
18.0
TIME (s)
MEASURED
EXT. FORCHHEIMER
S1; T=2s; A=7%
a = 0.33
b = 9.0
c = 0
k = 0.0050
w = 1.00
MRA V GENT/12-92

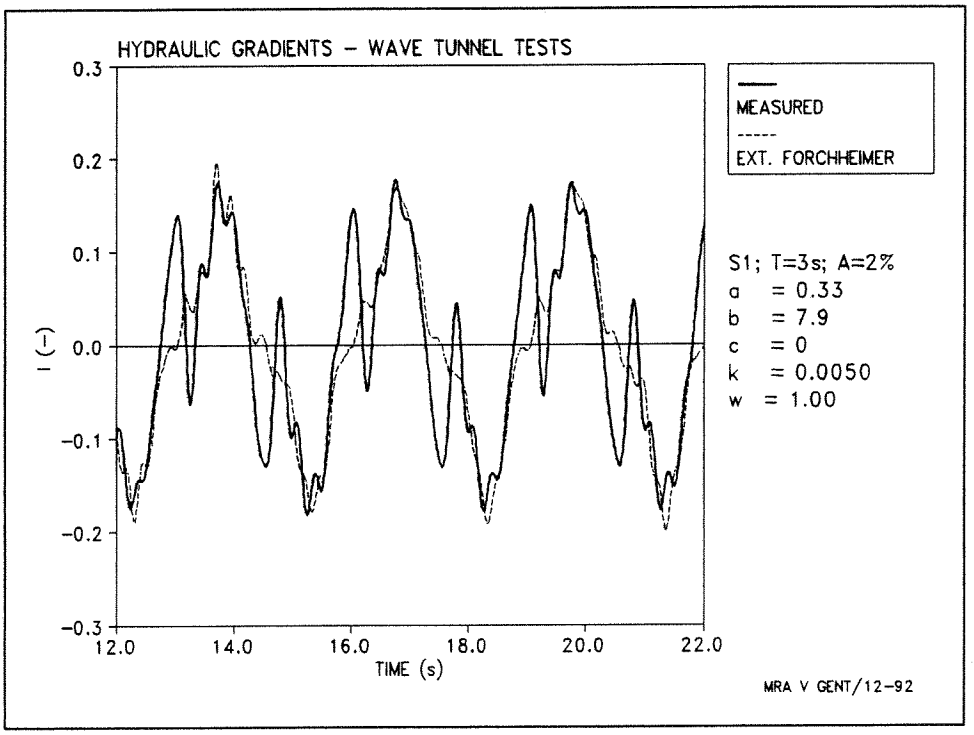
HYDRAULIC GRADIENTS – WAVE TUNNEL TESTS
0.3
0.2
0.1
0.0
-0.1
-0.2
-0.3
I (-)
12.0
14.0
16.0
18.0
20.0
22.0
TIME (s)
MEASURED
EXT. FORCHHEIMER
S1; T=3s; A=2%
a = 0.33
b = 7.9
c = 0
k = 0.0050
w = 1.00
MRA V GENT/12-92

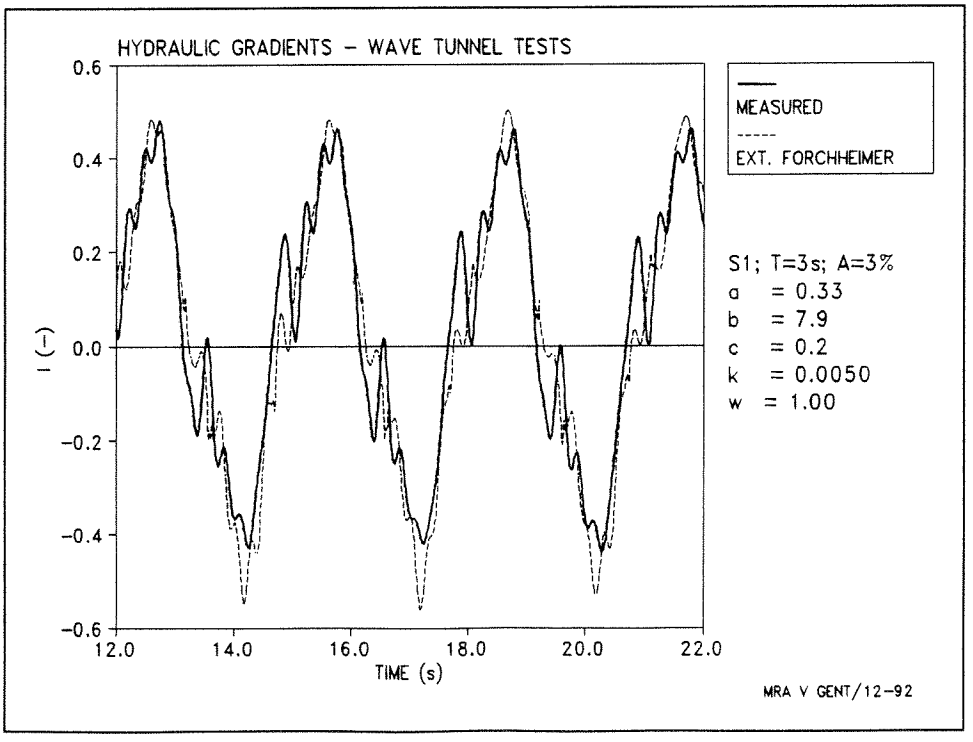
HYDRAULIC GRADIENTS – WAVE TUNNEL TESTS
0.6
0.4
0.2
0.0
-0.2
-0.4
-0.6
I (-)
12.0
14.0
16.0
18.0
20.0
22.0
TIME (s)
MEASURED
EXT. FORCHHEIMER
S1; T=3s; A=3%
a = 0.33
b = 7.9
c = 0.2
k = 0.0050
w = 1.00
MRA V GENT/12-92

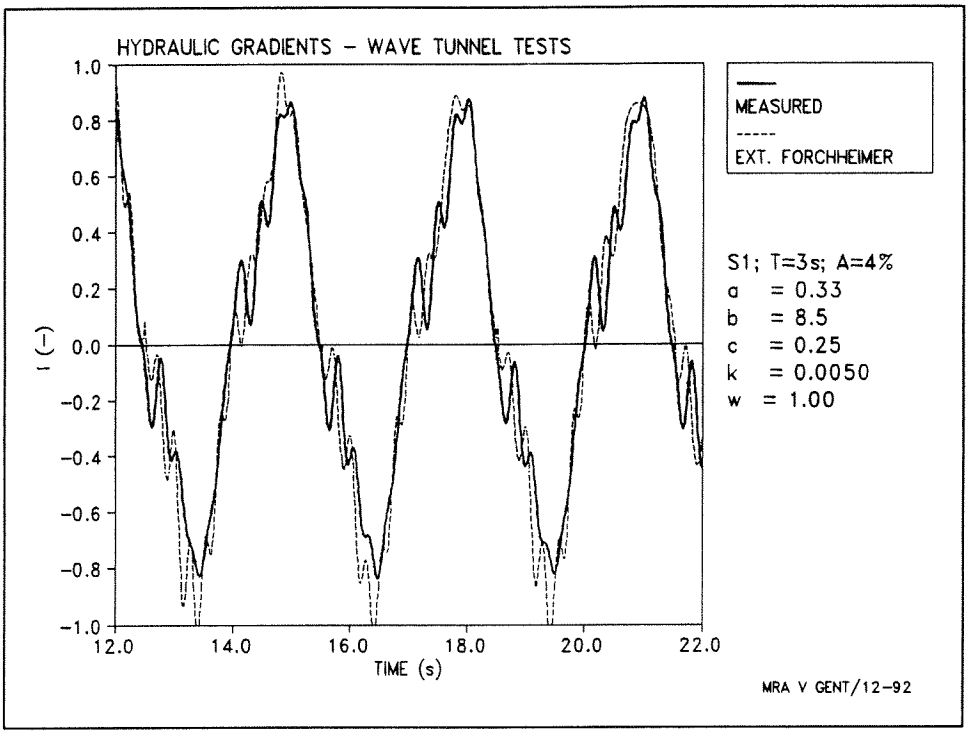
HYDRAULIC GRADIENTS – WAVE TUNNEL TESTS
I (–)
TIME (s)
MEASURED
EXT. FORCHHEIMER
S1; T=3s; A=4%
a = 0.33
b = 8.5
c = 0.25
k = 0.0050
w = 1.00
MRA V GENT/12-92

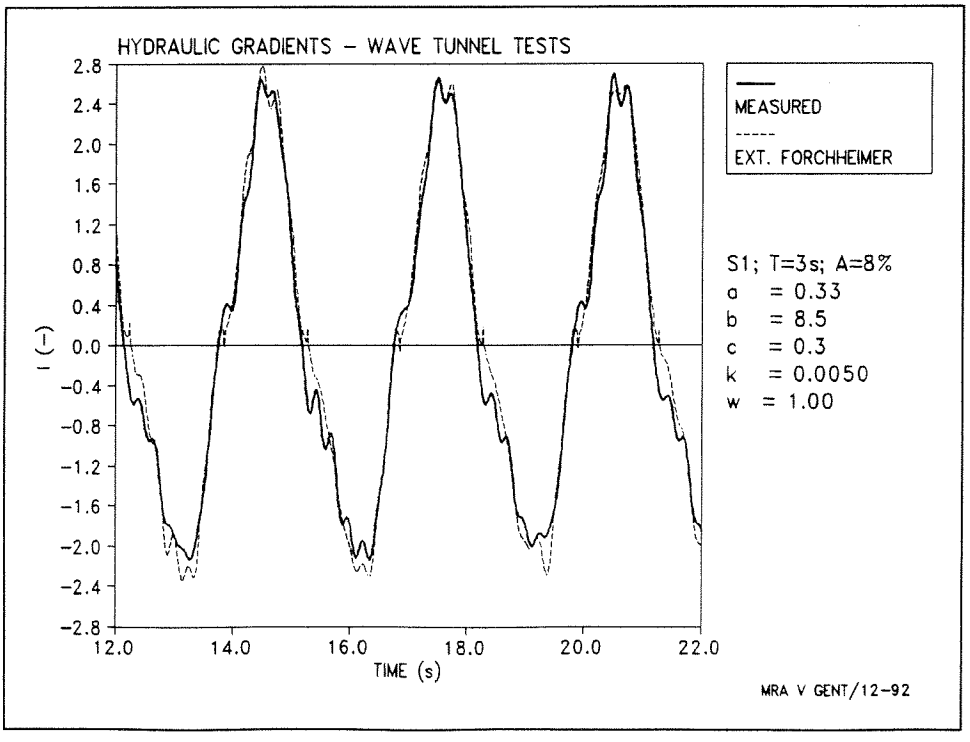
HYDRAULIC GRADIENTS – WAVE TUNNEL TESTS
I (–)
TIME (s)
MEASURED
EXT. FORCHHEIMER
S1; T=3s; A=8%
a = 0.33
b = 8.5
c = 0.3
k = 0.0050
w = 1.00
MRA V GENT/12-92

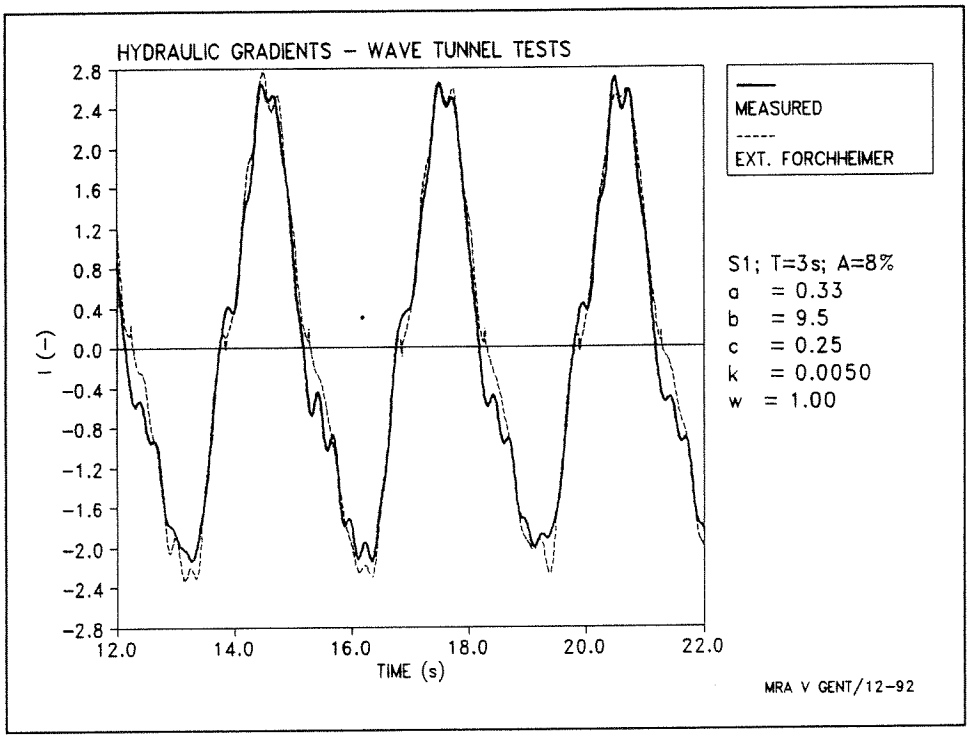
HYDRAULIC GRADIENTS – WAVE TUNNEL TESTS
I (-)
TIME (s)
MEASURED
EXT. FORCHHEIMER
S1; T=3s; A=8%
a = 0.33
b = 9.5
c = 0.25
k = 0.0050
w = 1.00
MRA V GENT/12-92

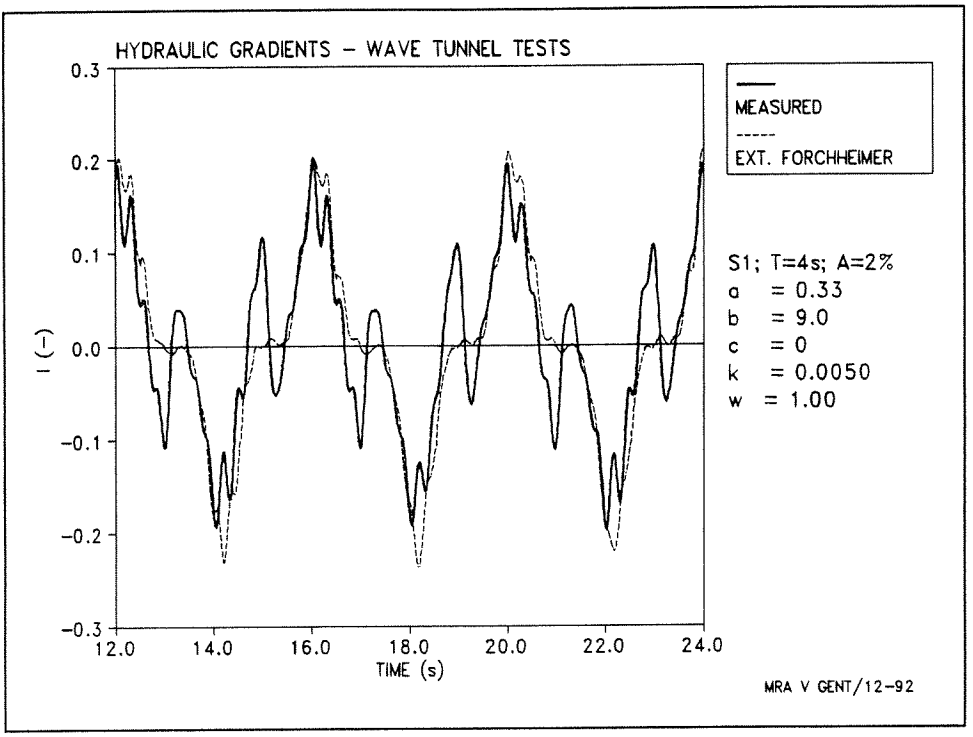
HYDRAULIC GRADIENTS – WAVE TUNNEL TESTS
I (-)
TIME (s)
MEASURED
EXT. FORCHHEIMER
S1; T=4s; A=2%
a = 0.33
b = 9.0
c = 0
k = 0.0050
w = 1.00
MRA V GENT/12-92

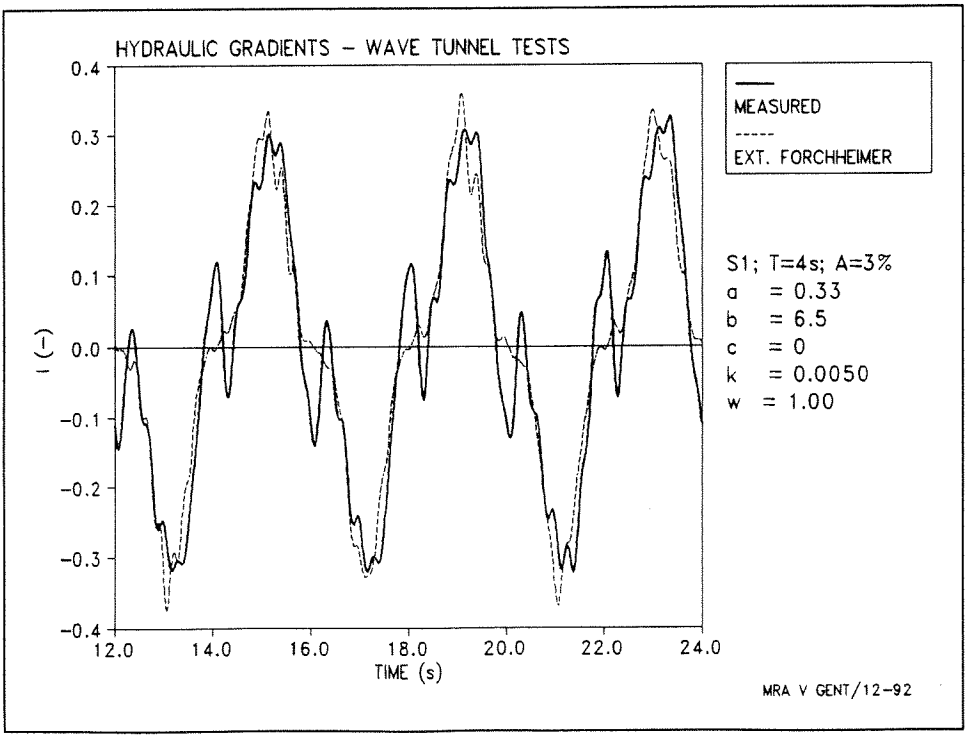
HYDRAULIC GRADIENTS – WAVE TUNNEL TESTS
I (-)
TIME (s)
MEASURED
EXT. FORCHHEIMER
S1; T=4s; A=3%
a = 0.33
b = 6.5
c = 0
k = 0.0050
w = 1.00
MRA V GENT/12-92

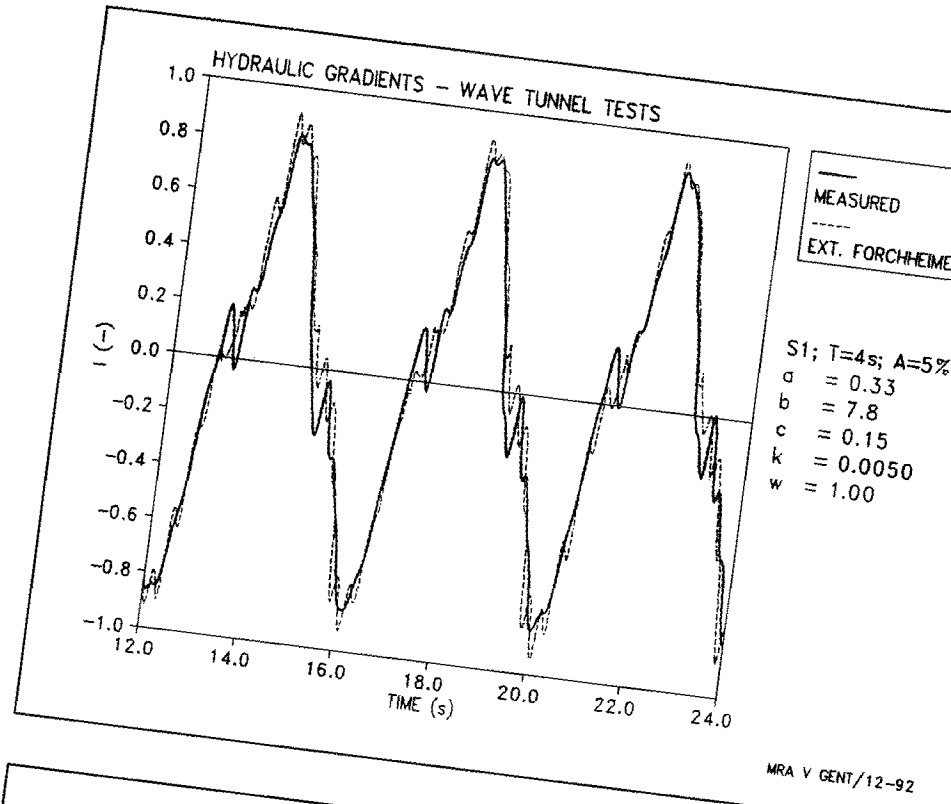
HYDRAULIC GRADIENTS – WAVE TUNNEL TESTS
1.0
0.8
0.6
0.4
0.2
0.0
−0.2
−0.4
−0.6
−0.8
−1.0
i
12.0
14.0
16.0
18.0
20.0
22.0
24.0
TIME (s)
MEASURED
EXT. FORCHHEIME
S1; T=4s; A=5%
a = 0.33
b = 7.8
c = 0.15
k = 0.0050
w = 1.00
MRA V GENT/12-92

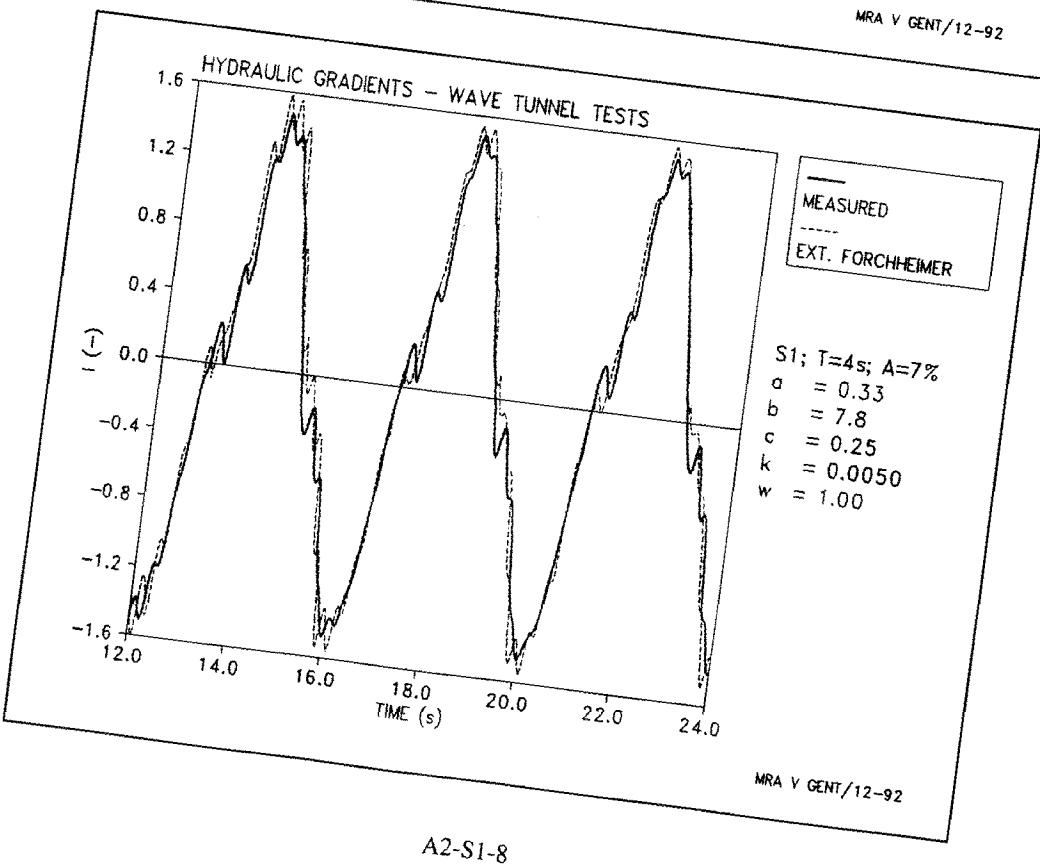
HYDRAULIC GRADIENTS – WAVE TUNNEL TESTS
1.6
1.2
0.8
0.4
0.0
−0.4
−0.8
−1.2
−1.6
i
12.0
14.0
16.0
18.0
20.0
22.0
24.0
TIME (s)
MEASURED
EXT. FORCHHEIMER
S1; T=4s; A=7%
a = 0.33
b = 7.8
c = 0.25
k = 0.0050
w = 1.00
MRA V GENT/12-92

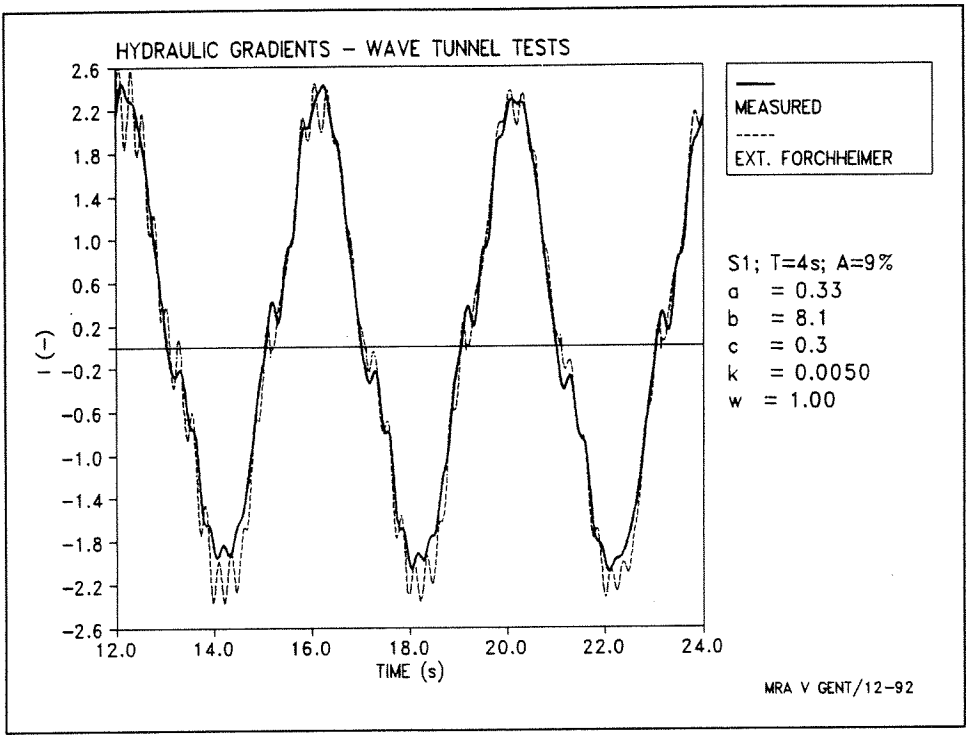
HYDRAULIC GRADIENTS – WAVE TUNNEL TESTS
I (-)
2.6
2.2
1.8
1.4
1.0
0.6
0.2
-0.2
-0.6
-1.0
-1.4
-1.8
-2.2
-2.6
12.0
14.0
16.0
18.0
20.0
22.0
24.0
TIME (s)
MEASURED
EXT. FORCHHEIMER
S1; T=4s; A=9%
a = 0.33
b = 8.1
c = 0.3
k = 0.0050
w = 1.00
MRA V GENT/12-92

APPENDIX 3

TABLES OSCILLATORY FLOW

R1 - IRREGULAR ROCK (D_{EQ}=0.076; n=0.442)				
û	T	a	b	c
0.14	2	0.23	11.5	0.10
0.24	2	0.23	10.0	0.30
0.33	2	0.23	8.2	0.35
0.39	2	0.23	7.2	0.40
0.43	2	0.23	7.2	0.40
0.13	3	0.23	10.2	0.10
0.22	3	0.23	8.7	0.15
0.28	3	0.23	8.0	0.30
0.35	3	0.23	7.6	0.35
0.40	3	0.23	7.4	0.35
0.13	4	0.23	9.8	0
0.19	4	0.23	9.0	0
0.23	4	0.23	8.3	0
0.34	4	0.23	7.9	0.20
0.43	4	0.23	7.7	0.20
0.50	4	0.23	7.4	0.20

R3 - SEMI ROUND ROCK (D_{EQ}=0.0607; n=0.454)				
û	T	a	b	c
0.12	2	0	18.0	0.30
0.29	2	0	15.0	0.40
0.38	2	0	14.0	0.45
0.13	3	0	17.0	0
0.26	3	0	12.5	0.35
0.37	3	0	12.0	0.35
0.44	3	0	12.0	0.30
0.13	4	0	16.0	0
0.22	4	0	14.0	0.22
0.32	4	0	12.5	0.25
0.40	4	0	12.3	0.30
0.45	4	0	12.1	0.35

R4 - VERY ROUND ROCK (D_{EQ}=0.0606; n=0.393)				
û	T	a	b	c
0.14	2	0.34	12.0	0.20
0.24	2	0.34	9.0	0.40
0.32	2	0.34	8.8	0.45
0.38	2	0.34	8.8	0.45
0.42	2	0.34	9.0	0.45
0.45	2	0.34	9.2	0.45
0.13	3	0.34	10.5	0.10
0.21	3	0.34	9.5	0.10
0.27	3	0.34	9.1	0.3
0.33	3	0.34	9.2	0.35
0.38	3	0.34	9.2	0.35
0.42	3	0.34	9.2	0.40
0.12	4	0.34	10.3	0
0.18	4	0.34	9.2	0.10
0.23	4	0.34	8.6	0.15
0.28	4	0.34	8.6	0.15
0.33	4	0.34	8.6	0.30
0.37	4	0.34	8.6	0.35
0.41	4	0.34	8.8	0.35
0.44	4	0.34	8.4	0.40
0.49	4	0.34	8.1	0.40

R5 - IRREGULAR ROCK (D_{EQ}=0.0251; n=0.449)				
û	T	a	b	c
0.05	2	1.81	50	0.25
0.14	2	1.81	40	0.40
0.20	2	1.81	35	0.40
0.05	3	1.81	40	0
0.08	3	1.81	34	0
0.14	3	1.81	32	0
0.18	3	1.81	32	0
0.25	3	1.81	32	0.30
0.05	4	1.81	34	0
0.08	4	1.81	33	0
0.13	4	1.81	31	0
0.21	4	1.81	31	0
0.25	4	1.81	31	0.25

R8 - IRREGULAR ROCK (D_{EQ}=0.0385; n=0.388)				
û	T	a	b	c
0.10	2	0.89	28	0.35
0.22	2	0.89	23	0.40
0.28	2	0.89	22	0.45
0.09	3	0.89	25	0.10
0.17	3	0.89	24	0.30
0.20	3	0.89	22	0.40
0.29	3	0.89	22	0.45
0.32	3	0.89	22	0.45
0.09	4	0.89	24	0
0.18	4	0.89	22	0.15
0.26	4	0.89	22	0.25
0.30	4	0.89	22	0.35
0.34	4	0.89	21	0.35

S1 - Spheres-cubic packing (D_{EQ}=0.046; n=0.476)				
û	T	a	b	c
0.07	2	0.33	21.0	0
0.15	2	0.33	12.0	0
0.27	2	0.33	9.0	0.30
0.33	2	0.33	9.0	0.30
0.49	2	0.33	9.0	0
0.13	3	0.33	7.9	0
0.22	3	0.33	7.9	0.20
0.31	3	0.33	8.5	0.25
0.45	3	0.33	8.5	0.25
0.10	3	0.33	8.5	0.30
0.13	4	0.33	9.0	0
0.20	4	0.33	6.0	0
0.31	4	0.33	7.8	0.15
0.42	4	0.33	7.8	0.25
0.51	4	0.33	8.1	0.30